


Fall 2017

## Effects of Carboxylated Nanodiamonds on Macrophages During and After Differentiation

Maisoun E. Bani Hani  
*Old Dominion University*, [mbani002@odu.edu](mailto:mbani002@odu.edu)

Follow this and additional works at: [https://digitalcommons.odu.edu/biology\\_etds](https://digitalcommons.odu.edu/biology_etds)

 Part of the [Immunology and Infectious Disease Commons](#), [Molecular Biology Commons](#), [Nanomedicine Commons](#), and the [Toxicology Commons](#)

---

### Recommended Citation

Bani Hani, Maisoun E.. "Effects of Carboxylated Nanodiamonds on Macrophages During and After Differentiation" (2017). Doctor of Philosophy (PhD), Dissertation, Biological Sciences, Old Dominion University, DOI: 10.25777/6pdw-9r12  
[https://digitalcommons.odu.edu/biology\\_etds/25](https://digitalcommons.odu.edu/biology_etds/25)

This Dissertation is brought to you for free and open access by the Biological Sciences at ODU Digital Commons. It has been accepted for inclusion in Biological Sciences Theses & Dissertations by an authorized administrator of ODU Digital Commons. For more information, please contact [digitalcommons@odu.edu](mailto:digitalcommons@odu.edu).

**EFFECTS OF CARBOXYLATED NANODIAMONDS ON MACROPHAGES DURING  
AND AFTER DIFFERENTIATION**

by

Maisoun E. Bani Hani

B.S. June 2007, Jordan University of Science and Technology, Jordan

M.S. June 2012, Jordan University of Science and Technology, Jordan

A Dissertation Submitted to the Faculty of  
Old Dominion University in Partial Fulfillment of the  
Requirements for the Degree of

DOCTOR OF PHILOSOPHY

BIOMEDICAL SCIENCES

OLD DOMINION UNIVERSITY  
December 2017

Approved by:

Christopher J. Osgood (Advisor)

Stephen J. Beebe (Member)

Lesley H. Greene (Member)

## **ABSTRACT**

### **EFFECTS OF CARBOXYLATED NANODIAMONDS ON MACROPHAGES DURING AND AFTER DIFFERENTIATION**

Maisoun E. Bani Hani  
Old Dominion University, 2017  
Advisor: Dr. Christopher J. Osgood

Nanodiamonds (ND) are a carbon-based nanomaterial that are increasingly being proposed for developing novel imaging techniques, as carriers of biomolecules and therapeutic drugs, as coatings for implants, and for other biomedical applications. The exceptional chemical, mechanical, and optical properties of ND make this material suitable in a wide range of fields. The application of ND in the biomedical field is attractive but requires more in-depth investigation into the safety of ND and its interactions with different cells and systems. The effects of ND on the immune system are not fully understood or investigated and there are several controverting reports regarding ND biocompatibility. Macrophages are found in almost all tissues of the body and are key players in the vertebrate immune system, maintaining homeostasis and initiating immune response to a wide range of pathogens and foreign or host mediators. I hypothesized that ND can affect macrophages and interfere with their functions, and aimed to study interactions of ND with these cells to better understand the potential impact of ND on the immune system. My studies included monitoring both cultured and bone-marrow-derived macrophages *in vitro* after different exposure conditions and assessment of their effects on cellular processes using molecular laboratory techniques. Results showed that these particles do not significantly increase cell death or changes in cell morphology. These

macrophages internalized ND via phagocytic and clathrin-dependent endocytosis in a time- and dose-dependent manner. The internalized ND localized to the cytoplasm without eliciting an inflammatory response in macrophages. Investigations on the macrophage functions showed that treatment of macrophages with ND did not affect their ability to respond to lipopolysaccharides. On the other hand, their endocytic activity was reduced significantly, irrespective of ND dose. Exposure of bone marrow cells to ND early during their differentiation did not affect their morphology or reduce the percent of cells expressing macrophage surface markers. Nonetheless, ND exposure reduced the number of surface markers expressed on each cell. My findings suggest that ND are not cytotoxic to macrophages at the tested concentrations, but they can interfere with macrophage functions and differentiation. Further studies are needed to explore the mechanisms by which ND suppress macrophages endocytic activity and expression of surface markers and the downstream impact of these suppressed immune functions. In addition, the effects of ND on other cells' immune functions and expression of other immune mediators yet to be studied before concluding the immunotoxicity or compatibility of ND.

Copyright, 2017, by Maisoun E. Bani Hani. All Rights Reserved.

*All my work is dedicated to my family*

## ACKNOWLEDGMENTS

First and most importantly, I thank God for giving me strength to take challenges, for his countless blessings in my life, and for giving me a lot more than what I hoped. There have been so many wonderful people who have contributed to the successful completion of this dissertation and no words are enough to thank them. I would like to thank the best advisor ever, Dr. Christopher Osgood, who guided me throughout my work. This work would not have been possible without his efforts, understanding, knowledge, and endless support. I would also like to acknowledge the special efforts of Dr. Stephen Beebe for his encouragement and support to stay focused along this dissertation journey and gave me all the time and valuable input to make my work successful. I would like to thank my committee member Dr. Lesley Greene for reviewing my dissertation and for her comments. I'm also grateful to Dr. Michael Stacey for his time and efforts and for helping me in learning lab techniques at the beginning of my lab work. Special thanks to Dr. Ralph Stevens who shared his knowledge and always supported me during the good or bad times. I'm also thankful for Dr. Anthony Asmar who has always been a great friend and helped and advised me in my lab work.

All my love and gratitude for my parents who encouraged me throughout all my studies, my husband, Khaled, for his endless love and support, and my angels; Sara, Ghazal, Mahmoud, Adam, Jued, and Sam for their patience and precious help. Special thanks for my sisters Rania, Maryan, and Furat and brothers Khaled, Mohammad, Ali, and Wadee'a for being always there for me. I would also like to thank Mohammad Salem for his support and encouragement during these years. Finally, I would like to thank all my friends and colleagues and everyone at Old Dominion University and specially College of Sciences.

**ACRONYMS**

µg	Microgram
ANOVA	Analysis of variance
APC	Antigen-presenting cells
BMDM	Bone marrow derived macrophages
BSA	Bovine serum albumin
CCL	C-C motif ligand
CD	Cluster of differentiation
cDNA	Complimentary DNA
CLR	C-type lectin receptors
CPZ	Chlorpromazine hydrochloride
ct	Threshold cycle
CXCL	C-X-C motif ligand
CYTO	Cytochalasin D
DAMP	Damage-associated molecular patterns
DMSO	Dimethyl sulfoxide
DNA	Deoxyribonucleic acid
DOX	Doxorubicin



EIPA	5-(N-Ethyl-N-isopropyl) amiloride
FACS	Fluorescence-activated cell sorting
FBS	Fetal bovine serum
GAPDH	Glyceraldehyde 3-phosphate dehydrogenase
GC	Glucocorticoids
HIV	Human immunodeficiency virus
HPHT	High pressure high temperature
HSC	Hematopoietic stem cells
IACUC	Institutional animal care and use committee
IC	Immune complexes
IFN	Interferon
IL	Interleukin
iNOS	Inducible nitric oxide synthase
LPS	Lipopolysaccharide
MAC-1	Macrophage-1 antigen
MBC	Methyl-beta-cyclodextrin
M-CSF	Macrophage-colony stimulating factor
MFI	Mean fluorescence intensity

MHC	Major histocompatibility complex
MSC	Mesenchymal stem cells
MWNT	Multi-walled carbon nanotubes
ND	Nanodiamonds
ng	Nanogram
NK	Natural killer cells
NLS	Nuclear localization sequence
nm	Nanometer
NOD	Nucleotide oligomerization
NV	Nitrogen vacancy
NYST	Nystatin
OD	Optical density
PAMP	Pathogen-associated molecular patterns
PBS	Phosphate buffer saline
PDGF	Platelet-derived growth factor
PEG	Polyethylene glycol
PHYN	Phenylarsine oxide
PLLA	Poly L-lactic acid

PRR	Pattern recognition receptors
RGD	Arginine-glycine-aspartic acid
RNA	Ribonucleic acid
ROS	Reactive oxygen species
RT-qPCR	Real time-quantitative polymerase chain reaction
SEM	Standard error mean
SiV	Silicon vacancy
SSC	Side scatter
SWNT	Single-walled carbon nanotubes
TCR	T cell receptors
TGF	Transforming growth factor
TLR	Toll-like receptor
TNF	Tumor necrosis factor
VEGF	Vascular-endothelial growth factor

## TABLE OF CONTENTS

	Page
LIST OF FIGURES.....	xiv
LIST OF TABLES.....	xvi
 Chapter	
1. INTRODUCTION.....	1
1.1 NANOMEDICINE.....	1
1.2 CARBONE-BASED NANOPARTICLES.....	4
1.2.1 GRAPHENE.....	6
1.2.2 NANOTUBES.....	7
1.2.3 FULLERENES .....	9
1.2.4 NANODIAMONDS .....	10
1.3 BIOMEDICAL APPLICATIONS OF NANODIAMONDS.....	14
1.3.1 IMAGING AND TRACKING APPLICATIONS .....	14
1.3.2 NANODIAMONDS AS A DRUG DELIVERY CARRIER .....	15
1.3.3 TISSUE ENGINEERING AND SURGICAL IMPLANTS.....	17
1.4 THE VERTEBRATE IMMUNE SYSTEM.....	19
1.4.1 ANTIGEN PRESENTATION .....	21
1.4.2 MACROPHAGES.....	26
1.5 IMMUNE RESPONSE TO NANOPARTICLES.....	30
1.5.1 TOXICITY STUDIES ON ND.....	32
2. SPECIFIC AIMS.....	34

Chapter	Page
3. MATERIALS AND METHODS.....	36
3.1 NANODIAMONDS AND CELL CULTURE.....	36
3.2 CELL VIABILITY ASSAYS.....	38
3.3 ND UPTAKE AND SUBCELLULAR LOCALIZATION.....	39
3.4 GENE EXPRESSION .....	40
3.5 EFFECTS OF ND ON MACROPHAGES ENDOCYTIC ACTIVITY.....	43
3.6 DIFFERENTIATION OF BMDM.....	44
3.7 STATISTICAL ANALYSIS.....	44
4. RESULTES AND DISCUSSION.....	45
4.1 PHENOTYPIC CHARACTERIZATION OF BMDM .....	45
4.2 INTERACTIONS OF ND WITH MACROPHAGES.....	46
4.3 CELL VIABILITY.....	54
4.4 QUANTITATION OF ND UPTAKE AND THEIR INTERNALIZATION MECHANISM.....	65
4.5 EFFECTS OF ND ON GENE EXPRESSION IN MACROPHAGES.....	69
4.6 EFFECTS OF ND ON MACROPHAGE FUNCTIONS AND DIFFERENTIATION.....	76
5. DISCUSSION.....	85
5.1 PRIMARY CELLS AND MACROPHAGE-LIKE CELL LINE.....	85
5.2 EFFECTS OF ND ON CELL MORPHOLOGY.....	86
5.3 SUBCELLULAR LOCALIZATION.....	87

5.4 INTERFERENCE OF ND WITH ABSORBANCE AND FLUORESCENCE.....	88
5.5 CELL VIABILITY.....	89
5.6 QUANTIFICATION OF THE ND UPTAKE AND UPTAKE MECHANISM.....	91
5.7 EFFECTS OF ND ON GENE EXPRESSION.....	94
5.8 EFFECTS OF ND ON MACROPHAGE RESPONSE TO LPS.....	97
5.9 EFFECTS OF ND ON MACROPHAGE ENDOCYTIC ACTIVITY.....	97
5.10 DIFFERENTIATION OF BMDM IN THE PRESENCE OF ND.....	99
5.11 SIZE-DEPENDENT EFFECTS.....	102
6. CONCLUSION.....	104
REFERENCES.....	108
APPENDIX.....	131
VITA.....	134

## LIST OF FIGURES

Figure	Page
1.1 Nanoparticles-based theragnostic medicine.....	3
1.2 Carbon based nanomaterials.....	5
1.3 Carbon hybridization states.....	6
1.4 Transmission electron micrograph of a single ND particle.....	12
1.5 ND-DOX complex inhibits tumor growth.....	17
1.6 Differentiation of Hematopoietic stem cells into the different types of blood cells....	20
1.7 Antigen presentation by macrophages.....	22
1.8 Endocytic pathways include phagocytosis and pinocytosis.....	24
1.9 Activation of macrophages.....	29
4.1 Phenotypic characterization of BMDM .....	45
4.2 Fluorescent microscope images.....	47
4.3 Figure 4.3: ND-treated cells decrease in size.....	49
4.4 Granularity of ND-treated cells.....	50
4.5 Effects of ND treatment on FSC and SSC parameters.....	52
4.6 Confocal microscope images.....	53
4.7 Absorbance of ND-treated cells at different wavelengths.....	55

4.8 Effect of cell culture supernatant transfer.....	57
4.9 MTS standard curve.....	58
4.10 Cell viability assay of ND-treated cells.....	60
4.11 Cell viability assay 1, 2, and 3 days after ND treatment.....	62
4.12 Fluorescence of ND.....	63
4.13 Apoptosis assay.....	65
4.14 Quantification of ND uptake.....	66
4.15 Endocytic pathways.....	68
4.16 RT-qPCR graphs.....	70
4.17 Gene expression in macrophages in response to ND.....	72
4.18 Cytokines ELISAs.....	74
4.19 Effects of ND treatment on macrophages response to LPS.....	77
4.20 Endocytic activity.....	79
4.21 Microscopic images of BMDM differentiated in the presence of ND.....	81
4.22 FACS graphs for determination of effects of ND on surface markers expression..	82
4.23 Expression of surface markers in ND-treated and untreated BMDM.....	83
4.24 Effects of ND on the number of surface markers expressed per cell.....	84



**LIST OF TABLES**

Table	Page
1.1 Tissue-resident macrophages.....	27
3.1 Endocytic pathway inhibitors.....	40
3.2 RT-qPCR Primers.....	42

## CHAPTER 1

### INTRODUCTION

#### 1.1 Nanomedicine

The study and application of nanometer-sized materials in medicine opened the door for new diagnostic and therapeutic strategies. Nanomedicine has gained exponential interest with highly promising results in the last decade. Some of the advantages of using nanomaterials in medicine are early diagnosis of diseases at the molecular level, improved drug delivery and targeting, and the reduction of side effects from overdosing and nonspecific or off-target effects. Hundreds of nanoparticle-containing products such as food and food packaging products, health and fitness, cosmetics, clothing, home and automotive products, reached the market in consumer products and more than 50 therapeutic drugs such as liposomal doxorubicin (cancer), pegylated interferons (hepatitis B and C), and carbohydrate-coated iron oxide (anemia of chronic kidney disease), have already entered clinical practice and many more are in the pre-clinical or clinical phases (Zhang et al. 2015; Min et al. 2015; Caster et al. 2017).

Advancement in the nanotechnology field made it possible to manipulate nanoparticles to achieve or enhance any required properties. Nanoparticles-based therapeutics can overcome many complex problems with the old therapeutic interventions. These nanoparticles can be designed to stay in the body long enough to reach their target and avoid removal by immune system components. They can also be

designed to concentrate more drug molecules in each particle, accumulate and deliver the drug to the targeted tissue but not to other healthy tissues, and to overcome biological barriers (Rizzo et al. 2013; Arranja et al. 2017).

Inorganic nanoparticles such as gold, silver, fluorescent quantum dots and iron oxides have been widely tested for diagnosis and imaging applications (Kolosnjaj-Tabi et al. 2017). Their unique physical and chemical properties such as inertness, stability, optical or magnetic properties made these materials suitable for these applications (Huang et al. 2011). With their higher sensitivity and specificity, inorganic nanoparticles may allow for diagnosis of early stage cancers and to better classify specific types of cancers (Huang et al. 2011; Kolosnjaj-Tabi et al. 2017).

Nanotechnology enabled the combination of diagnosis, targeted therapy, and monitoring the efficacy of drugs using a single platform in so called theragnostic nanomedicine (Figure 1.1). These platforms offer less invasive imaging techniques or enhance the current techniques and at the same time, lower the opportunity to expose the patient to multiple potentially harmful drugs and imaging contrast agents (Kolosnjaj-Tabi et al. 2017). In addition to their valuable roles as theragnostic nanoparticles, these platforms are highly useful for personalizing nanomedicine-based therapeutic interventions (Rizzo et al. 2013).

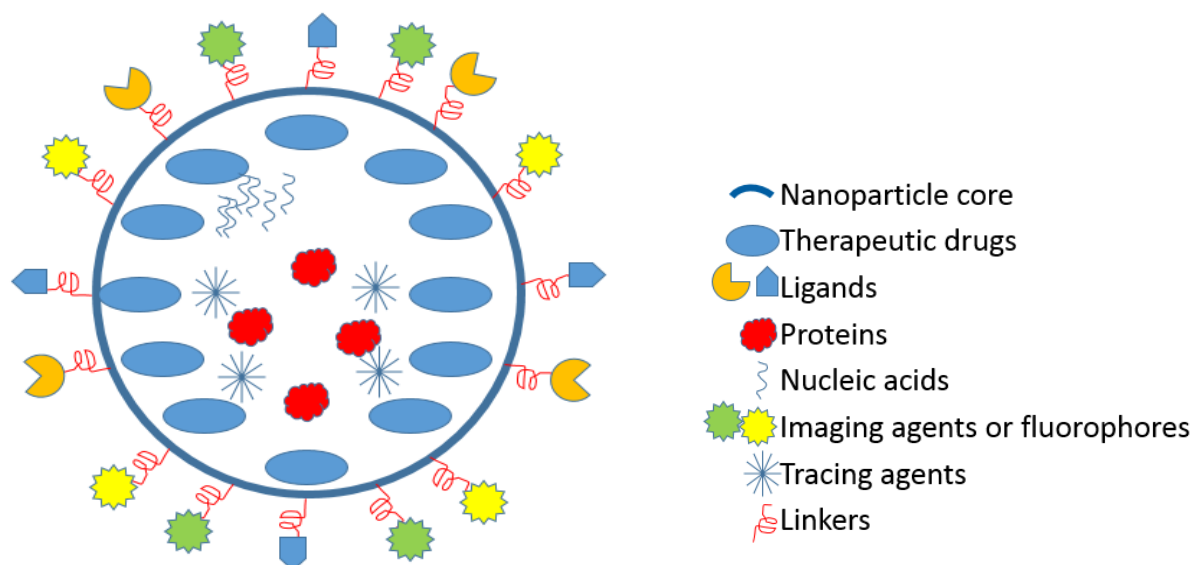


**Figure 1.1:** Nanoparticles-based theragnostic medicine. Nanoparticles can be designed to achieve diagnosis, targeted therapy, and monitoring the efficacy of drugs. The nanoparticle core can be conjugated with proteins or ligands to target specific tissue or cell type and with tracking agents for imaging and monitoring nanoparticles *in vivo* along with therapeutic drugs in the same platform.

Nanoparticles have also been suggested as adjuvants or delivery vehicles for vaccines. Traditional vaccines contain attenuated or killed microbes or microbial components and these have been essential for control of many infectious diseases. However, some of these vaccines fail to offer protection or are not safe to use specifically in the growing population of immunocompromised people (Gregory et al. 2013). For example, two vaccine candidates for *Staphylococcus aureus* (*S. aureus*) infection have been evaluated previously but failed to demonstrate efficacy and no licensed vaccine is currently available against *S. aureus* infection (Giersing et al. 2016). A recent study on a

nanoparticle-based *S. aureus* vaccine reported high protective immunity against this infection (Wang et al. 2016). For many other infectious diseases such as HIV, malaria, dengue, and Chagas disease, no vaccine is available to provide good protection. Nanoparticles can serve as a delivery vehicle for vulnerable antigens such as microbe's isolated proteins, polysaccharides, or naked DNA molecules protecting them from degradation and enhancing their presentation for immune cells.

## **1.2 Carbon-based nanoparticles**

A wide variety of starting materials have been suggested for biomedical applications in addition to the many possible modifications to enhance their biocompatibility and efficiency. Carbon-based nanoparticles such as nanotubes, graphene, fullerenes, and nanodiamonds (ND), have been tested for different imaging and therapeutic modalities (Fisher et al. 2012; Khabashesku et al. 2005). All of these particles are pure carbon materials that differ in their molecular configuration (carbon allotropes) (Figure 1.2).

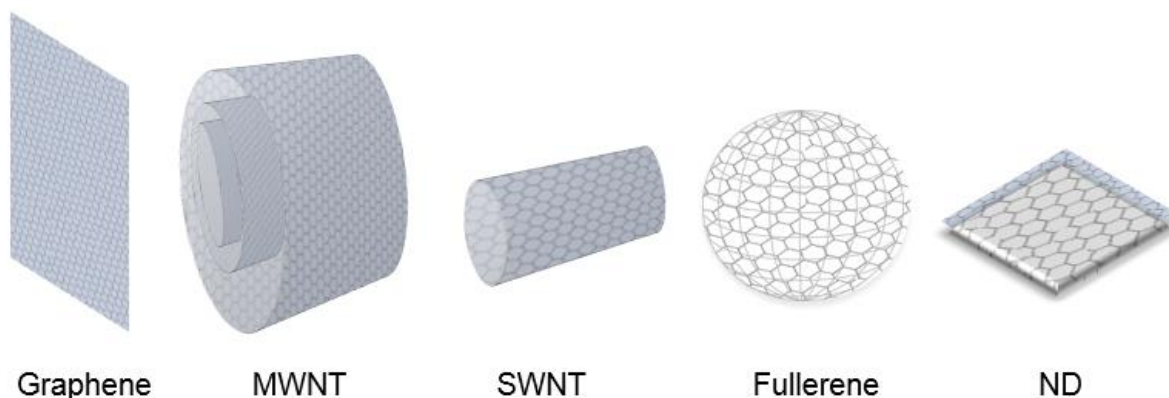


**Figure 1.2:** Carbon based nanomaterials. Graphene sheet is the parent for these carbon allotropes. Single-walled carbon nanotubes (SWNT) are cylindrical tubes, multi-walled carbon nanotubes (MWNT) are concentric cylinders, fullerenes are spherical, and nanodiamonds (ND) are rounded or faceted crystals.

The six electrons of carbon atom are arranged as  $1s^2, 2s^2, 2p^2$ . One of the  $s$  orbital electrons can promote to the empty, higher energy  $p$  orbital due to the narrow energy gap between  $2s$  and  $2p$  electron shells, allowing carbon to hybridize into an  $sp$ ,  $sp^2$ , or  $sp^3$  configuration (Figure 1.3) (Mauter and Elimelech 2008). These different hybridization states affect the overall characteristics of the carbon compound. The trigonometric  $sp^3$  configuration dominates the carbon-carbon bond in ND while the planar  $sp^2$  state dominates in fullerene, nanotubes, and graphene (Ajayan 1999). By controlling variables including temperature and pressure during the synthesis of carbon particles, scientists are able to force the formation of these types of bonds producing the different carbon allotropes.

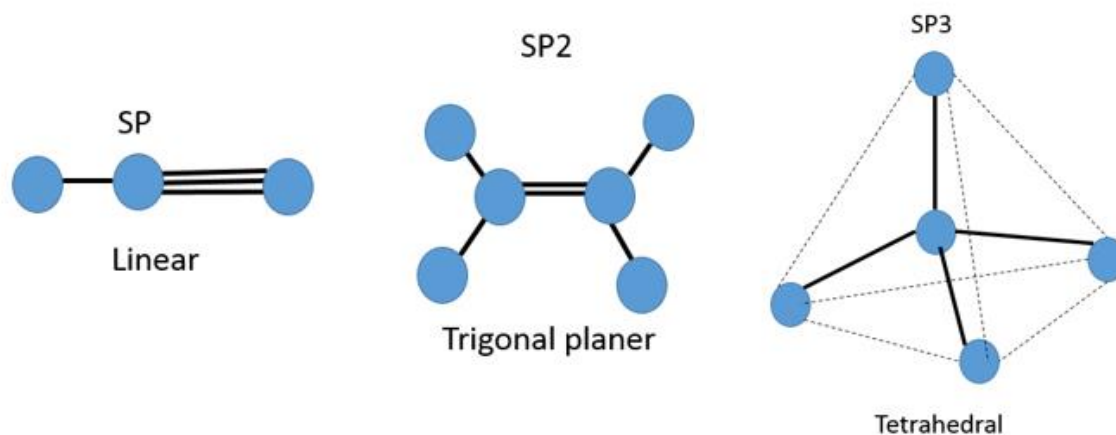


**Figure 1.3:** Carbon hybridization states.

### 1.2.1 Graphene

Graphene is the first known two-dimensional atomic crystal composed of a single layer of  $sp^2$ -hybridized carbon atoms in a honeycomb lattice with exceptional structural, optical, mechanical, electrical, and thermal properties (Yin et al. 2015; Novoselov et al. 2012). Geim and Novoselov won the Noble prize in physics in 2010 for their groundbreaking experiments using regular adhesive tape to isolate a single atom thick graphene from a piece of graphite. Different methods have been used for the mass production of graphene and its derivatives depending on the cost, quality and required properties of the product. The most common methods include chemical vapor deposition, mechanical, thermal, or liquid-phase exfoliation, and chemical, electrochemical, or thermal reduction of graphene oxide (Novoselov et al. 2012).

Since its first appearance in 2004, graphene evoked enormous interest to investigate its potential in several scientific applications (Geim and Novoselov 2007; Liu et al. 2013). This relatively new material found its path into a wide range of fields and showed promising results for its capabilities. In biomedicine, graphene and graphene oxide have been extensively studied for their use as sensors to detect biomolecules, drug and gene delivery vehicles, nanoprobe for bioimaging, phototherapy, and antimicrobial agents (Wang et al. 2011; Feng et al. 2013; Maleki Dizaj et al. 2015; Yang et al. 2013). More derivatives are being investigated particularly with the ease of functionalization of graphene and with the advancements in this rapidly growing area.

### **1.2.2 Nanotubes**

Graphene is the building block of the carbon nanotubes where these tubes are formed from folding of the graphene sheets into the cylindrical structure. Single-wall carbon nanotubes (SWNT) and multi-wall carbon nanotubes (MWNT) have distinct features making them suitable for different applications. The inner diameter ranges from 0.4 to 3 nm in the SWNT and from 0.4 up to few nanometers in the MWNT while the outer diameter of MWNT is 2-30 nm (Eatemadi et al. 2014). The length of the tube is relatively high compared to the diameter (typically in the micrometer range and up to several micrometers) which gives nanotubes the highest aspect ratio (length-to-diameter) compared to other nanomaterials (Akiladevi and Basak 2011; Kaushik and Majumder 2015). Another interesting feature of carbon nanotubes is their high tensile strength (resistance to being pulled apart). The  $sp^2$  bonds between carbon atoms are stronger



than the sp<sup>3</sup> bonds in diamonds and theoretically, these tubes may have tensile strength hundreds of times higher than that of steel (Eatemadi et al. 2014).

Carbon nanotubes were first introduced by Somio Iijima in 1991 (Iijima 1991). Iijima used carbon arc discharge method to produce MWNT. This method applies a direct current between two graphite rods in a chamber filled with ambient gas to induce evaporation of the anode carbon which deposit on the top of the cathode producing MWNT (Ando and Zhao 2006; Eatemadi et al. 2014). Other commonly used methods to produce carbon nanotubes include laser ablation which uses a high-power laser to vaporize pure graphite, and chemical vapor deposition which involve chemical breakdown of hydrocarbons and deposition on a metal substrate (Cha et al. 2013; Kaushik and Majumder 2015; Eatemadi et al. 2014). Each of these methods has variations but in general, all of them produce similar yield rate and can produce both SWNT and MWNT (Eatemadi et al. 2014).

In addition to their valuable capabilities for electronics, nanotechnology, manufacturing, and construction, carbon nanotubes were tested for many biomedical applications. Studies on interactions of bone cells (osteoblasts) and mesenchymal stem cells (MSC) with carbon nanotubes showed that these tubes positively affect bone formation by enhancing differentiation of MSC into osteogenic lineage, osteoblast proliferation, and expression of calcium and alkaline phosphatase (Elias et al. 2002; Khang et al. 2006; Stout and Webster 2012; Nayak et al. 2010). Other studies investigated the suitability of carbon nanotubes as *in vivo* biosensors such as tissue-implantable insulin sensor, and showed promising results for detection of biomolecules (Iverson et al. 2013; Kruss et al. 2013; Bisker et al. 2015). The ability to modify these nanotubes by

functionalization with biomolecules allowed the production of more effective materials enhancing biocompatibility and solubility in aqueous media (Eatemadi et al. 2014).

### 1.2.3 Fullerenes

Buckminsterfullerene, C<sub>60</sub>, is the smallest and the most abundant fullerene from the currently used preparations (Hirsch and Brettreich 2005). Fullerenes are composed of carbon hexagons, like graphene, but fused with pentagons to provide the curvature. Other larger fullerenes, in addition to the many manipulated derivatives, are also produced for specific applications. These spheres are less stable thermodynamically than graphite or diamonds and are less water-soluble. However, the solubility of fullerenes in organic solvents allowed the chemical modifications enhancing their solubility in aqueous media and stability (Schinazi et al. 1993; Yamago et al. 1995; Hirsch and Brettreich 2005).

Production of fullerenes was first reported by Curl, Kroto, and Smalley in 1985 which later led to a Noble prize in chemistry in 1996 (Noble prize.org 1996). They used the laser irradiation method to vaporize graphite producing clusters of 60 carbon atoms (C<sub>60</sub>) and 70 carbon atoms (C<sub>70</sub>) (Kroto et al. 1985). Since then, scientists have developed other methods to generate fullerenes and fullerenes derivatives. The first method to produce macroscopic quantities of fullerenes also included the vaporization of graphite but this method used resistive heating of graphite instead of laser irradiation (Kratschmer et al. 1990). Fullerenes were found in the sooting flames which led to new methods for synthesis of fullerenes based on combustion (Howard et al. 1991). Using different pressures, temperatures, and carbon to oxygen ratios, combustion of a premixed benzene, oxygen, and argon flames producing fullerenes in addition to other combustion

products (Hirsch and Bretterich 2005). Another method to produce fullerene is the pyrolysis of naphthalene in argon stream at 1000 °C which is based on the full dehydrogenation of naphthalene to produce C<sub>60</sub> and C<sub>70</sub> but in low yield (Taylor et al. 1993). The yield and purity of fullerenes produced by the available current production methods vary and all require purifications after synthesis due to the use of metallic catalysts and by products of the production reaction.

Due to the unique physical and chemical features of the fullerene family, and especially C<sub>60</sub>, these nanomaterials were tested in biological fields. Schinazi and co-workers (1993) reported anti-HIV activity of a water-soluble fullerene C<sub>60</sub> derivative in acutely and chronically HIV-infected cells (Schinazi et al. 1993). Two major targets were found for anti-HIV fullerenes derivatives; the anti-protease and anti-reverse transcriptase activities, which were enhanced by surface modifications of the fullerenes (Friedman et al. 1993; Friedman et al. 1998; Mashino et al. 2005). An interesting feature of fullerene C<sub>60</sub> is its ability to quench various free radicals (Krusic et al. 1991). This feature is of special importance in biomedical field as it shows a higher efficiency than conventional antioxidants. In addition, fullerene can produce highly reactive singlet oxygens when exposed to light which can react with a wide range of biomolecules such as DNA (Arbogast et al. 1991; Markovic and Trajkovic 2008; Bosi et al. 2003).

#### **1.2.4 Nanodiamonds**

The nanometer-sized diamond particles are a new addition to the carbon-based nanomaterials and are currently available in different sizes (up to hundreds of nanometers) and surface chemistries (Figure 1.4). Synthesis of nanodiamonds requires

termination with functional groups or reconstruction into an  $sp^2$  carbon (Mochalin et al. 2011). These functional groups can be oxygen- or nitrogen-containing groups which can be easily conjugated with other desired molecules. The rigid diamond structure is formed by the  $sp^3$  hybridization of carbon atoms with tetrahedral symmetry (Kaur and Badea 2013). This hybridization state means that the four valence electrons of the carbon atom are engaged in a  $\sigma$  bond with the neighboring atoms resulting in a lack of free electrons and hence, producing a chemically inert core structure. This structure gives ND their outstanding properties such as chemical stability and extremely high hardness and strength. However, the chemical stability of the core does not hinder the ability of ND surface from engaging in interactions and modifications with chemicals and biomolecules. ND are chemically inert but can be easily conjugated with drugs or biomolecules which is essential for targeted therapy and diagnostic applications (Vaijayanthimala et al. 2015; Kong, Huang, Hsu et al. 2005; Kong, Huang, Liao et al. 2005).

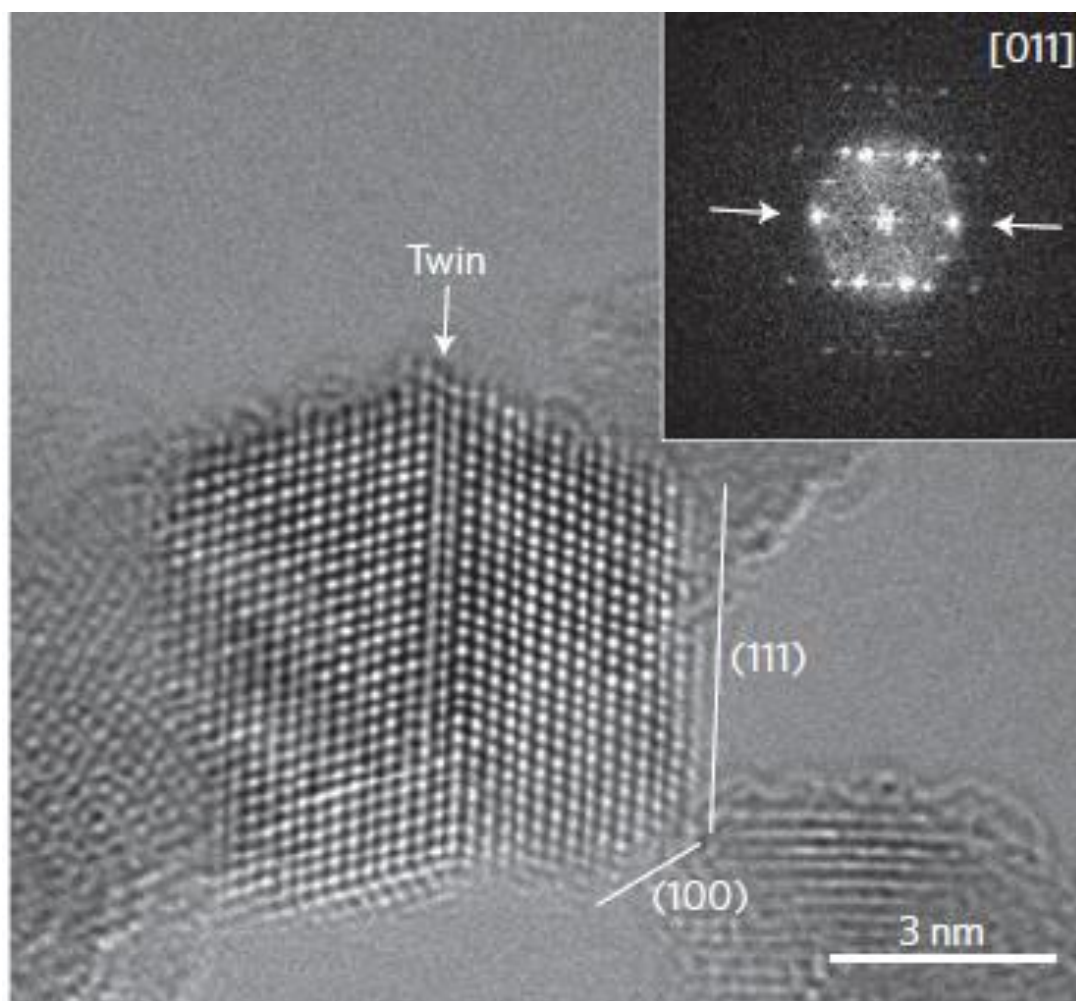


**Figure 1.4:** Transmission electron micrograph of a single ND particle. The ND core is highly ordered  $sp^3$  carbons and the surface can be  $sp^2$  or functionalized with other groups. ND surface can be rounded or have facets like the one shown here. Reprinted with permission from (Shenderova et al. 2011. Surface chemistry and properties of ozone-purified detonation nanodiamonds. *The Journal of Physical Chemistry C*. 115(20):9827-9837). © (2011) American Chemical Society.

In addition to their unique optical capabilities, ND are now being produced with enhanced intrinsic fluorescence. Their fluorescence originates from crystal defects that form in their lattice during production. High energy irradiation of ND knocks carbon atoms out of the diamond structure creating vacancies which move closer to the nitrogen centers to produce the nitrogen-vacancy (NV) centers (Davies et al. 1992). Two types of NV centers are produced by this method; the neutral and the negatively charged centers which differ in their emission spectra (Mochalin et al. 2011). The neutral NV centers emit at 575 nm, weaker than the emission of the negatively-charged NV which peaks above 700 nm with no signs of photobleaching or photoblinking (Davies and Hamer 1976; Gruber et al. 1997; Yu et al. 2005). Yet another type of fluorescence-producing center is the silicon vacancy (SiV) which were shown to be stable in as small as 1.6 nm ND (Vlasov et al. 2014).

Production of ND is commercially achieved by three main approaches; detonation, high pressure-high temperature (HPHT), and chemical vapor deposition methods. Detonation of carbon explosives produces around 4-5 nm ND and is a relatively low-cost production method (Shenderova et al. 2002). These small ND are well suited for biomedical applications but they require extensive purification due to the impurities in and on their crystals (Kaur and Badea 2013; Shenderova et al. 2011). The chemical vapor deposition method is of major interest to produce ND films suitable for implant coatings due to their outstanding mechanical and wear-resistant properties (Gracio et al. 2010; Kaur and Badea 2013). The HPHT-ND are produced in large scale with a primary particle size >20 nm and are preferred for imaging and tracking applications due to their intrinsic fluorescence (Shenderova and McGuire 2015).

### 1.3 Biomedical applications of Nanodiamonds

Among all carbon-based nanomaterial, ND stand out as the most biocompatible material and are increasingly being proposed as diagnostic, imaging, and therapeutic agents in biomedicine (Schrand, Huang et al. 2007; Kaur and Badea 2013; Perevedentseva, Lin et al. 2013; Lim et al. 2016; Vijayanthimala et al. 2015). Their stable fluorescence makes it possible to track ND both *in vitro* and *in vivo* (Fang et al. 2011; Yu et al. 2005; Fu et al. 2007; Schirhagl et al. 2014; Hemelaar et al. 2017). In addition to their fluorescence potential, ND can easily be conjugated with fluorophores to enhance their fluorescence. ND can also be conjugated with biomolecules to serve as a nano-carrier of drugs and biomolecules. However, unlike the other carbon-based nanomaterials, susceptibility of ND to biodegradation is still unknown (Bhattacharya et al. 2016).

#### 1.3.1 Imaging and tracking applications

The HPHT-ND are preferred for imaging applications due to the ability to incorporate hundreds of parts per million of NV centers producing high fluorescence (Mochalin et al. 2011). Fu et al. (2007) studied the fluorescence of 100 nm ND and found that they can function as a tracking agent for biomolecules and intracellular interactions (Fu et al. 2007). Carboxylated ND were used for tracking cell division and differentiation and were found to be equally divided between the two daughter cells without affecting gene or protein expression (Liu et al. 2009). In another study, ND were used to image interactions of transferrin with its receptor on HeLa cells (Weng et al. 2009). This study also showed that conjugation of ND with transferrin did not affect the fluorescence of ND or the binding of transferrin to its receptor (Weng et al. 2009).

Several *in vivo* studies also investigated the usefulness of ND as imaging or tracking agents. Haziza and co-workers (2017) used fluorescent ND to measure changes in intraneuronal transport induced in the brain of two transgenic mouse models that mimic the slight changes in protein concentrations found in the brain of brain-disease patients such as autism and Alzheimer's disease (Haziza et al. 2017). Another group tracked the intradermally, intraperitoneally, and subcutaneously administered fluorescent ND in mice and rats and reported that these particles are non-toxic and suitable for long term *in vivo* imaging (Vaijayanthimala et al. 2012). Studies of the use of fluorescent ND for imaging were also tested by other groups in cultured cells, *Caenorhabditis elegans* (*C. elegans*), and mice and reported good imaging contrast even in the presence of background fluorescence (Mohan et al. 2010; Igarashi et al. 2012).

### **1.3.2 Nanodiamonds as a drug delivery carrier**

The requirements for drug delivery systems including biocompatibility, ease of attachment to different drugs or molecules, and dispersability, are all met by ND. In addition, ND allow the combination of drug delivery with imaging for assessment of delivery efficacy. The high loading capacity of ND is due to its large surface area; thus, it provides higher concentrations of these loads to be delivered. Li et al. (2010) reported that an anticancer drug conjugated with ND had a higher efficacy as compared to the drug alone (Li et al. 2010). Fluorescent ND were coated with a polymer shell and conjugated with cyclic RGD peptide and were shown to selectively target glioblastoma cells with high internalization efficacy (Slegerova et al. 2015). Protein functionalized-ND were used to deliver bone morphogenetic proteins to osteoblast progenitor cells to



promote bone formation (Moore et al. 2013). This study showed that the delivery system enhanced bone cell proliferation and differentiation. A short peptide-functionalized ND (DGEA-ND) and loaded with doxorubicin (DOX) was shown to successfully target bone metastatic prostate cancer cells *in vitro* which are known to over express  $\alpha 2\beta 1$  integrins during metastasis, and caused much higher cell death with higher specificity as compared to DOX alone, even at lower drug doses (Salaam et al. 2014). PEGylated ND loaded with DOX were shown to deliver the drug into human liver cancer cells *in vitro* with enhanced DOX uptake and a slow and sustained release of the drug (Wang D et al. 2013). DOX-ND complex was also tested in mouse models of liver cancer and mammary cancer and revealed an enhanced cancer inhibition establishing a very promising foundation for ND-based drug delivery systems (Figure 1.5) (Chow et al. 2011). These studies and many others, confirmed that the use of ND as a drug delivery vehicle enhances drug efficacy, allows sustained release of the drug, reduces side effects, and decreases toxicity and high drug doses.

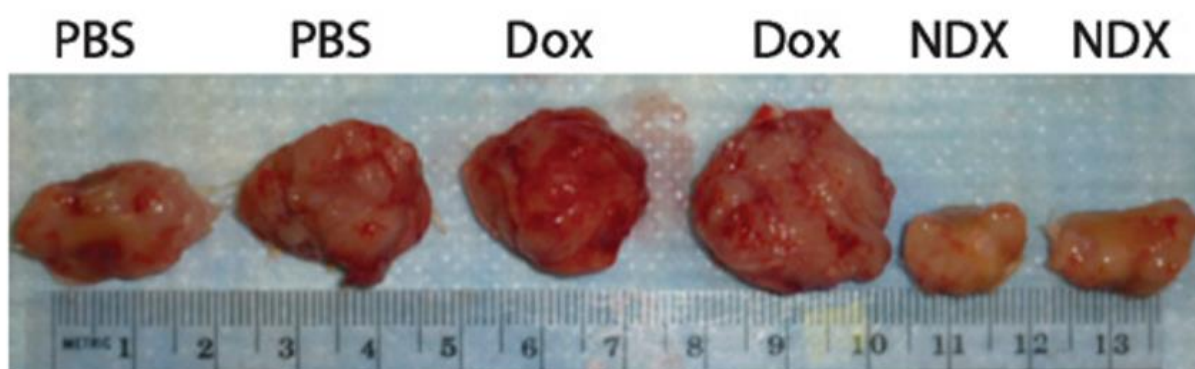


**Figure 1.5:** ND-DOX complex inhibits tumor growth. Mammary carcinoma mouse model was injected by tail with PBS, DOX, or NDX (ND-DOX complex). Excised tumors from treated mice showed that ND-DOX complex treatment efficacy is much higher than the other treatments. From (Chow et al. 2011. Nanodiamond therapeutic delivery agents mediate enhanced chemoresistant tumor treatment. *Science translational medicine*. 3(73):73ra21). Reprinted with permission from AAAS.

### 1.3.3 Tissue engineering and surgical implants

Restoration of damaged tissues is a core aim in the field of tissue engineering and regenerative medicine. In this field, ND can deliver growth factors to enhance cell proliferation (Moore et al. 2013), provide mechanical support for cells to grow on, and can be used as coatings of implantable medical devices. The superior features of ND such as chemical stability and hardness, presented ND as a preferred candidate for surgical implant coatings. Diamond-like carbon coatings were shown to enhance wear resistance and reduce the release of metal ions from orthopedic and dental implants (Gutensohn et

al. 2000; Roy and Lee 2007; Catledge et al. 2013). In a recent wear simulation study, two diamond surfaces (Convex and concave) produced by chemical vapor deposition of ND and after 5 million cycles of rotations of the diamond-on-diamond, showed that the ND surfaces remained intact and uniform thereby protecting the underlying metal (Baker et al. 2016). This study verify that ND deposition improves the longevity of joint replacement devices as compared to existing devices. Another study suggested the addition of ND to Mg-based biodegradable implants to reduce corrosion rate of the implant (Gong et al. 2015). Authors reported high cell viability and healthy cell morphology of cells grown in contact of Mg-ND composite. Investigation on the effect of various surface features of ND on osteoblast adhesion and proliferation reported that these features can be controlled to support or inhibit bone growth in different regions of an orthopedic implant (Yang et al. 2009).

In addition to implants coatings, Zhang and co-workers (2011) produced a poly L-lactic acid (PLLA)-ND composite bone scaffold material for bone tissue engineering (Zhang et al. 2011). In their work, the PLLA-ND composite provided improved mechanical property, bright fluorescent to monitor bone re-growth, and options to load drugs. They also suggested the use of this composite as a surgical tool such as fixation devices (Zhang et al. 2011). A recent study on ND-based scaffolds showed that functionalized ND improve characteristics of bone implants and vascularization within bone substituents (Wu et al. 2017). Another study investigated the potential of cellulose-nanodiamond composites for bone tissue regeneration and showed that this composite can serve as a biointerface promoting cell adhesion, proliferation, and differentiation of bone cells (Vega-Figueroa et al. 2017).

All the above-mentioned studies, and many others, showed the advantages of using ND in several biomedical applications (Zhu et al. 2012; Turcheniuk and Mochalin 2017). However, introduction of ND into the body allows these particles to interact with other tissues and organs and hence, may affect or interfere with normal biological processes. The system that is responsible for discrimination between self/nonself and perform sequential reactions to eliminate any hazard is the immune system. Any foreign particle or pathogen enter the body is expected to encounter components of this system.

#### **1.4 The vertebrate immune system**

The functions of the immune system are essential for the body's homeostasis, survival and health. Immune cells are generated from pluripotent hematopoietic stem cells (HSCs). These cells can self-renew and differentiate into the common lymphoid progenitor or the common myeloid progenitor (Figure 1.6). The common lymphoid progenitor cells further differentiate into the different lymphocytes; B lymphocytes (B cells), T cells, natural killer cells (NK), and the NK-T cells (Chaplin 2010). The common myeloid progenitor cells go through successive differentiation steps to generate megakaryocytes (which produces thrombocytes, platelets), erythrocytes (red blood cells), mast cells, granulocytes (neutrophils, basophils, and eosinophil), and monocytes (which can differentiate into macrophages or dendritic cells). After differentiation in the bone marrow, these cells are released to the blood and other tissues to perform their specialized functions.

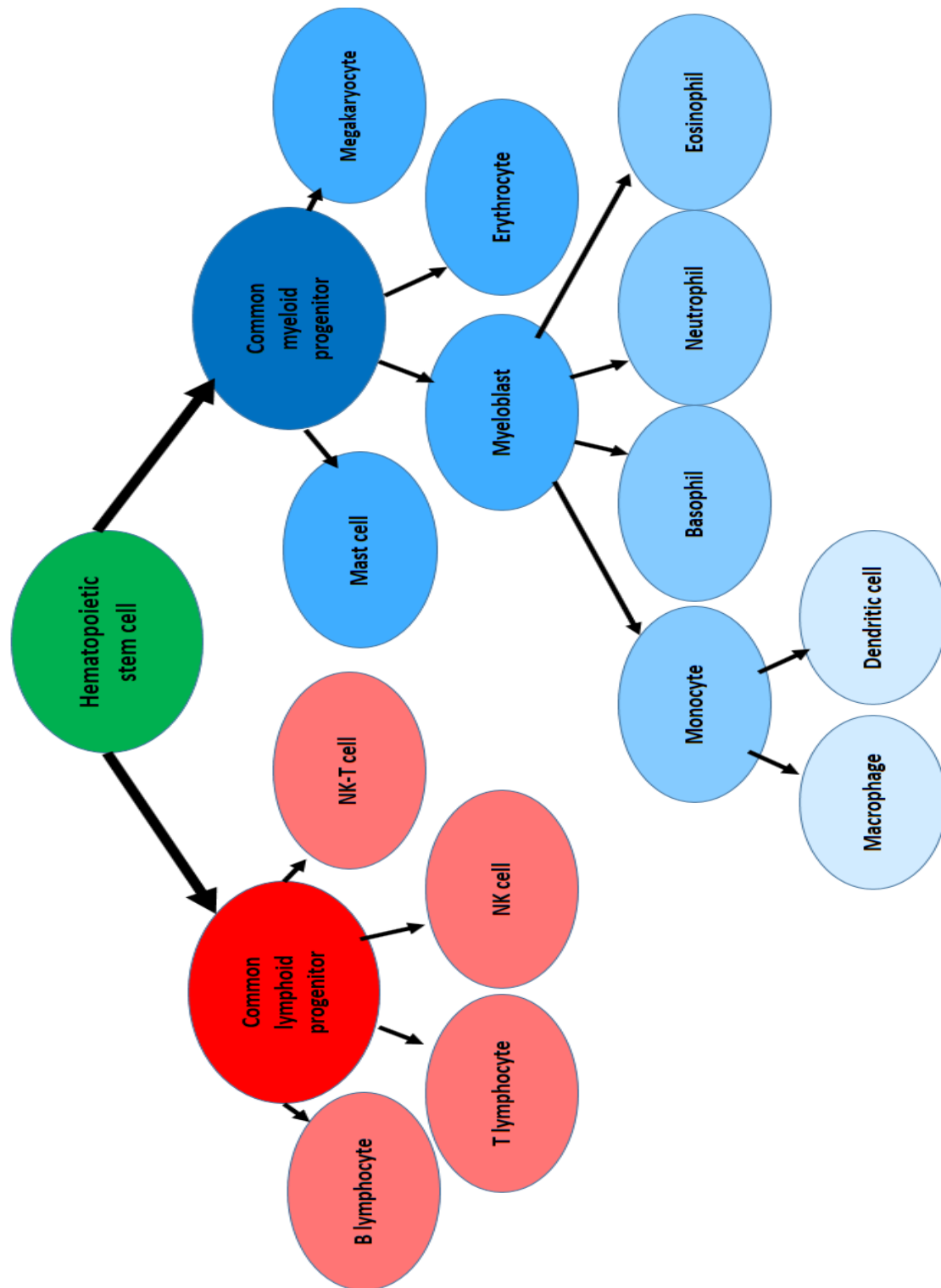


**Figure 1.6:** Differentiation of hematopoietic stem cells into the different types of blood cells.

The immune system is composed of two arms, innate and adaptive immunity, which coordinate together to provide protection against invading pathogens, cancer cells, toxins, and clearance of dead cells and self-proteins, as well as for tissue remodeling and wound healing. The innate immunity initiates the immune response and activates the adaptive immune component to control any invading threat. Innate immunity is the non-specific, early response (within hours) while the adaptive immunity can take days to develop the highly specific responses (late response). Thus, the innate immune cells can keep the infection in check if not being able to eliminate it, until the more specialized adaptive responses are activated.

#### **1.4.1 Antigen presentation**

The first signals for the initiation of an immune response are produced mainly by the cells that are usually present at the barriers interacting with the outer, or inner, environment. Professional antigen-presenting cells (APC) are macrophages, dendritic cells, and B cells but other cell types can also participate in antigen presentation during infection (Murphy 2011). These cells can recognize, engulf, process, and present antigens on their surfaces for T cells (Figure 1.7). Each of these steps is highly regulated and requires participation of many APC's components at different levels in the immune response.

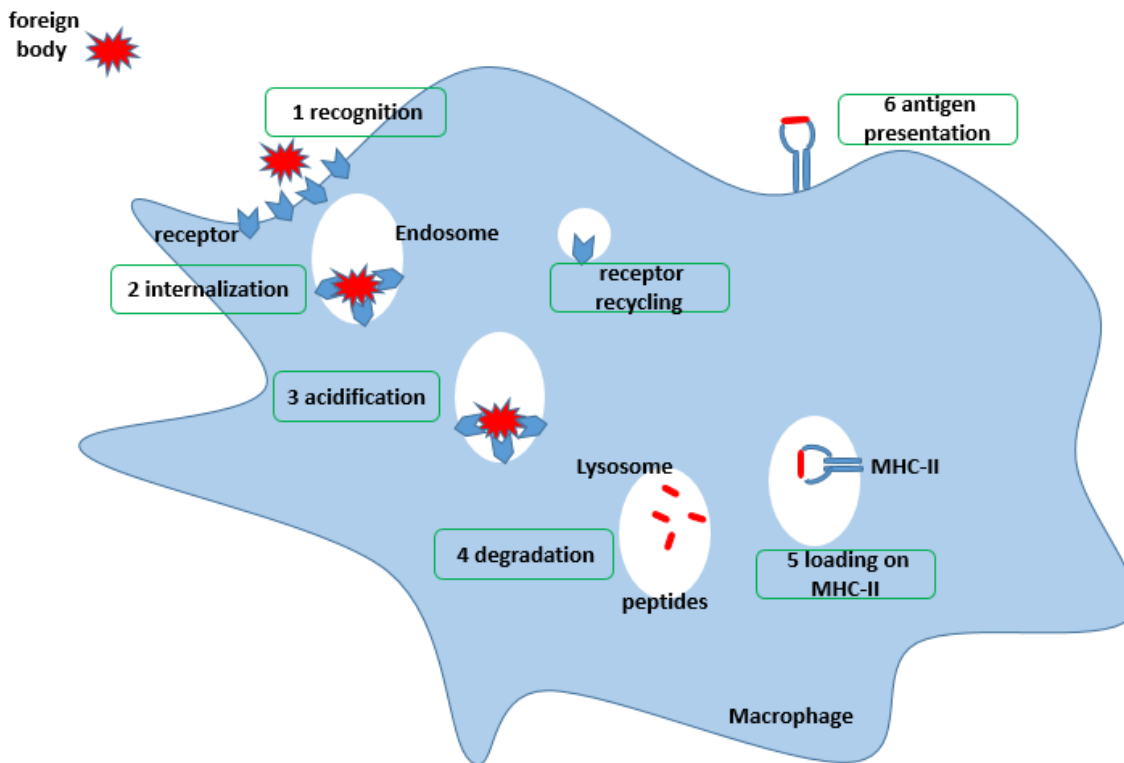


**Figure 1.7:** Antigen presentation by macrophages. Starts with recognition (1) where surface receptors recognize then bind to the pathogen or other components followed by internalization (2). The internalized endosome starts acidification (3) by decreasing the pH and fusing with or becoming lysosomes. The proteolytic enzymes along with reactive species help degrade (4) the pathogen into small peptides. These small peptides are then loaded onto the MHC-II molecules (5) and directed to the cell surface where they can be presented (6) and recognized by T cell's receptors.

Antigen recognition involves interactions between innate immune cell pattern recognition receptors (PRR) and the foreign substances known as pathogen-associated molecular patterns (PAMPs), or with the damage-associated molecular patterns (DAMPs). The PRR are localized on the cell membrane to detect extracellular patterns, also in the endosomal/lysosomal membrane to detect patterns in the endocytosed materials, and in the cytosol recognizing the intracellular pathogens and their components. They can also be secreted to the extracellular environment to detect extracellular pathogens. These receptors provide an initial discrimination between self and nonself (Murphy 2011).

Toll-like receptors (TLRs) are membrane-bound receptors (expressed on the cell surface membrane or in the endosomal membrane), that recognize different pathogenic patterns such as lipoproteins, lipopolysaccharides (LPS), and nucleic acids. Other membrane-bound PRRs such as C-type lectin receptors (CLRs), recognize other pathogenic components such as mannose, fucose, and glucans that are present on many pathogens. The cytosolic PRRs such as nucleotide oligomerization (NOD)-like receptors (NLRs), recognize peptidoglycans and are involved in regulation of inflammation. Certain stimuli can induce oligomerization of NLRs into a caspase 1-activating scaffold called inflammasome (Guo et al. 2015).

After recognition, these cells can internalize the pathogen (if it is still in the extracellular matrix), start the degradation process, and carry out presentation and initiation of signaling pathway cascades that are essential for host defense. Internalization of pathogens can happen in a specific or non-specific manner depending on the type (and size) of the internalized component (Malhotra et al. 2011). Endocytic pathways include



several diverse mechanisms by which different cells use to internalize nutrients, growth factors, hormones, antibodies, antigens, or extracellular particles and fluids (Figure 1.8). These pathways are essential for the cell to survive and to respond to the external signals.

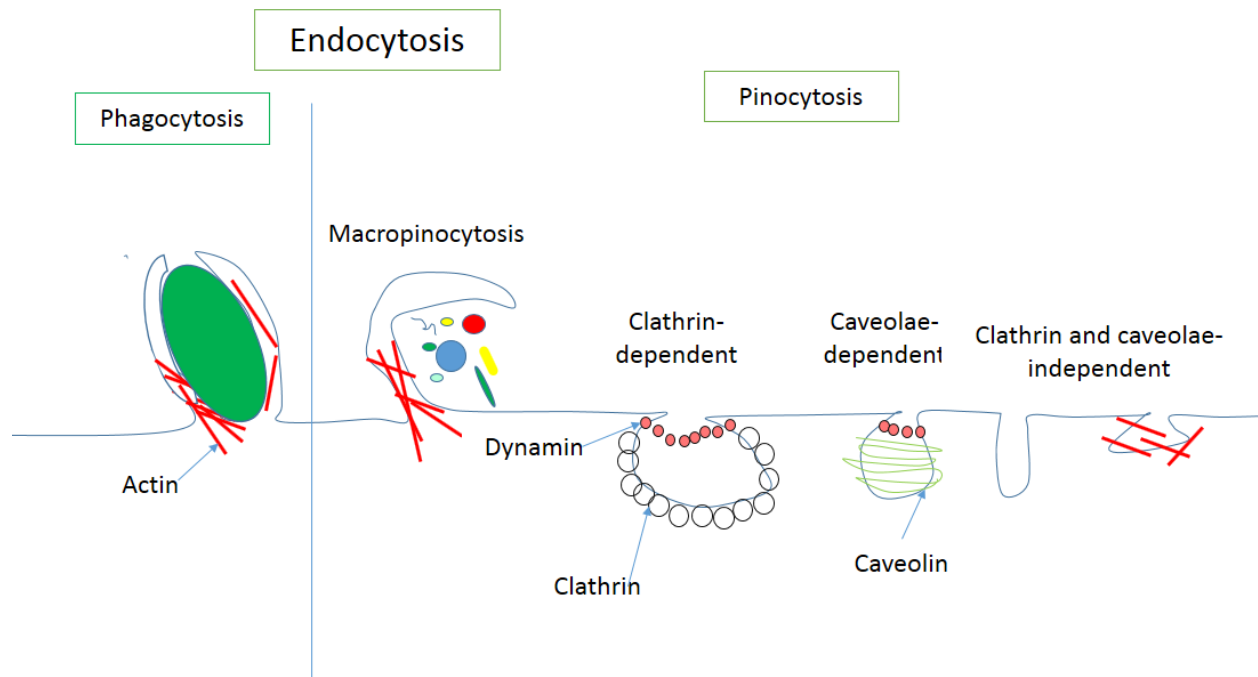


**Figure 1.8:** Endocytic pathways include phagocytosis and pinocytosis. There are different classifications for the endocytic pathways based on size of the cargo or vesicle or based on the dependence of the pathway on specific proteins. (Modified from Mayor and Pagano 2007; Murphy 2011).

Phagocytosis is a process by which professional phagocytic cells such as monocytes/macrophages, engulf large (>200 nm and up to 10  $\mu\text{m}$ ) pathogens and

particles or remnants of dead cells (Conner and Schmid 2003; Malhotra et al. 2011). This process is highly regulated, it involves recognition by cell-surface receptors such as the Fc receptor that recognizes the antigen-coated pathogens leading to the activation of the cell's inflammatory response. Phagocytosis is a crucial process not only for immune response, but also for clearing damaged tissues and during development without activation of inflammatory responses (Conner and Schmid 2003).

Unlike phagocytosis which is primarily associated with phagocytes, the other endocytic pathways (collectively called pinocytosis) occur in all immune or non-immune cell types. Pinocytosis, also known as fluid-phase endocytosis, includes macropinocytosis, clathrin-mediated, caveolae-mediated, and clathrin-and-caveolae-independent endocytosis. These endocytic pathways engulf smaller particles (50-200 nm) along with extracellular fluids and are referred to as “cell drinking” while phagocytosis which internalize larger particles (like a whole bacterium or a dead cell) is called “cell eating” (Malhotra et al. 2011). Phagocytosis and macropinocytosis (in addition to some other clathrin-and-caveolae-independent pinocytosis) are actin-dependent pathways that require rearrangement of cytoskeletal actin filaments to form the membrane extensions/invaginations (Mayor and Pagano 2007). The other pinocytosis mechanisms have smaller vesicle sizes where the plasma membrane invaginates to form a bud coated or un-coated with specialized proteins.

After internalization, the fate of internalized vesicle and its content depends on the endocytic pathway used. In the case of internalized pathogens or their components, these vesicles fuse with organelles in the endocytic pathway which contain proteolytic enzymes and a very low pH (high acidity). The early endosome starts to acidify by pumping more

H<sup>+</sup> ions to their lumen to become late endosomes and then, lysosomes. In APCs, the degraded content usually contains many antigens that are loaded on the major histocompatibility complex class II (MHC-II) and displayed on the cell surface. T cell receptors (TCR) can only recognize the antigen bounded by MHC-II but not the free antigens, which is a crucial process for T cells activation. Also, TCR are highly specific for the antigens they bind to, unlike the less specific receptors on innate immune cells surfaces.

### **1.4.2 Macrophages**

In addition to their role in antigen presentation (Figure 1.7), macrophages play crucial roles: in development; initiation of the immune response and its regulation; ingestion and killing of microbes; in the clearance of dead cells and cell debris; and in the repair of damaged tissues by promoting angiogenesis and fibrosis (Abbas 2015). Macrophages are found in almost all tissues of the body and they represent the first line of defense in innate immunity. Different subsets of macrophages are tissue-resident macrophages (Table 1.1), such as alveolar (dust cells) macrophages in the lung, Kupffer cells in the liver, microglia in the central nervous system, sinusoidal cells in the spleen, and Langerhans cells of the skin (Davies and Taylor 2015; Davies et al. 2013; Abbas 2015). Each type of tissue-resident macrophages has distinct features and roles and respond differently to extracellular signals due to the tissue-specific environment and epigenetic effects (Davies and Taylor 2015).

**Table 1.1:** Tissue-resident macrophages. Reprinted, with modification, by permission from Macmillan Publishers Ltd: [Nature Immunology] (Davies et al. 2013), copyright (2013).

<b>Tissue</b>	<b>Cell type</b>	<b>Function</b>
Lung	Alveolar cells	Immune surveillance and homeostatic regulation of tissue function
Liver	Kupffer	Clearance of microorganisms, aged erythrocytes, and cell debris from the blood
Central nervous system	Microglia	Involved in frontline immune surveillance, removal of dead neurons and synaptic remodeling.
Spleen	Sinusoidal cells	Erythrocyte clearance and iron metabolism
Skin	Langerhans	Interaction with T lymphocytes

Monocytes migrate from the blood to tissues and differentiate into macrophages which are activated in response to a wide range of pathogens and host mediators. Activated macrophages usually migrate from the site of infection to the draining lymph nodes where they participate in antigen presentation (Bellingan et al. 1996). Macrophages are dynamic because they can respond to and acquire different activation states depending on the stimulus, tissue distribution, and their parent monocytes (Benoit et al. 2008). One of the main hallmarks of macrophages is their remarkable plasticity and

ability to differentiate into different populations/phenotypes. In fact, it was suggested that the number of different macrophages populations may be as diverse as the number of the distinct stimuli that activated them (Mosser and Zhang 2008).

There are different ways to classify macrophages populations but in general, they are classified broadly into M1 and M2 (classically activated and alternatively activated, respectively) macrophages to mimic the Th1 and Th2 classification of T cells. Classically activated macrophages are stimulated by microbial components such as LPS, or by products of activated T cells such as interferon gamma (IFN  $\gamma$ ), to become more efficient at killing microbes and secrete many pro-inflammatory cytokines and chemokines (Figure 1.9). On the other hand, alternative activation is stimulated by other types of stimuli such as interleukin (IL) 4 and IL 13 to promote tissue repair and remodeling and secrete anti-inflammatory cytokines and chemokines. More recent studies explored the heterogeneity of the M2 macrophages and sub-classified them into M2a, M2b, M2c, and M2d to cover a range of stimuli that induces the anti-inflammatory effects (Roszer 2015).

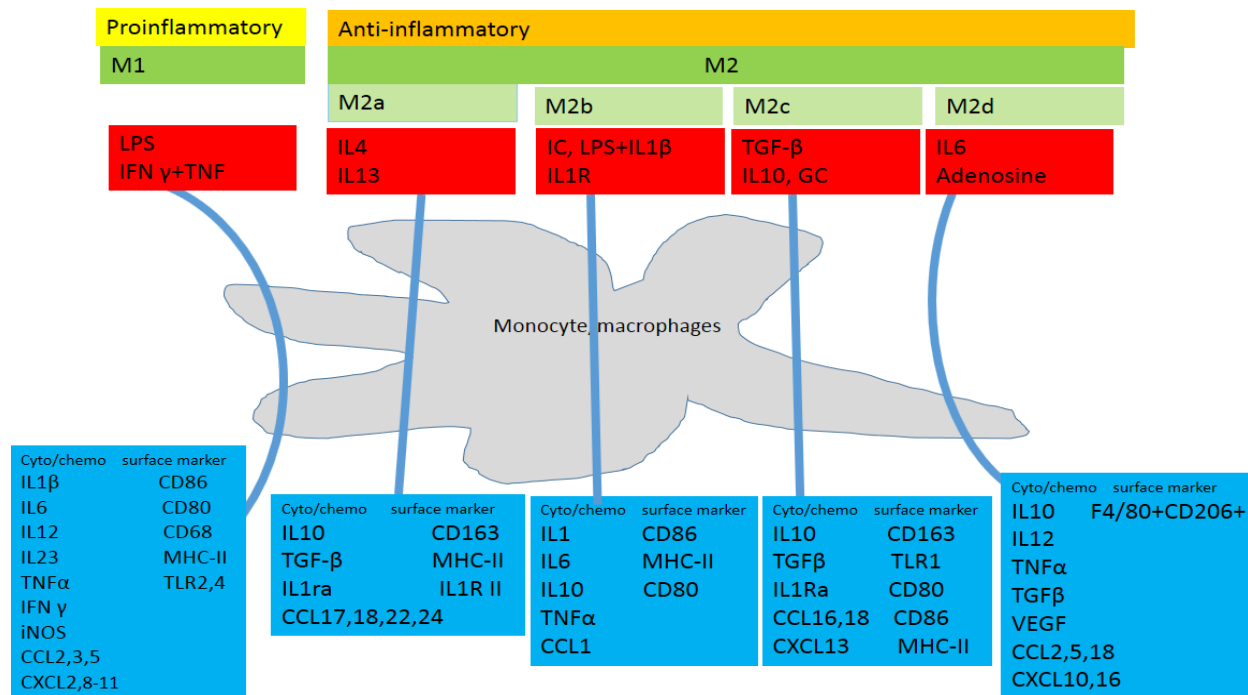


**Figure 1.9:** Activation of macrophages. M1 macrophages produce pro-inflammatory cytokines and chemokines to induce inflammation and recruitment of other immune cells. M2 macrophages produce anti-inflammatory cytokines and chemokines to inhibit inflammation, assess in healing, tissue repair and remodeling processes. The M2 macrophages are sub-classified into M2a, M2b, M2c, and M2d based on the stimulation signals and production of cytokines, chemokines, and surface markers. Abbreviations, LPS: lipopolysaccharides, IFN: interferon, TNF: tumor necrosis factor, IL: interleukin, iNOS: inducible nitric oxide synthase, CCL: C-C motif ligand, CXCL: C-X-C motif ligand, CD, cluster of differentiation, MHC: major histocompatibility complex, TLR: Toll-like receptor, TGF: transforming growth factor, IC: immune complexes, GC: glucocorticoids, VEGF: vascular-endothelial growth factor. (Summarized from Gordon 2003; Benoit et al. 2008; Roszer 2015; Colin 2014; Ferrante and Leibovich 2012; Martinez and Gordon 2014; Wang et al. 2010; da Silva and Gordon 1999; Duluc et al. 2007).

## 1.5 Immune response to nanoparticles

Nanoparticles are foreign materials to the body and hence, they might be recognized by immune cells, initiate an immune response, modulate functions of immune cells, or deplete them. Immunotoxicity is any negative effect on the immune cells' viability, proliferation, differentiation, or function. Immunotoxicity can be induced by exposure to nanoparticles leading to detrimental effects on the immune system and the whole body (Wang X et al. 2013). Over stimulation of the immune function can lead to allergies and autoimmune diseases, and suppression of the immune function can lead to increased incidence and severity of infectious diseases (Ghoneum et al. 2014; Wang X et al. 2013; Mitchell et al. 2009). Therefore, the immune system is highly regulated at all levels and modulation of its function can affect the health and survival of all other systems in the body.

Innate immune cells represent the fast, nonspecific, first responders to any foreign substance or organism and had been studied extensively in immunotoxicity studies of nanoparticles. Exposure of innate immune cells to titanium dioxide or silicon dioxide nanoparticles induced the formation of the inflammasome, production of the pro-inflammatory cytokine IL1- $\beta$ , and activation of caspase-1 (Yazdi et al. 2010). Similar effects were reported, in addition to the increased production of reactive oxygen species (ROS) upon exposure of innate immune cells to silver nanoparticles (Yang et al. 2012). Nanometer-sized titanium dioxide particles were also reported to induce production of cytokines and expression of costimulatory molecules on dendritic cells and subsequently led to the activation of the adaptive immunity by priming the activation and proliferation of naïve CD4<sup>+</sup> T cells (Schanen et al. 2009). Carbon nanotubes were reported to activate

components of the complement system, which is part of the innate immunity, via classical and alternative activation pathways (Salvador-Morales et al. 2006). These and many other studies, showed that exposure of innate immune cells to nanoparticles can induce an inflammatory response and activate the adaptive immunity.

Suppression of immune function has also been reported. Dutta et al. (2007) found a reduction in LPS-mediated response from mouse macrophages after exposure to carbon nanotubes (Dutta et al. 2007). In addition, Mitchell et al. (2009) reported a suppressed systemic immune function in response to inhaled carbon nanotubes (Mitchell et al. 2009). The effects of ND on immune cells may go in either direction, suppression or over stimulation, and thus need to be further evaluated.

Safety/toxicity of a nanomaterial cannot be drawn from that of the bulk material. The small size of these materials allows them to enter cells and/or bring in toxic elements, interact directly with cells and biomolecules, or interfere with biological processes. Several studies showed that internalization and toxicity of nanomaterials are size-dependent (Carlson et al. 2008; Manolova et al. 2008; Kunzmann et al. 2011; Tsai et al. 2012). In addition to size, the shape may also affect phagocytosis of the nanomaterial and production of cytokines. Carbon nanotubes were found to cause frustrated phagocytosis and the release of pro-inflammatory cytokines and ROS in macrophages (Brown et al. 2007; Murphy et al. 2012). Charge and surface chemistries can be modulated during or after synthesis of the nanomaterial and by interactions with proteins and ions before they encounter cells which affect their toxicity (Choi et al. 2010; Kong et al. 2015).



### 1.5.1 Toxicity studies on ND

In addition to their unique physical and chemical properties, NDs are described as a highly biocompatible material (Yu et al. 2005; Liu et al. 2007; Schrand, Dai et al. 2007; Schrand, Huang et al. 2007; Liu B et al. 2016). Yu and colleagues (2005) showed that the 100 nm-sized ND did not affect metabolic activity in human kidney cells significantly (Yu et al. 2005). Schrand et al. (2007) investigated the toxicity of ND of sizes 2-10 nm and showed that ND are nontoxic to a variety of cell types with no significant ROS production (Schrand, Huang et al. 2007). Similar *in vitro* studies with different cell types reported the minimal toxicity of ND as compared to other carbon-based nanoparticles (Schrand, Dai et al. 2007; Liu et al. 2007). A ND-based probe for nitric oxide detection showed low toxicity and favorable biocompatibility in human adenocarcinoma cell line (Liu B et al. 2016).

In addition to the *in vitro* studies, several *in vivo* studies also investigated the toxicity of ND. Mohan et al. (2010) tested the ND toxicity by feeding or microinjecting of ND in *C. elegans* and reported that ND were nontoxic and did not cause any detectable stress to the worm (Mohan et al. 2010). Interactions of ND with blood and blood components did not affect oxygenation state of red blood cells and did not induced an immune response (Tsai et al 2016). Other studies of ND for *in vivo* imaging applications in mice and rats demonstrated the good biocompatibility of ND administered via various routes (Vaijayanthimala et al. 2012; Igarashi et al. 2012).

However, the controversy about biocompatibility of ND persists. Dworak et al. (2014) reported that ND of a size <10 nm were cytotoxic; inhibited proliferation, and induced apoptosis in lymphocytes at concentrations of  $\geq 50$   $\mu\text{g/ml}$  (Dworak et al. 2014). In

their work, DNA oxidative damage and changes in chromatin stability were observed even at very low ND concentrations (Dworak et al. 2014). Another study also reported a decrease in cell proliferation after treatment with ND (6-100 nm) at lower concentrations (50 µg/ml) and a reduction in cell proliferation and metabolic activity at higher concentrations (200 µg/ml) (Thomas et al. 2012). The study also showed that ND with variable sizes induced a reduction in cell viability but did not promote inflammation (Thomas et al. 2012). A recent *in vivo* study showed toxic effects of ND in zebrafish embryos model, increasing mortality rate in early stages and changes in morphological features of the developing embryos (Lin et al. 2016). The potential impacts of ND on the immune system are still not fully understood and further studies are needed to evaluate their potential immunotoxicity.

## CHAPTER 2

### SPECIFIC AIMS

Nanodiamonds (ND) are being tested for a wide range of biomedical applications. Although they are described as a non-toxic, biocompatible material, the controversy about their immunotoxicity persists. I hypothesized that ND may induce an immune response in macrophages, and can affect or interfere with their differentiation and normal functions such as endocytosis and initiation of an immune response to conventional threats. I aimed to investigate the effects of ND on murine macrophage-like cell line in addition to primary cells isolated from mouse bone marrow and differentiated into macrophages.

**Aim 1:** Investigate the initial interactions between mouse macrophages and ND.

1. Examining of ND uptake by mouse macrophages using the fluorescence microscopy. Two mouse macrophage types treated or untreated with ND and mounted under fluorescence microscope to detect ND internalization and changes in cells morphology.
2. Define the subcellular localization of ND in cells using confocal microscopy.
3. Quantitate ND uptake using flow cytometer for cells treated with different concentrations and at different time points.
4. Determine the uptake pathways of ND using endocytic pathways inhibitors.
5. Assess cell viability of cells treated with varying doses of ND and for varying treatment intervals directly after ND treatment and on day one, two, and three after treatment using the MTS assay.

6. Assess the percent of apoptotic cells after ND treatment.

**Aim 2:** Determine the effects of ND on gene expression in macrophages.

1. Use real time-quantitative polymerase chain reaction (RT-qPCR) to assess response of these cells to ND. I chose the immune markers, IL1 $\beta$ , IL4, IL6, IL10, IL12, TNF $\alpha$ , CXCL2, and CCL2, to assess the pro- and anti-inflammatory cell response to ND.
2. Confirm the RT-qPCR results using Enzyme-Linked Immunosorbent Assay (ELISA) to detect changes in IL1 $\beta$ , IL6, IL10, IL12, CCL2, and TNF $\alpha$  protein production.

**Aim 3:** Determine the effects of ND on macrophage function and differentiation.

1. Challenge the ND-treated and untreated cells with LPS to compare LPS-mediated responses in macrophages using RT-qPCR.
2. Assess the endocytic activity of ND-treated cells. Expose the ND-treated and untreated cells to fluorescently-labeled dextran particles to compare their ability to internalize the dextran particles using flow cytometer.
3. Determine the effects of ND on differentiating bone marrow cells. Treat the isolated bone marrow cells with ND before they differentiate into macrophages, then assess the cell morphology and expression of macrophage surface markers (CD11b and F4/80).

## CHAPTER 3

### MATERIALS AND METHODS

#### 3.1 Nanodiamonds and cell culture

Carboxylated, HPHT ND (COOH-ND), with average size of 100 nm, containing >900 NV/particle, and excitation/emission of 532/700 nm, were purchased (Adámas Nanotechnologies, Inc. Raleigh, NC), and were used as received without any further modifications. The ND were sonicated for 10-15 minutes in water bath sonicator before each use and suspended in complete growth media at concentrations 1-100 µg/ml.

Murine monocytes/macrophage cell line, J774A.1, originally isolated from ascites of an adult female BALB/cN mouse with reticulum cell sarcoma (American Type Culture Collection, Manassas, VA), were maintained in Dulbecco's Modified Eagle's Medium (DMEM, Lonza, USA) supplemented with 10% heat-inactivated fetal bovine serum (FBS, Gibco USA), 100 units/ml penicillin and 100 µg/ml streptomycin (Gibco) at 37°C in a 5% CO<sub>2</sub> humidified incubator.

Bone marrow derived macrophages (BMDMs) were isolated and differentiated directly or frozen as previously described with some modifications (Weischenfeldt and Porse 2008; Marim et al. 2010). Briefly, C57BL/6, CD-1, DBA/2J, or BALB/cJ, mice 1-4 months old, were euthanized in CO<sub>2</sub> chamber. Bone marrow cells of femurs and tibias were flushed with phosphate buffer saline (PBS), passed through a 40 µm cell strainer (Celltreat), centrifuged at 200 g for 5 minutes, and re-suspended in freezing media; 90%

FBS and 10% DMSO. One milliliter of the cell suspension was added into each cryotube and left in the -80 freezer for 24 hours before transferring into liquid nitrogen tank for later use. Mice femurs and tibias were obtained through tissue sharing from IACUC approved protocols (14-003, 14-007, 15-027, 16-016).

To prepare the BMDM, fresh or frozen bone marrow cells were re-suspended in differentiation media; RPMI 1640 (Mediatech Manassas, VA) supplemented with 20% FBS, 100 units/ml penicillin, 100 µg/ml streptomycin and 10 ng/ml macrophage-colony stimulating factor (M-CSF, Biolegend, San Diego, CA). Cells incubated at 37°C in a 5% CO<sub>2</sub> humidified incubator were fully differentiated after day 7 and were harvested by scraping or detachment with 5 mM EDTA/PBS, counted and plated with cultivation media (same constituent as differentiation media except for 10% FBS).

The primary mouse bone marrow cells usually acquire the macrophage phenotype within 7 to 10 days after isolation under M-CSF induction (Wang C et al. 2013; Weischenfeldt and Porse 2008). To confirm the BMDM phenotype, antibodies to macrophage surface markers, CD11b and F4/80 (AbD Serotec®) were used. After differentiation, cells were harvested and re-suspended in flow buffer (1% bovine serum albumin, BSA, in PBS) with blocking antibody (CD 16/32) for 10 minutes. One microliter of each FITC-CD11b and PE-F4/80 were added and incubated in the dark at room temperature. After 30 minutes, cells were washed and re-suspended in 300 µl flow buffer for Fluorescence-activated cell sorting (FACS) analysis (BD FACSAria™ cell sorter BD Biosciences San Jose, CA).

### 3.2 Cell viability assays

Cell viability was assessed using the MTS viability assay (CellTiter 96® AQueous Non-Radioactive Cell Proliferation Assay, Promega). The MTS assay is a colorimetric method to determine the number of viable cells based on their ability to reduce the tetrazolium compound into a soluble formazan product. The absorbance measured at 490 nm is proportional to the number of viable cells. To determine the optimum seeding density for macrophages, cells were plated at varying densities and a standard curve was generated. Cells were plated at  $2-3 \times 10^4$  cells per well of a 96-well plate. After 24 hours, cells were incubated with different concentrations of ND and for different time intervals. The MTS reagent was added directly or after 1, 2, or 3 days after ND treatment. After 2-4 hours, supernatants were transferred into new wells and the absorbance at 490 nm was measured using a plate reader (SpectraMax i3, Molecular devices). The cell viability was obtained by normalizing the absorbance of the ND-treated cells against the control, untreated cells, and expressed as percentage.

The apoptosis assay kit was used to assess the percent of cells at the early apoptosis phase after ND treatment (CellEvent™ Caspase- 3/7 Green Flow Cytometry Assay Kit, Thermo Fisher). This kit consists of a green detection reagent which defines apoptotic cells based on the ability of activated caspase 3 and caspase 7 to cleave this reagent to emit a bright green fluorescence. Cells were plated at  $10^5$  cells/well in 6-well plates. After 24 hours, the cells were treated for another 24 hours with 10, 50, or 100  $\mu\text{g/ml}$  ND, with the untreated cells as a negative control, and 10  $\mu\text{M}$  staurosporine (Sigma) or a 100  $\text{ng/ml}$  LPS (Xaus et al. 2000) as positive controls. Harvested cells were suspended in flow buffer and the kit was used per the user manual except that the dead

cell stain (SYTOX<sup>TM</sup> AADvanced<sup>TM</sup>), the second component of this kit, was not used due to the interference from ND.

### **3.3 ND uptake and subcellular localization**

To study the ND uptake with the microscope, J774A.1 and BMDM were plated on coverslips. After 24 hours, cells were treated with 50 µg/ml ND for another 24 hours, stained with DAPI, and examined with fluorescent microscopy (Olympus BX51) at 535-50 nm excitation and 610-75 nm emission, and with confocal microscopy to determine their subcellular localization (Leica TCS SP8, Leica Microsystems).

To quantitate ND uptake, cells were harvested and plated at 10<sup>5</sup> cell/well in 6-well plates. After 24 hours, cells were treated with different concentrations of ND and for different time points. Each sample was harvested, centrifuged for 5 minutes at 1000 RPM, and re-suspended in flow buffer before FACS analysis.

The uptake pathways were investigated through the application of endocytic pathways inhibitors (Sigma). Each inhibitor was prepared and applied separately for 30 minutes at 37°C, prior to the treatment of cells with ND. The fluorescence signals from cells pre-treated or untreated with each inhibitor were measured using FACS. The inhibitors that were used are summarized in table 3.1.



**Table 3.1:** Endocytic pathway inhibitors.

<b>Inhibitor</b>	<b>Pathway</b>	<b>Reference</b>	<b>Concentration</b>
Chlorpromazine hydrochloride	Clathrin-dependent endocytosis	Wang et al. 1993; Shamsul et al. 2010	20 µg/ml
Phenylarsine oxide	Clathrin and receptor-mediated endocytosis	Gibson et al. 1989; Cai et al. 2015	0.5 µg/ml
Methyl-beta-cyclodextrin	Caveolae and clathrin-dependent endocytosis	Rodal et al. 1999; Li et al. 2014	10 mM
Nystatin	Caveolae/lipid raft dependent endocytosis	Payne et al. 2007; Shamsul et al. 2010	40 µg/ml
5-(N-Ethyl-N-isopropyl) amiloride; EIPA	Macropinocytosis	West et al. 1989; Gerondopoulos et al. 2010	66 µM
Cytochalasin D	Actin-dependent endocytosis	Sampath and Pollard 1991	6 µM

### 3.4 Gene expression

To assess the ability of ND to induce an inflammatory response in macrophages, cells were plated at  $1-2 \times 10^5$  cell per well of a 12-well plate and incubated at 37°C, 5% CO<sub>2</sub> for 24 hours. Fresh media were added and the ND were sonicated for 15 minutes

before addition. Cells were incubated for 4 hours with or without 50 µg/ml ND before total RNA isolation.

LPS is a bacterial endotoxin localized in the outer layer of the membrane of gram-negative bacteria, and is known to induce a strong inflammatory response in human and animals. To investigate the ability of ND-treated cells to respond to LPS stimulation, cells were plated as above and treated with or without ND (50 µg/ml for 4 hours), then with or without 10 ng/ml LPS (Sigma) for 3 hours.

RNA extraction from ND or LPS-treated and untreated samples was performed in the plates using ISOLATE II RNA Mini Kit (Bioline USA) per the manufacturer instructions. Complimentary DNA (cDNA) was synthesized using SensiFAST™ cDNA synthesis kit (Bioline USA). Quality and quantity of RNA and cDNA were assessed with NanoVue (GE Healthcare). The cDNA was amplified using SensiFAST SYBR® Hi-ROX kit (Bioline USA) in a Bio Rad CFX Connect Real-Time PCR Detection System (BioRad, USA). Primers (IDT®) sequences were from previously published work (references and sequences are summarized in table 3.2). To confirm primers specificities and find expected amplicons sizes, each primer pair was checked with in silico PCR (<https://genome.ucsc.edu/cgi-bin/hgPcr>), and the resulted sequence were aligned to the target gene in blast nucleotide ([https://blast.ncbi.nlm.nih.gov/Blast.cgi?PROGRAM=blastn&PAGE\\_TYPE=BlastSearch&LINK\\_LOC=blasthome](https://blast.ncbi.nlm.nih.gov/Blast.cgi?PROGRAM=blastn&PAGE_TYPE=BlastSearch&LINK_LOC=blasthome)).

**Table 3.2.** RT-qPCR primers.

Gene	Forward primer	Reverse primer	Reference
GAPDH	TAT GTC GTG GAG TCT ACT GGT	GAG TTG TCA TAT TTC TCG T	Osterholzer et al. 2011; Davis et al. 2013
Actin	TGG AAT CCT GTG GCA TCC ATG AAA C	TAA AAC GCA GCT CAG TAA CAG TCC G	Osterholzer et al. 2011
IL1- $\beta$	CAA CCA ACA AGT GAT ATT CTC CAT G	GAT CCA CAC TCT CCA GCT GCA	Martinon et al 2010
IL 6	GAG GAT ACC ACT CCC AAC AGA CC	AAG TGC ATC ATC GTT GTT CAT ACA	Martinon et al 2010
TNF $\alpha$	CCT GTA GCC CAC GTC GTA GC	AGC AAT GAC TCC AAA GTA GAC C	Osterholzer et al. 2011
CCL2	CCC ACT CAC CTG CTG CTA CT	TCT GGA CCC ATT CCT TCT TG	Santoro et al. 2015
CXCL2	CCA CTC TCA AGG GCG GTC AAA	TAC GAT CCA GGC TTC CCG GGT	Thomas et al. 2012
iNOS	TTT GCT TCC ATG CTA ATG CGA AAG	GCT CTG TTG AGG TCT AAA GGC TCC G	Osterholzer et al. 2011
IL4	AAC GAG GTC ACA GGA GAA GG	TCT GCA GCT CCA TGA GAA CA	Liu T et al. 2016
IL10	ATA ACT GCA CCC ACT TCC CA	GGG CAT CAC TTC TAC CAG GT	Liu T et al. 2016
IL12	GAT GAC ATG GTG AAG ACG GC	AGG CAC AGG GTC ATC ATC AA	Liu T et al. 2016

The PCR reaction volumes were 20  $\mu$ l/sample and the program was 2 minutes at 95°C, then 40 cycles of 5 seconds at 95°C and 30 seconds at 60°C and the PCR products were assessed with the melt curves. Gene expression data were normalized to two housekeeping genes; Glyceraldehyde-3-phosphate dehydrogenase (GAPDH) and  $\beta$  actin, and the fold change was determined using the  $\Delta\Delta$ CT method. Briefly, the  $\Delta$ ct value is obtained by normalizing the threshold cycle (ct) value of the target gene with that of the housekeeping genes which are known to have stable expression under a wide range of treatments, to compensate for differences in the amount of loaded DNA or RNA. The fold change in the gene expression is obtained by calculating the difference between the  $\Delta$ ct of the treated sample and that of the control sample and raising the  $\Delta\Delta$ ct value to the base 2 ( $2^{-\Delta\Delta$ ct) because the PCR assumes an exponential increase in the number of copies of the original mRNA for each gene after each cycle.

To assess the amount of secreted proteins after ND treatment, macrophages were plated at  $10^6$  cell/ml in 6-well plates. After 24 hours, ND (50  $\mu$ g/ml) or LPS (10 ng/ml) were added with fresh media and incubated for another 24 hours. Cell culture supernatant was collected, centrifuged at 1500 RPM for 10 minutes at 4 °C, and stored at -80 until analyzed with ELISAs. Protein concentrations of IL1 $\beta$ , IL6, TNF $\alpha$ , CCL2, IL10, and IL12 were measured using a sandwich ELISA-based flow kit (LEGENDplex™ mouse inflammation panel, Biolegend®, San Diego, CA) according to the manufacturer instructions.

### **3.5 Effects of ND on macrophages endocytic activity**

BMDM were plated at  $10^5$  cells/well in a 6-well plate and after 24 hours, cells were treated with 0, 10, 20, or 50  $\mu$ g/ml ND. After 16 hours, cells were incubated with cascade

blue-labeled dextran particles (3000MW Invitrogen, Eugene OR) for 45 minutes, washed and re-suspended in flow buffer for FACS analysis.

### **3.6 Differentiation of BMDM**

Bone marrow cells were isolated from femurs and tibias as above and differentiated into BMDM in differentiation media with or without 50 µg/ml ND for 7 days. The mature cells were investigated for changes in surface markers expression (CD11b and F4/80) and changes in shape or morphology.

### **3.7 Statistical analysis**

Results are presented as the mean values  $\pm$  standard error of the mean (SEM) of at least three independent experiments. Test for significant was performed using one way ANOVA for multiple comparison followed by Dunnet's test. P value < 0.05 was considered statistically significant. Statistical calculations were performed using IBM SPSS version 24. Statistical significant was assessed with student's T test when comparing one treatment with one control.

## CHAPTER 4

### RESULTS

#### 4.1 Phenotypic characterization of BMDM

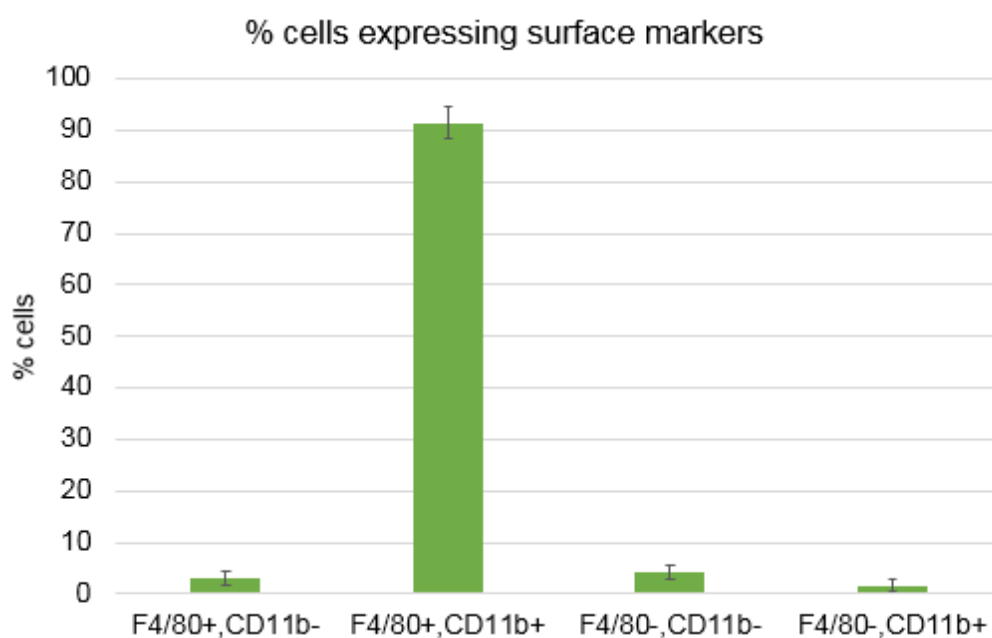


**Figure 4.1:** Phenotypic characterization of BMDM. Flow cytometry analysis showing the expression of macrophages surface markers. More than %90 of cells expressed the two markers; CD11b and F4/80 on their surfaces. Results are the average from four independent experiments  $\pm$  SEM.

Bone marrow cells were isolated from mice femurs and tibias and differentiated into BMDM for seven days under M-CSF induction. After day seven, cells were fully differentiated into macrophages and their phenotype was confirmed using antibodies against macrophage surface markers, CD11b and F4/80. The percent of cells expressing each or both surface markers were analyzed using FACS and are shown in Figure 4.1. More than 90% of cells expressed the two markers together on their surfaces which confirms the macrophage phenotype.

#### **4.2 Interactions of ND with macrophages**

Macrophages are professional phagocytes and thus, they engulf a wide range of foreign particles in addition to self, dead or infected cells or molecules. I found that upon exposure of macrophages to ND, these cells internalize the ND spontaneously. Microscopic images of J774A.1 and BMDM incubated with ND showed the uptake of ND by these cells (Figure 4.2). ND appear as dark spots in the bright field images with a red fluorescence in the TRITC channel. Images showed that the shape of the cell did not change dramatically due to ND treatment. ND-treated cells appeared to be larger in the microscopic images but on contrary, forward scatter (FSC) measurements in FACS analysis showed that the ND-treated cells size decreased in a time-and dose-dependent manner (Figure 4.3).

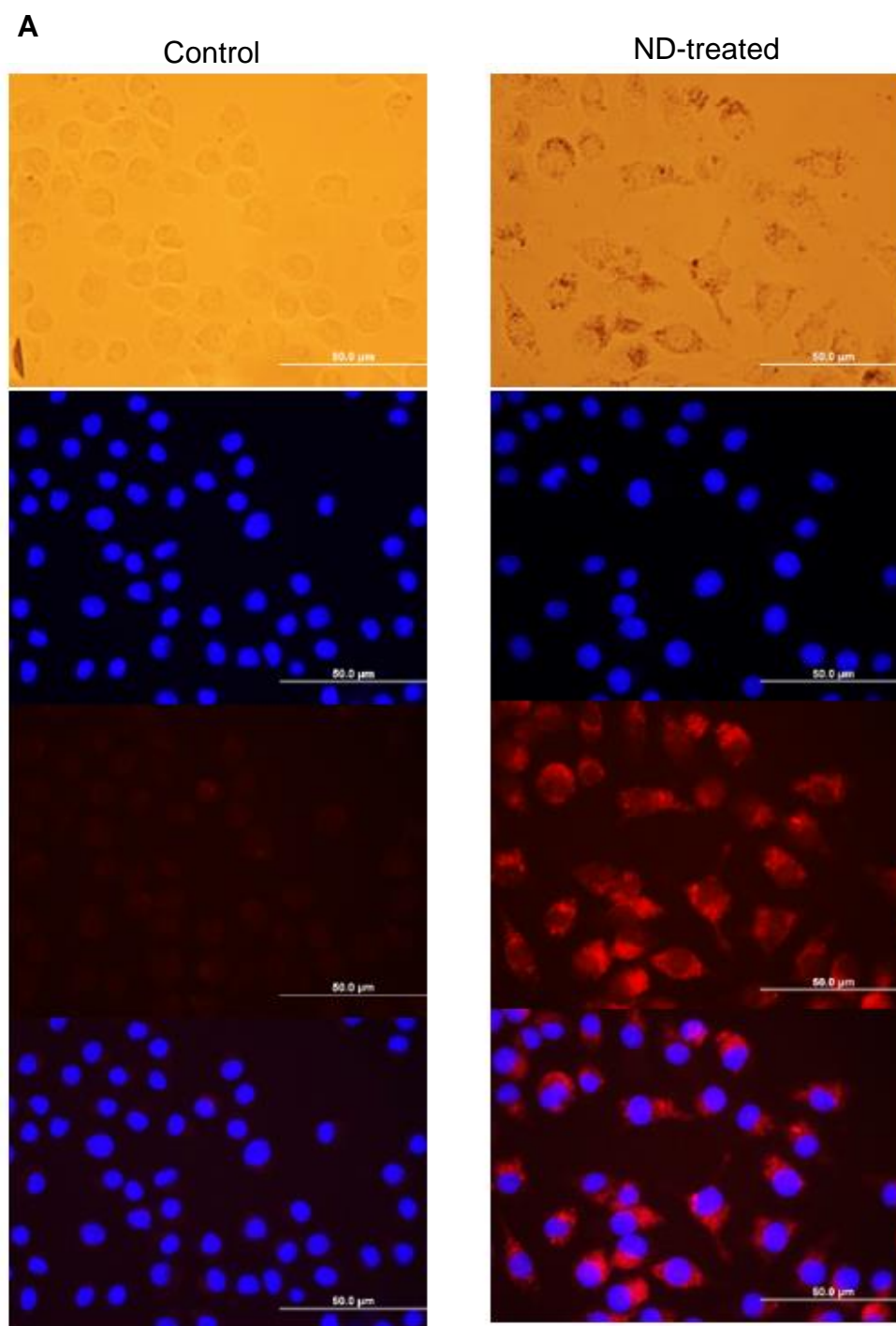


**Figure 4.2:** Fluorescent microscope images. J774A.1 (**A**) and BMDM (**B**) control and ND-treated (50  $\mu$ g/ml ND for 24 hours) images from top to bottom are bright field, DAPI, TRITC, and merged images.



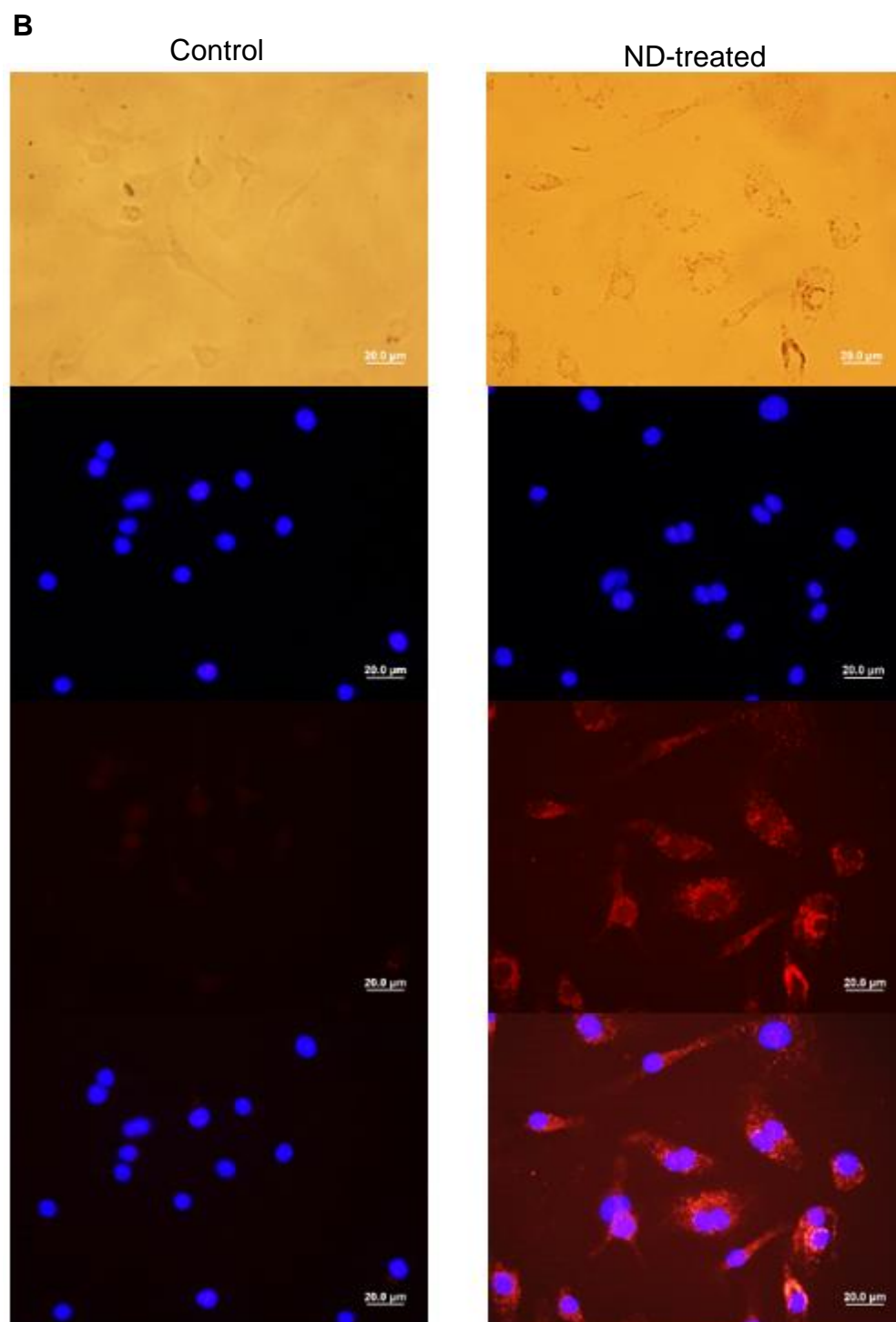


**Figure 4.2:** Continued.

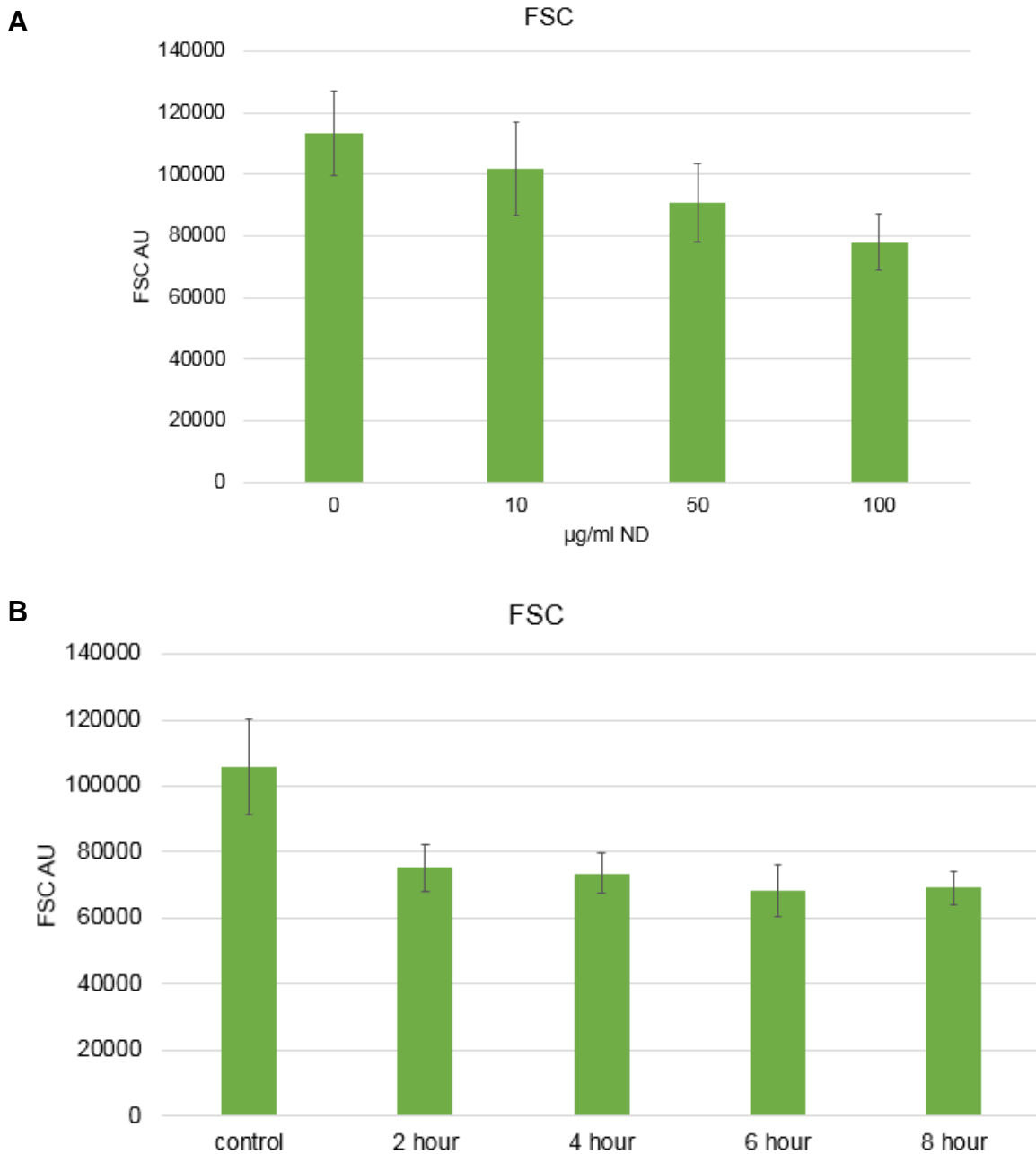


**Figure 4.3:** ND-treated cells decrease in size. BMDM were treated with 0, 10, 50, or 100  $\mu\text{g/ml}$  ND for 24 hours (**A**) or with 50  $\mu\text{g/ml}$  ND for 0, 2, 4, 6, or 8 hours (**B**). The size of ND-treated cells (Forward scatter, FSC parameter in arbitrary units, AU) was assessed using FACS. The decrease was dose- and time-dependent. Results represent the average of at least 3 independent experiments  $\pm$ SEM.

Other morphological features of ND-treated cells such as the cellular granularity, was also affected after ND treatment (Figure 4.4 A and B). Cells treated with different concentrations of ND and for different time intervals, showed an increase in granularity as measured with the side scatter (SSC) in flow analysis. The increase in granularity was dose- and time-dependent.

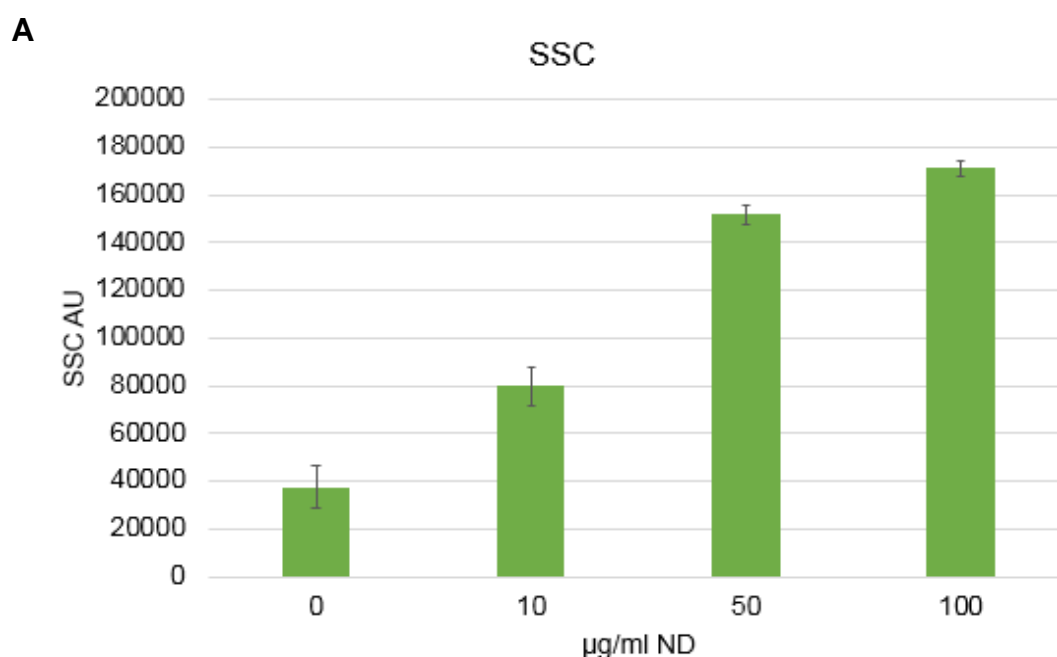


**Figure 4.4:** Granularity of ND-treated cells. BMDM were treated with 0, 10, 50, or 100 µg/ml ND for 24 hours (**A**) or with 50 µg/ml ND for 0, 2, 4, 6, or 8 hours (**B**). Cell granularity (SSC parameter) was assessed using FACS and the results shows a dose- and time-dependent increase in cell's granularity. Results represent the average of at least 3 independent experiments  $\pm$ SEM.

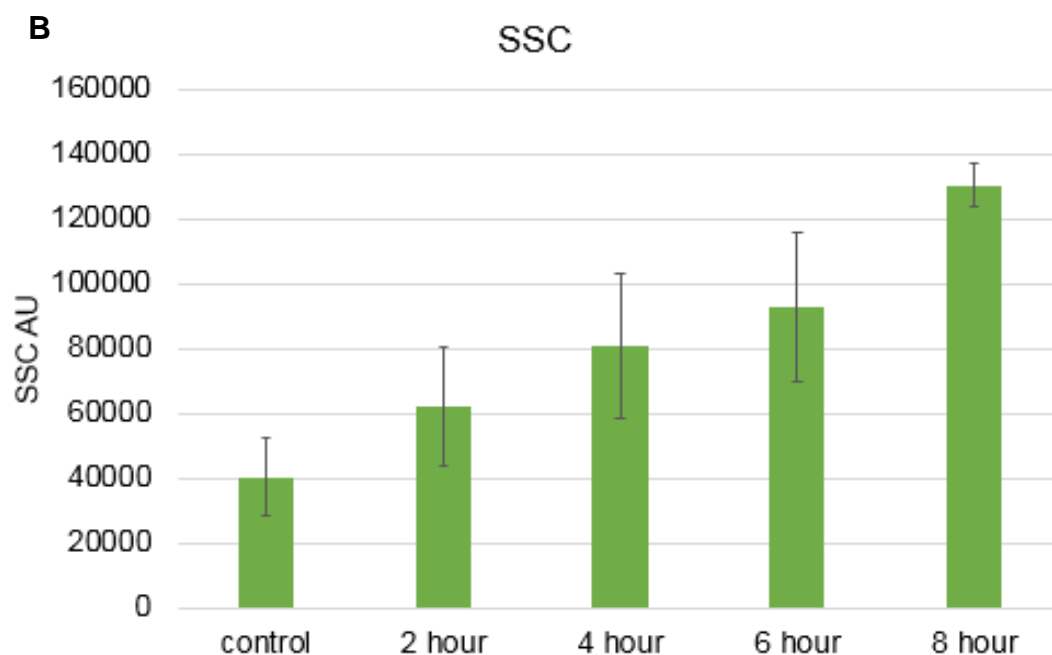


**Figure 4.4:** Continued.

Representative graphs showing changes in FSC and SSC of ND-treated or untreated cells are shown in Figure 4.5. Both FSC and SSC of cells changed after ND treatment but in opposite directions, the FSC decreased and the SSC increased with increasing ND doses.

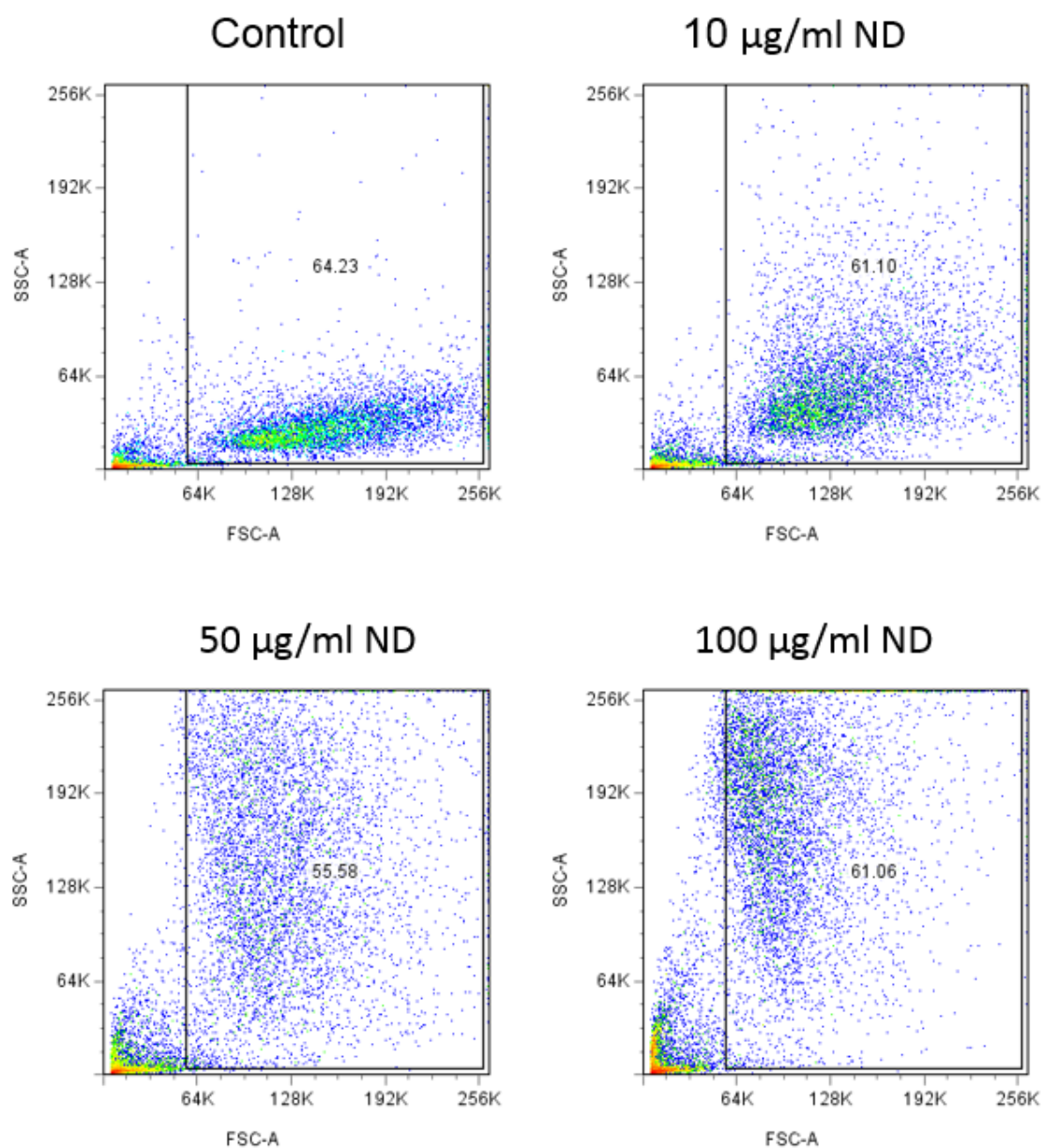


**Figure 4.5:** Effects of ND treatment on FSC and SSC parameters. Representative graphs of FACS analysis for cells treated with different concentrations of ND showed the increase in SSC (cell granularity) and decrease in FSC (cell size) with increasing ND concentration.

To define the sub-cellular localization of ND in macrophages, BMDM were incubated with ND (50  $\mu\text{g/ml}$ ) for 24 hours and the nuclei were stained with DAPI (Figure 4.6). The confocal microscope images showed that the ND entered the cell and localized to the cytoplasm but did not enter to the nucleus.

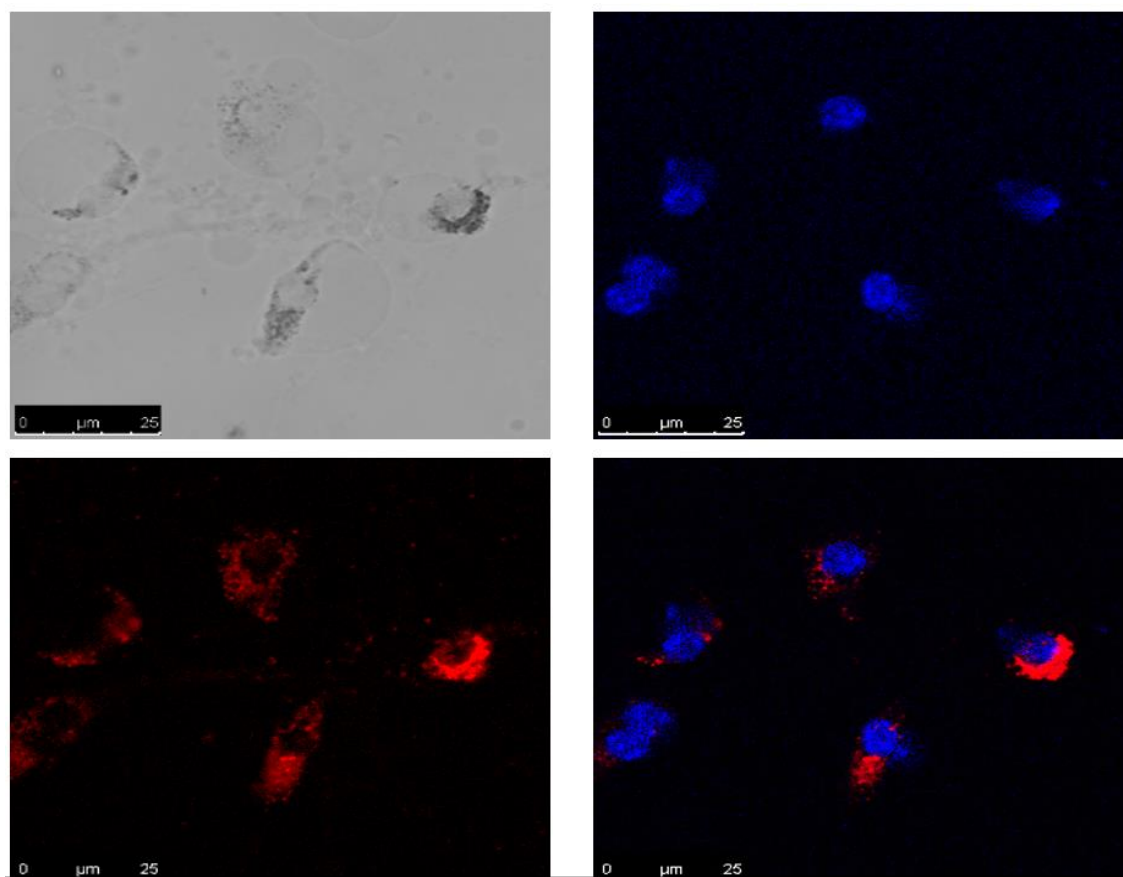


**Figure 4.6:** Confocal microscope images. BMDM treated with ND were imaged with confocal microscope to determine ND sub-cellular localization. DAPI staining was used to stain the nucleus. Image of bright field (top left), DAPI (top right), TRITC (bottom left), and merged (bottom right). ND entered to the cytoplasm but not into the nucleus.

### 4.3 Cell viability

The MTT and MTS assays measure the metabolic activity of cells indicating the number of metabolically active, i.e. live cells, through their ability to reduce tetrazolium compounds into formazan. One important difference between the two assays is that the MTT assay produce insoluble formazan that accumulates inside cells and requires cell lysis to be released into the media before measuring the absorbance while the MTS produces a soluble formazan that is released directly into the media without the need for cell lysis. I started with the MTT assay but suspected that the ND might be contributing to the absorbance. Therefore, I measured the absorbance of ND-treated cells at different wavelengths before performing the assay (Figure 4.7). These wavelengths are used for the MTT assay (570 and 690 nm) and for the MTS assay (490 nm). The result show that the absorbance increased with increasing ND concentrations and hence, they can give false increase in cells activity.

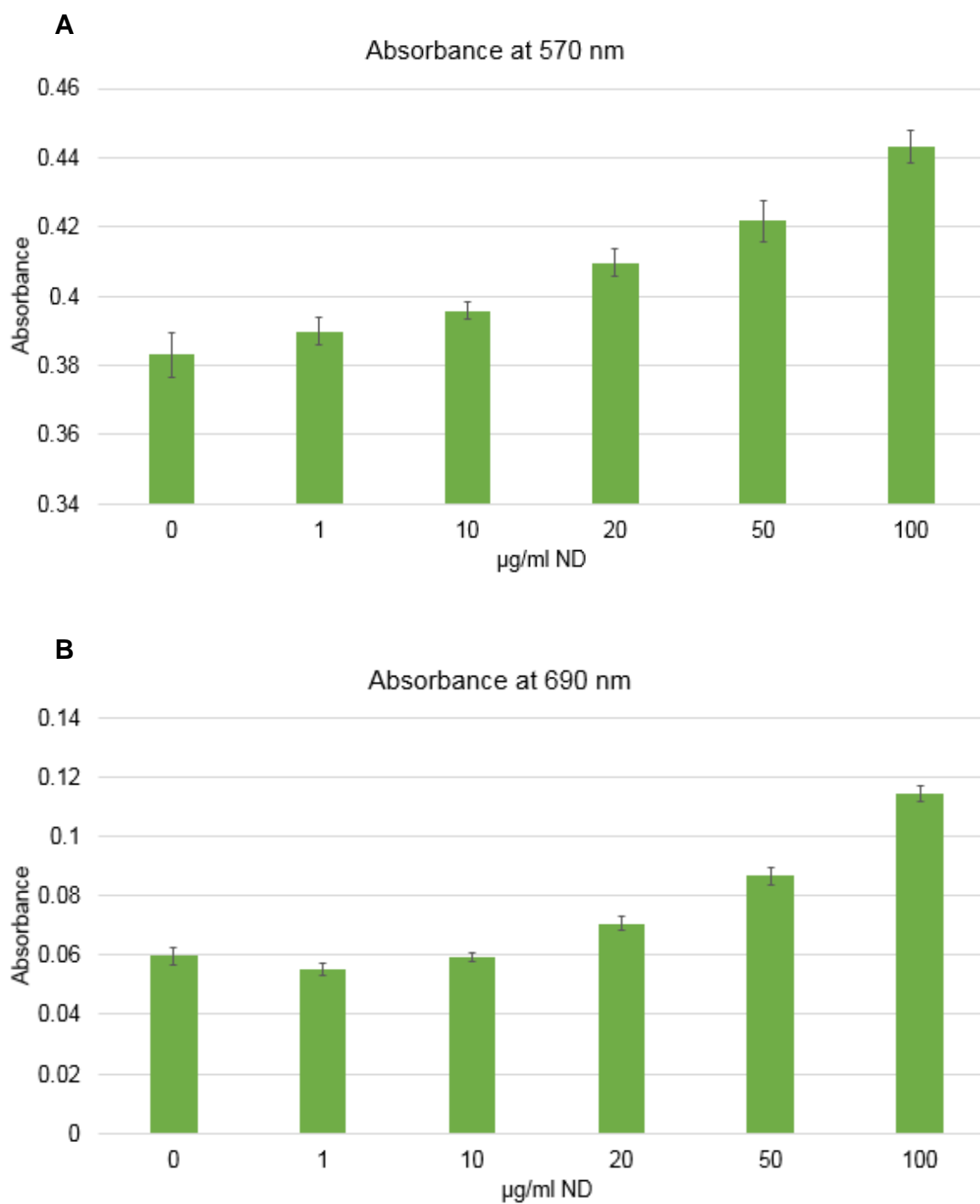


**Figure 4.7:** Absorbance of ND-treated cells at different wavelengths. J774A.1 cells were treated with 0, 1, 10, 20, 50, or 100 µg/ml ND and the absorbance was measured at 570 (A), 690 (B), and 490 (C) nm.



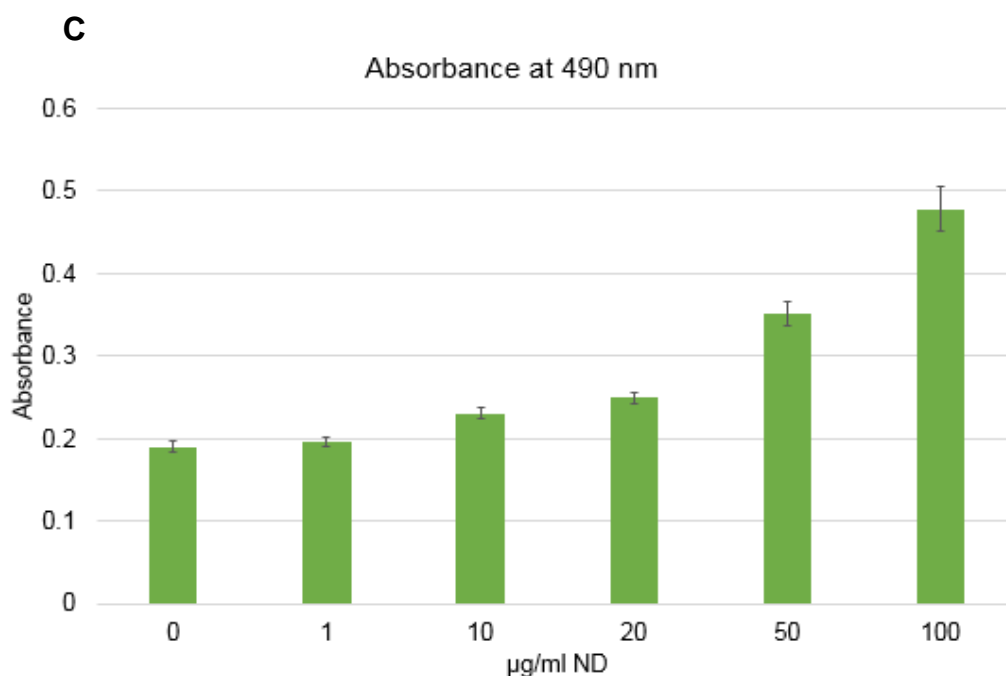


**Figure 4.7:** Continued.

I switched to the MTS assay because this assay does not require lysing of cells so that the media containing the released formazan can be transferred into new wells (without cells) before measuring the absorbance to avoid ND interference. To confirm that transfer of the supernatant did not affect the validity of MTS absorbance readings, I performed an MTS assay using a different cell type (4T1 cells), and the absorbance was read before and after transferring supernatant into new wells (Figure 4.8). Results showed that the absorbance of the formazan-containing cell culture media is lower after transferring into new wells but that did not affect the overall proportion with cell density.

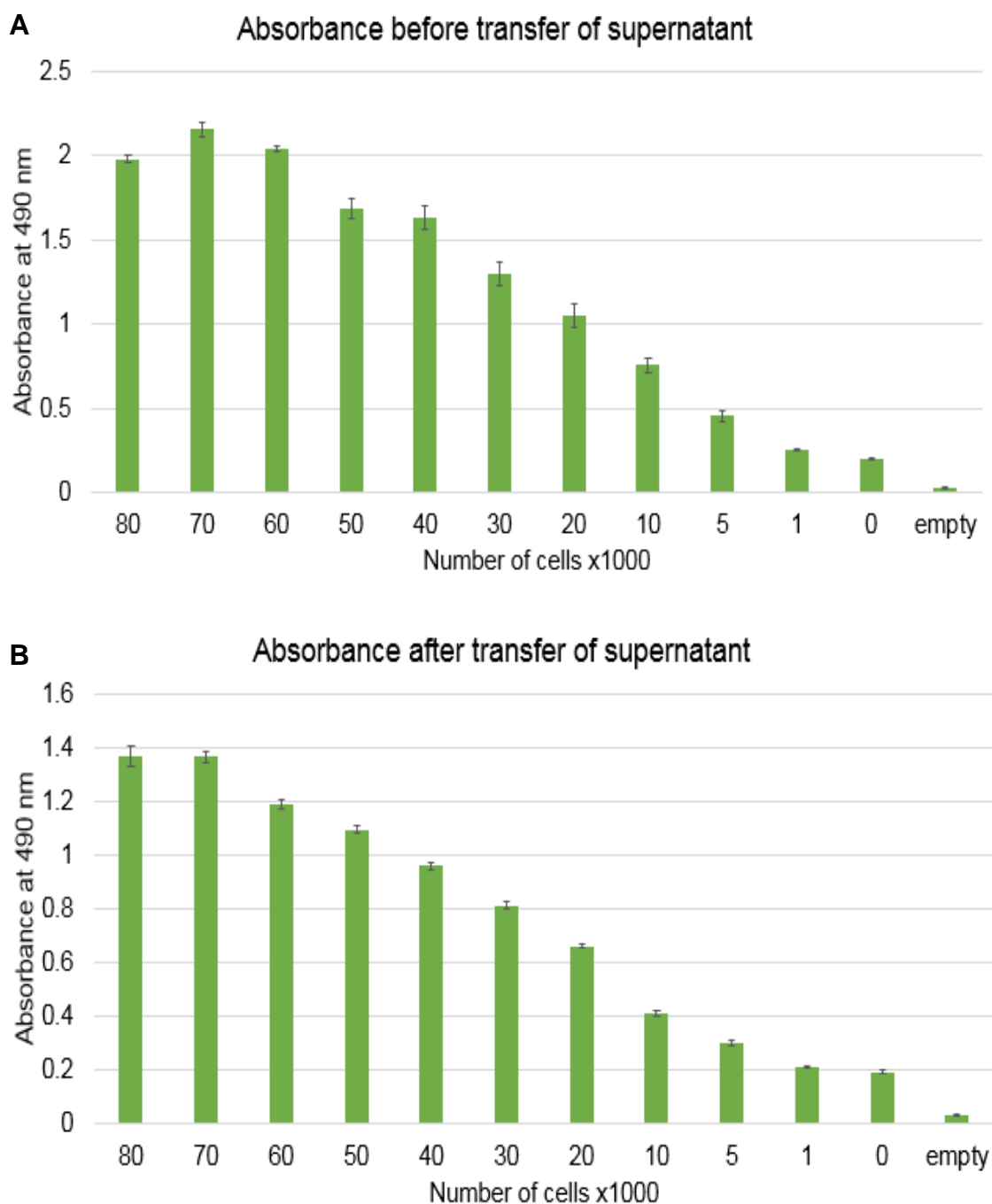


**Figure 4.8:** Effect of cell culture supernatant transfer. Cells were plated at different densities and after performing an MTS assay, the absorbance of formazan-containing cell culture supernatant was measured at 490 nm before (**A**) and after (**B**) transferring into new plates. Each result is the average of four replicates  $\pm$  SEM.

The MTS assay was used to assess metabolic activity of the two macrophage cell types after ND treatment. The optimum seeding density for macrophages was determined by plating cells at different densities and generation of the standard curve (Figure 4.9). The plating density that falls in the linear range of the standard curve graph and with absorbance readings less than 2 was chosen (between 5000 and 30,000 cells/well).

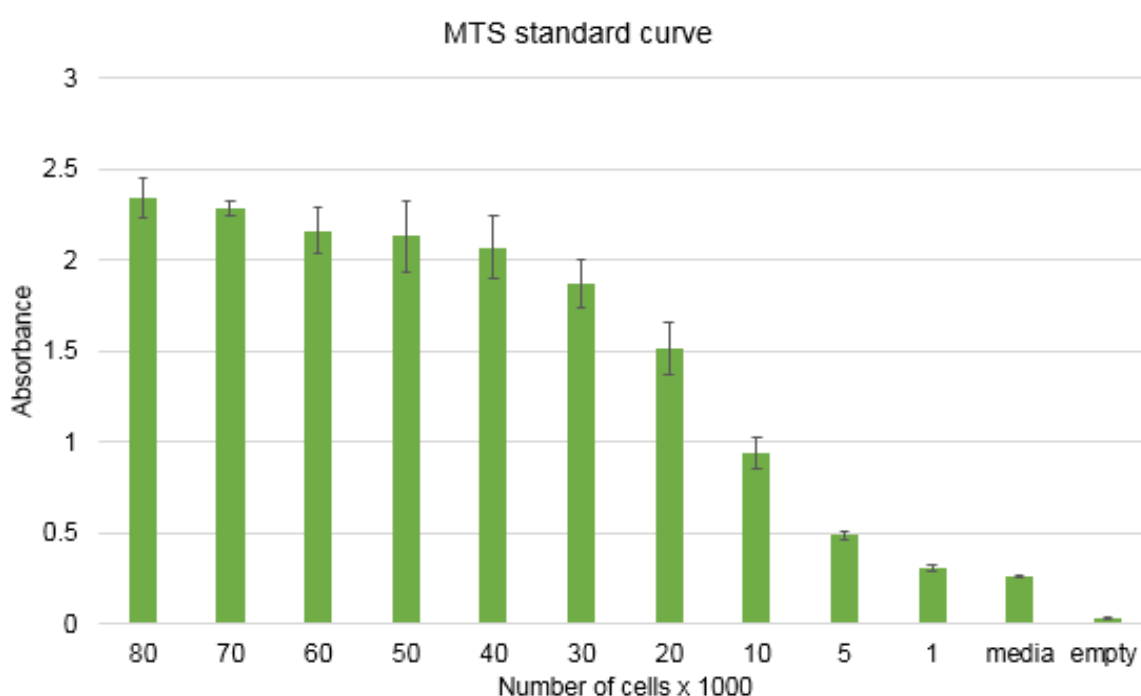


**Figure 4.9:** MTS standard curve. BMDM were plated in 96-well plates at densities from 0 to 80 thousand cell/well. Each result is the average of four replicates  $\pm$  SEM.

The first set of MTS experiments used the J774A.1 cell line treated for 24 hours with different concentrations of ND (Figure 4.10 A). In these experiments, the MTS assay was performed directly after ND treatment and results showed a slight decrease in metabolic activity of ND-treated cells though, it was not significant statistically even with the higher doses used (up to 100  $\mu\text{g/ml}$ ). Next, BMDM were treated with different concentrations of ND and for different incubation times and left for two days before performing the MTS assay (Figure 4.10 B). MTS assay with BMDM did not show a significant difference between ND-treated and untreated cells except for two concentrations/time points. The first significant difference was with the 8 hours treatment with 100  $\mu\text{g/ml}$  ND where there was a significant increase in metabolic activity. Second significant difference was with the 12 hours treatment with 10  $\mu\text{g/ml}$  ND where there was a decrease in metabolic activity. Overall, I detected no consistent effect of ND treatment on cellular viability.

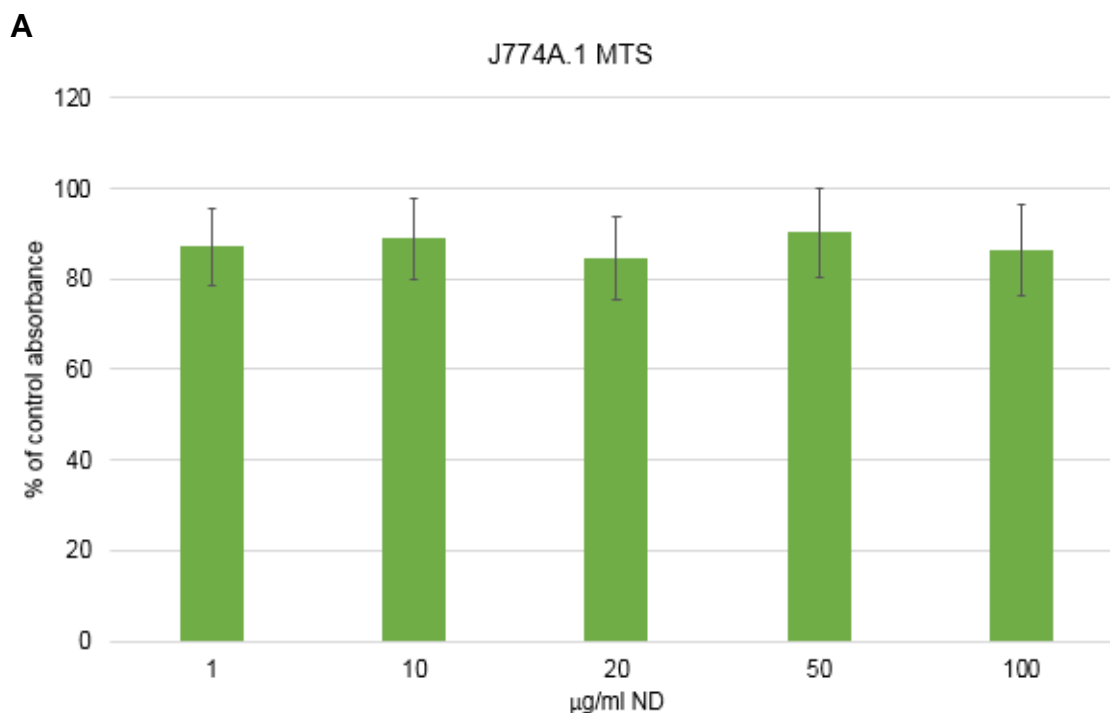


**Figure 4.10:** Cell viability assay of ND-treated cells. **(A)** J774A.1 treated with different doses of ND for 24 hours. **(B)** BMDM treated with different doses and time points, 2 days after ND treatment. One way ANOVA was not significant except for the 100  $\mu\text{g/ml ND}$  treatment for 8 hours and 10  $\mu\text{g/ml ND}$  for 12 hours. Results represent the optical density (OD) at 490 nm normalized to the OD of control cells averaged from at least three independent experiments each with four replicates  $\pm\text{SEM}$ .

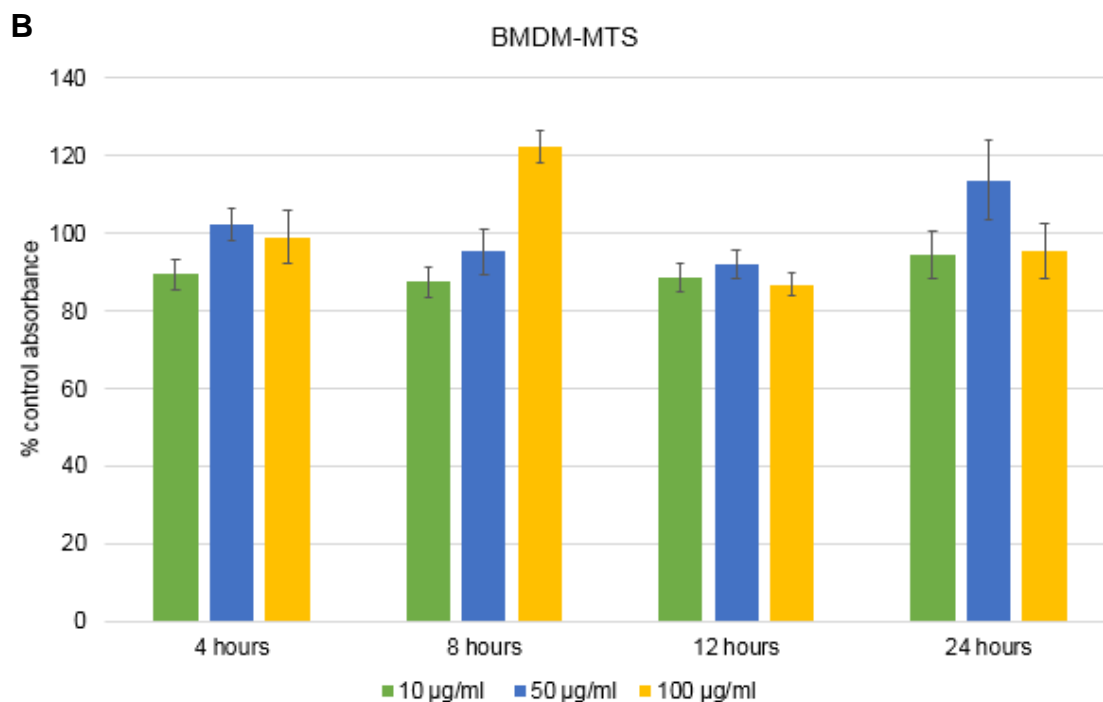


**Figure 4.10:** Continued.

Changes in cell metabolic activity may not accurately indicate cell health or death. Sometimes, the cell may undergo transient changes in metabolic activity temporarily upon exposure to certain conditions or treatments. Therefore, ND-treated and untreated cells were monitored for 1, 2 and 3 days after the ND treatment and the MTS assay was performed on each day. Results showed a reduction in the metabolic activity with increasing concentrations and days after incubation, although differences were not significant statistically even at high concentration (Figure 4.11).

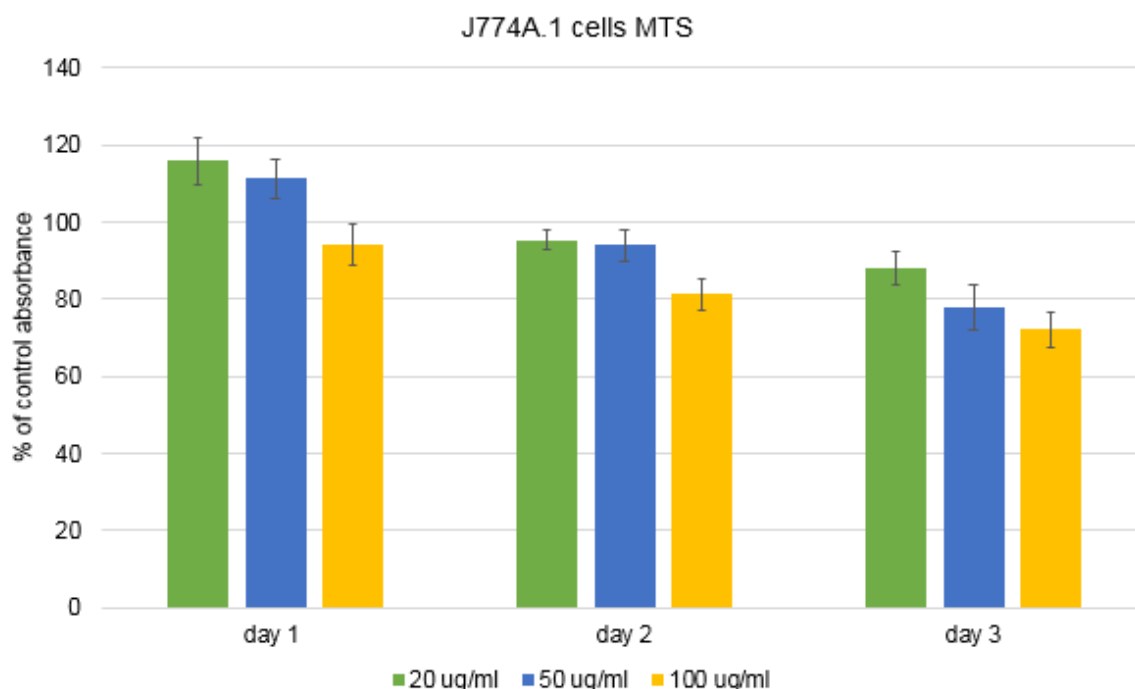


**Figure 4.11:** Cell viability assay 1, 2, and 3 days after ND treatment. MTS of J774A.1 at 1, 2 and 3 days after a 24-hour ND treatment with different concentrations. One way ANOVA from three independent experiment, each with four replicates, was not significant.

To further investigate cell viability, the apoptosis assay kit was used without adding the red dead cell stain of the kit (SYTOX™ AADvanced™) because the ND fluorescence was measured at different channels and was found to be interfering with that of this stain (Figure 4.12). Results from the apoptosis assay can indicate the percent of cells having the activated caspase 3 and caspase 7 but cannot distinguish between cells that are at the early or late apoptotic or necrotic cell death.

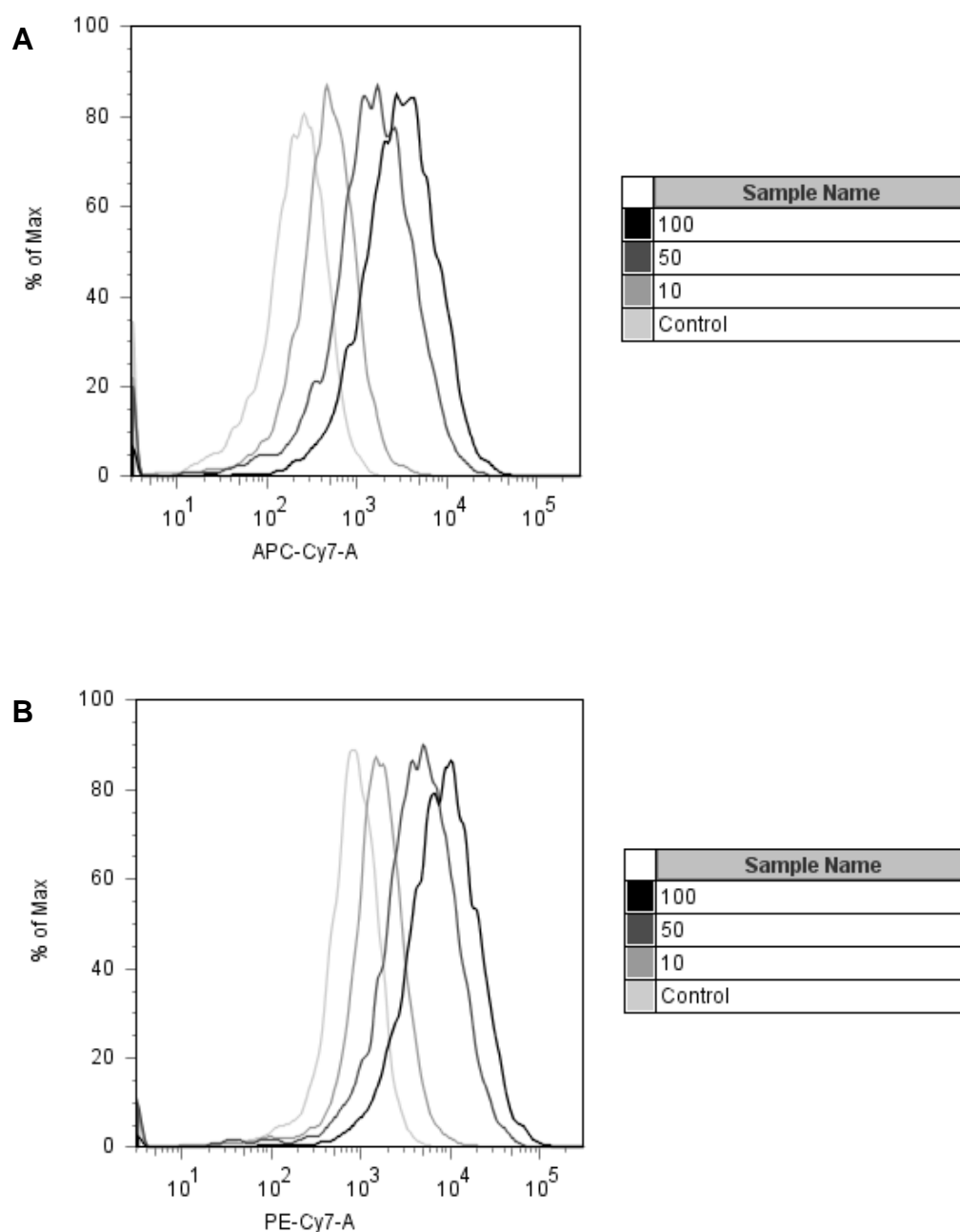


**Figure 4.12:** Fluorescence of ND. BMDM were treated with different concentrations of ND (0, 10, 50, or 100  $\mu\text{g/ml}$  ND), and the fluorescence signal was measured using FACS. Results showed that fluorescence of ND can be detected in different channels including APC-Cy7 (**A**), PE-Cy7 (**B**), and PerCP-Cy5.5 (**C**). Results represent average of at least three independent experiments  $\pm$ SEM.



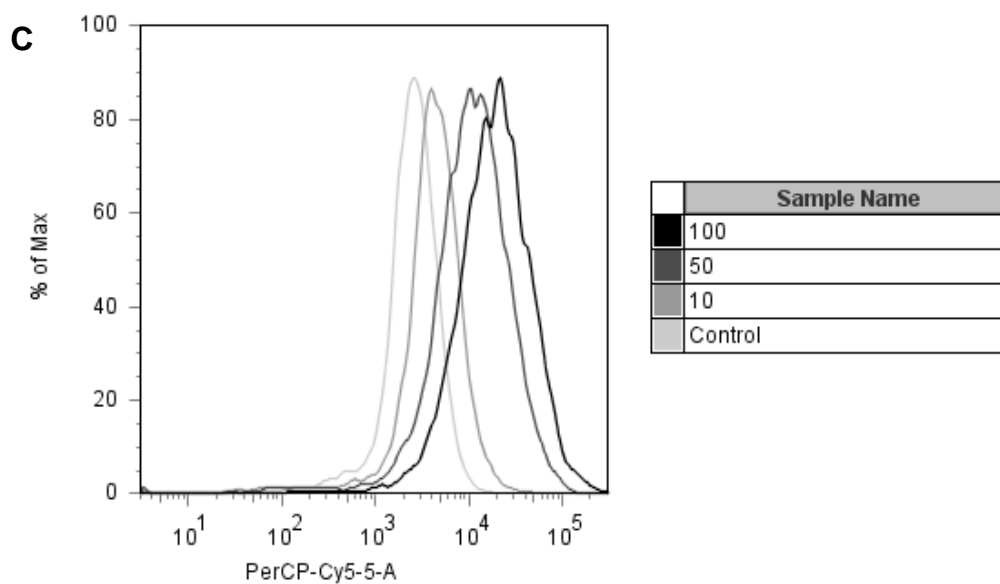


**Figure 4.12:** Continued.

I evaluated the percent of dead cells in macrophages treated with different concentrations of ND (Figure 4.13), and results showed an increase in the percent of dead cells in the ND-treated samples as compared to control, untreated cells. However, this increase was not significant.

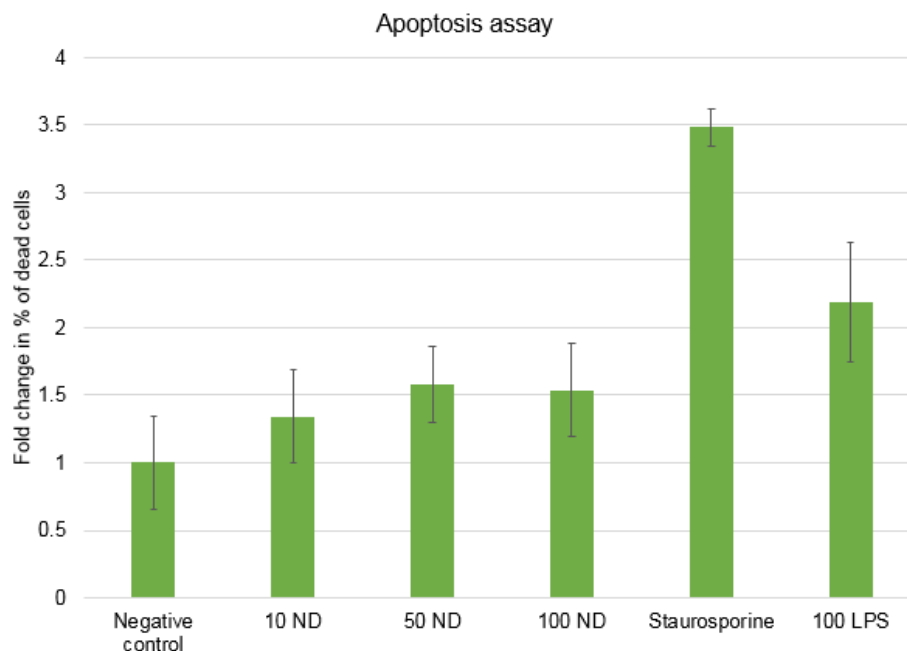


**Figure 4.13:** Apoptosis assay. BMDM were treated with 10, 50, or 100  $\mu\text{g/ml}$  ND for 24 hours. Negative control is untreated cells and positive controls are 100 ng/ml LPS and 20  $\mu\text{M}$  staurosporine for 24 hours. Results are average  $\pm$ SEM from four independent experiments.

#### 4.4 Quantitation of ND uptake and their internalization mechanism

The bright red fluorescence of ND enabled the detection of ND uptake with the fluorescent microscope (Figure 4.2), and quantification of ND uptake by cells using FACS. To quantitate the uptake of ND by these cells, BMDM were incubated with varying doses and for varying incubation times. The fluorescence of ND was measured in the APC-Cy7 channel (excitation 650 nm, emission 785 nm). Results showed an increase in

fluorescence intensities with increasing the ND concentration (Figure 4.14 A) or increasing the time of incubation (Figure 4.14 B).

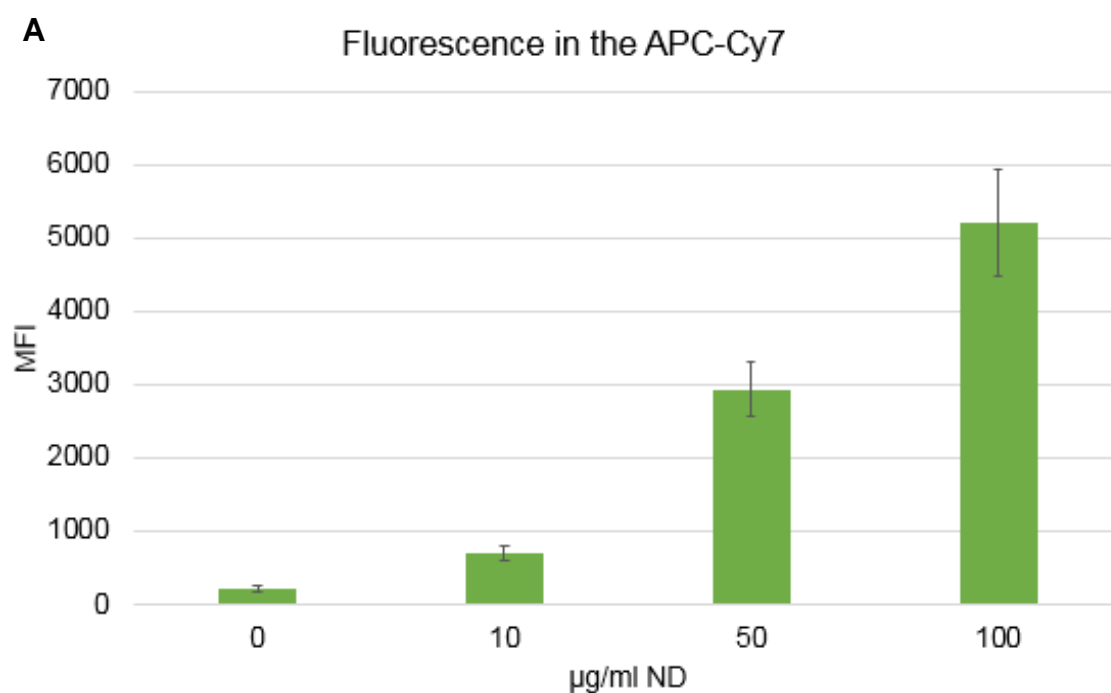


**Figure 4.14:** Quantification of ND uptake. FACS analysis of BMDM treated with 0, 10, 50, or 100 µg/ml ND for 24 hours (**A**) or with 50µg/ml ND for 0, 2, 4, 6, and 8 hours (**B**). Results represent average of the Mean fluorescence intensity (MFI) of cells in arbitrary unit  $\pm$  SEM from three independent experiments.

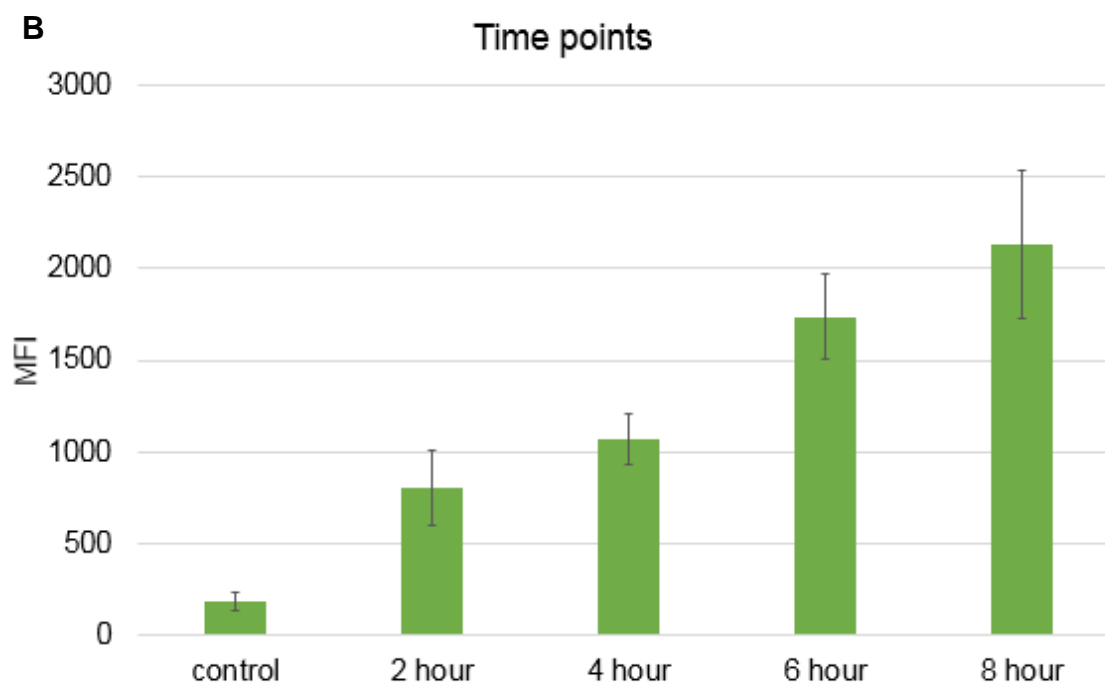


**Figure 4.14:** Continued.

To determine the uptake pathway of ND by macrophages, BMDM were pre-treated with different endocytic pathways inhibitors before exposing them to ND and the fluorescence signals were quantified using FACS (Figure 4.15). The results showed a reduction in ND uptake by about 40% when pre-treated with cytochalasin D (CYTO). Cytochalasin D is a known inhibitor of actin-dependent endocytosis pathways (Sampath and Pollard 1991). Both phagocytosis and macropinocytosis (In addition to other endocytic pathways) are actin-dependent pathways (Figure 1.7). However, only a slight reduction in ND uptake (< 10%) was noted when pre-treating with 5-(N-Ethyl-N-isopropyl) amiloride (EIPA), an inhibitor of macropinocytosis through the inhibition of  $\text{Na}^+/\text{H}^+$  exchangers (Gerondopoulos et al. 2010), which suggest that ND uptake was through

phagocytosis more than macropinocytosis. In addition, the clathrin-dependent endocytosis inhibitor also reduced the ND uptake by about 20% which also show the involvement of clathrin pathway in the uptake of ND by these cells.

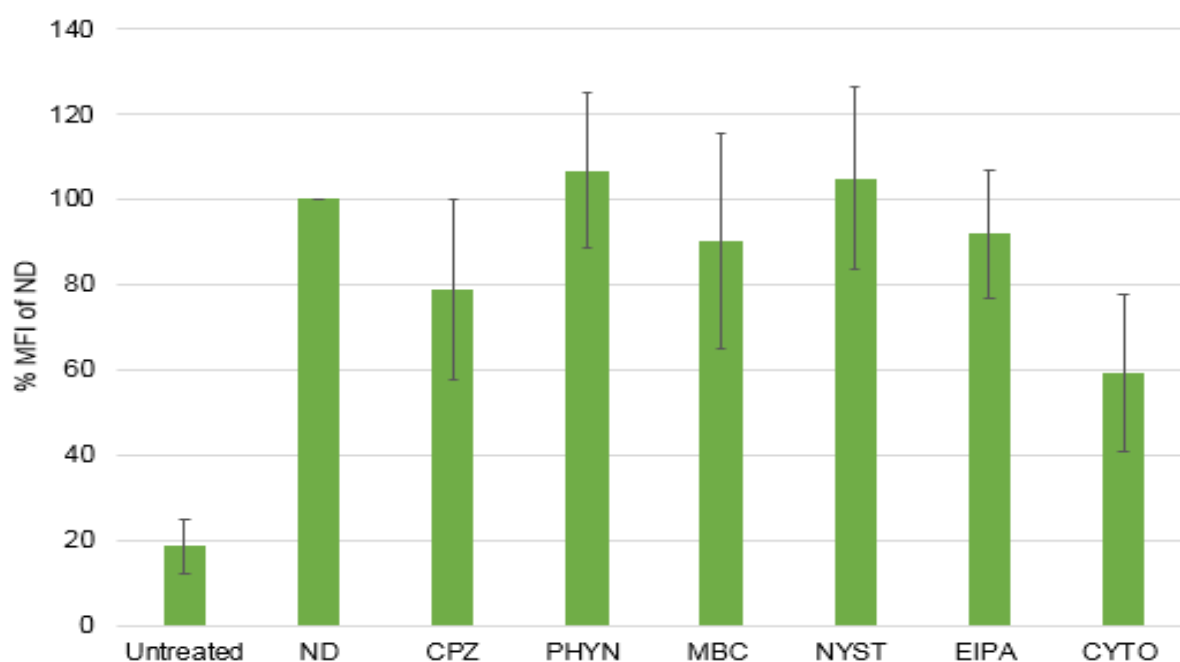


**Figure 4.15:** Endocytic pathways. FACS results showing the uptake of ND by cells pretreated or untreated with endocytic pathways inhibitor. BMDM were pretreated with each inhibitor for 30 minutes before exposing them to ND. Abbreviations, CPZ: chlorpromazine hydrochloride, PHYN: phenylarsine oxide, MBC: methyl-beta-cyclodextrin, NYST: nystatin, EIPA: 5-(N-Ethyl-N-isopropyl) amiloride, CYTO: cytochalasin D.

#### 4.5 Effects of ND on gene expression in macrophages

Macrophages are known to respond to a wide range of stimuli. Their responses include expression of surface activation markers, changes in their phagocytic activity, and secretion of cytokines, chemokines, and adhesion molecules. These events require activation or suppression of the transcription of certain genes and the subsequent translation and further processing to produce functional proteins. The aim of the following experiments was to assess the inflammatory response of macrophages upon exposure to ND. Macrophages cell line, J774A.1 and BMDM were exposed to 50  $\mu\text{g/ml}$  ND and total RNA was isolated, converted to cDNA, and followed by RT-qPCR.

The output files from the thermal cycler contains the ct values for each target gene which represents the threshold cycle or the cycle at which the amount of DNA reached the threshold value. The amplification curves showed the ct value of each reaction including the non-template controls (NTCs) and the melt curves confirmed the amplicon size (Figure 4.16). Some reactions may show amplification in the NTC which may indicate a contamination specially if the ct value of NTC is low. However, that amplification could be from primer dimers and this can be confirmed from the melt curve graph. The melting temperature of primer dimers is usually low because of its small size while in cases where there is a peak at a higher temperature (close to the melting temperature of the target amplicon), this indicates a contamination and the results are not valid.

When using the  $\Delta\Delta\text{ct}$  method to calculate the fold change, the ct value of the target gene is normalized to the ct value of the reference gene (or genes). These calculations give the  $\Delta\text{ct}$  value for each gene in each sample. Next, the  $\Delta\text{ct}$  value of each gene in the treated sample is compared to that in the control sample to find the fold change in gene

expression. The fold change that lies between 1 and -1 is not considered as a change in gene expression. Any fold change value above 2 or below -2 can be considered as a change but to determine if this change is significant, statistical tests are usually used to compare the fold change for each gene.

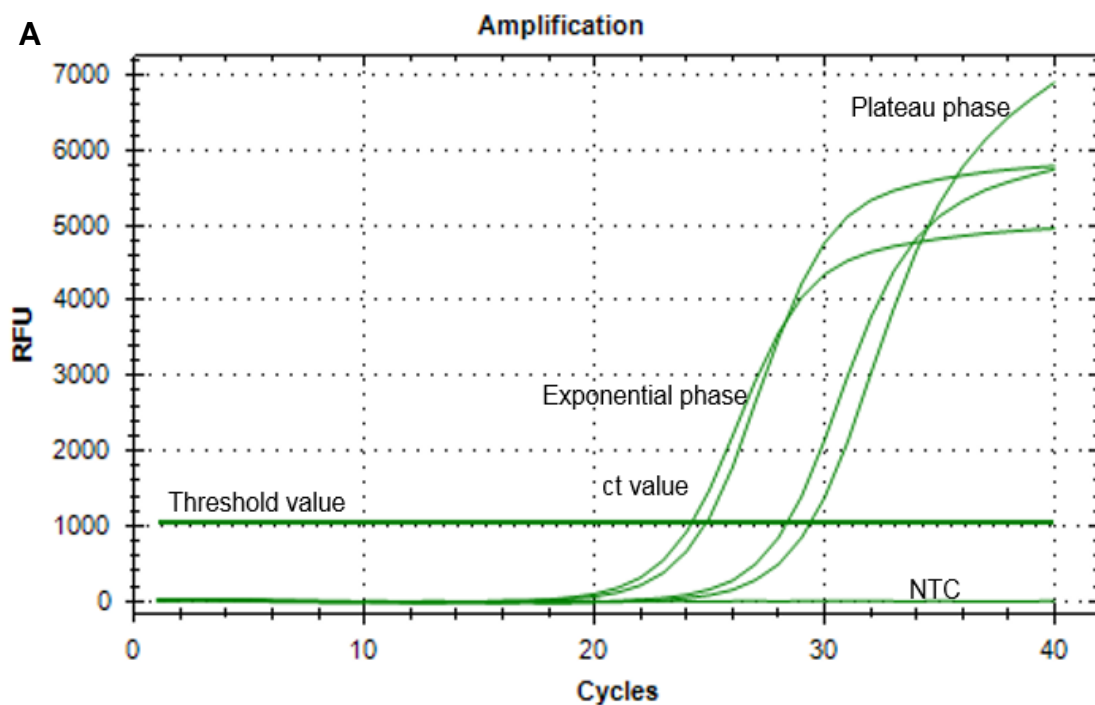


**Figure 4.16:** RT-qPCR graphs. Representative graphs from RT-qPCR experiments showing the amplification of cDNA for a target gene with differential gene expression (**A**) and non-differential expression (**B**). Melt curves for the amplicon in the reaction may show a second peak at a lower temperature from primer dimers (**C**). RFU: Relative fluorescence unit.

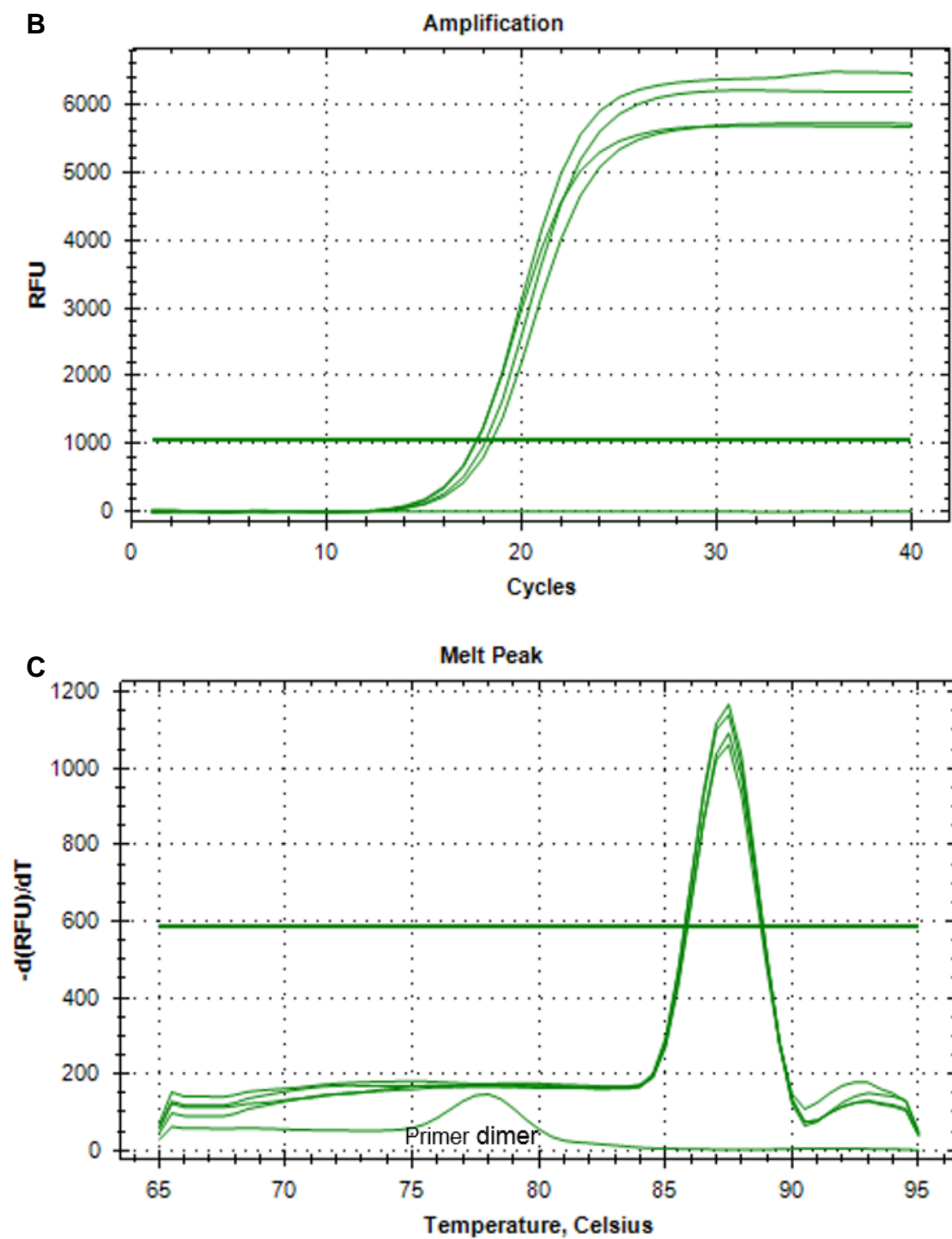
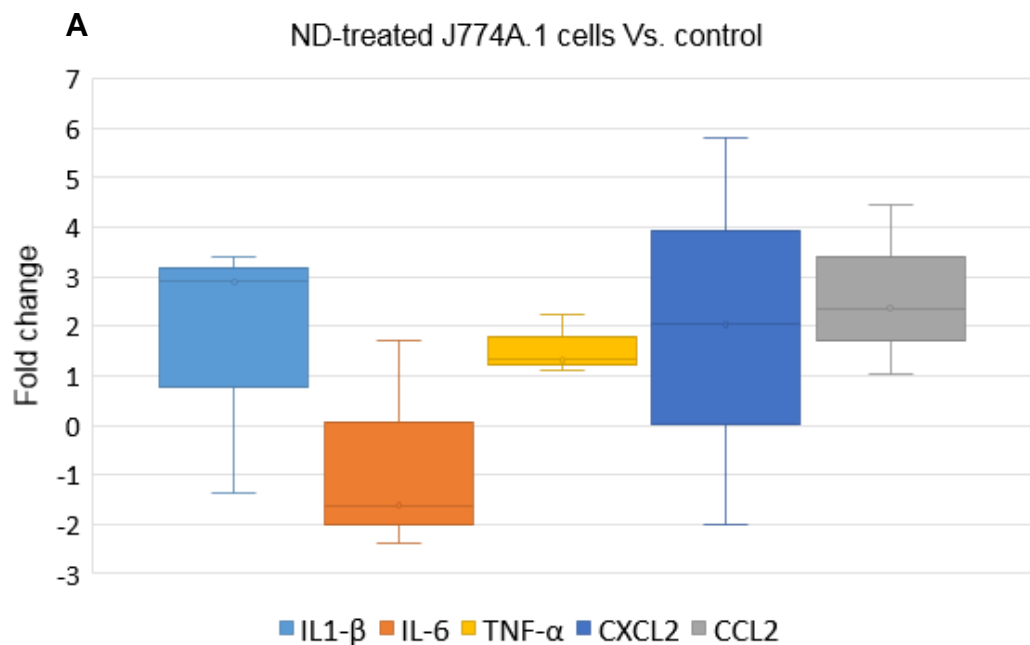


Figure 4.16: Continued.



I assessed the expression of inflammatory cytokines; IL1 $\beta$ , IL6, TNF $\alpha$ , and iNOS and chemokines; CXCL2, and CCL2 in both cell types at the mRNA level using RT-qPCR. In addition, BMDM were also assessed for IL4, IL10, and IL12 expression after ND treatment. Results showed differences in the response of the two cell types to ND (Figure 4.17).



**Figure 4.17:** Gene expression in macrophages in response to ND. Macrophage cell line, J774A.1 (**A**), and BMDM (**B**) exposed to 50  $\mu$ g/ml ND for 6-7 hours and the total RNA was isolated, converted to cDNA, and used for the RT-qPCR. Results obtained using the  $\Delta\Delta$ ct method and represent the mean fold change averaged from three independent experiment  $\pm$ SEM. Student's T test was not significant for all the tested genes ( $P>0.05$ ).

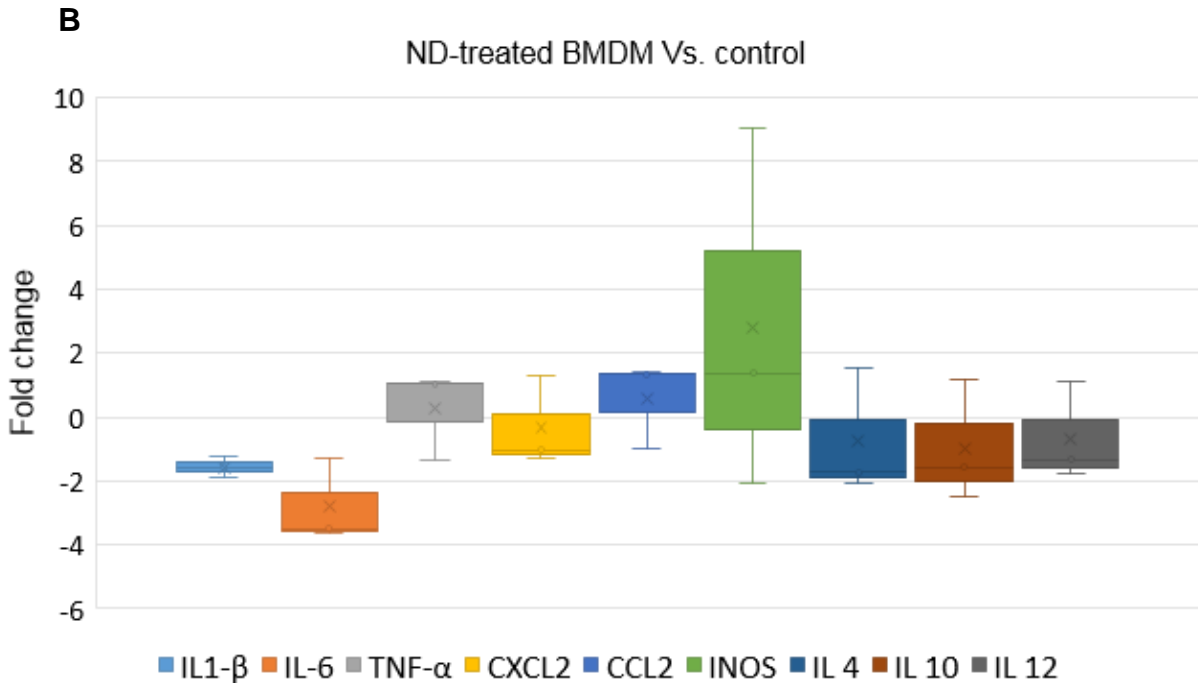


**Figure 4.17:** Continued.

Expression of iNOS was upregulated in BMDM but was not detected in the J774A.1 cell line. The macrophage cell line showed some upregulation in the pro-inflammatory genes except for IL6 whereas BMDM showed downregulation in all genes except for TNF $\alpha$ , CXCL2, and CCL2 that were unaffected. However, changes in all genes expression were not significant statistically in the two cell types.

To confirm the RT-qPCR results, protein concentrations of IL1 $\beta$ , IL6, TNF $\alpha$ , CCL2, IL10, and IL12, were assessed with ELISAs (Figure 4.18). Results showed no effect of ND treatment as compared to the negative control (untreated cells) and positive control (10 ng/ml LPS) except for CCL2 which was much higher in the ND-treated sample and IL1  $\beta$  which was not detected in all samples.

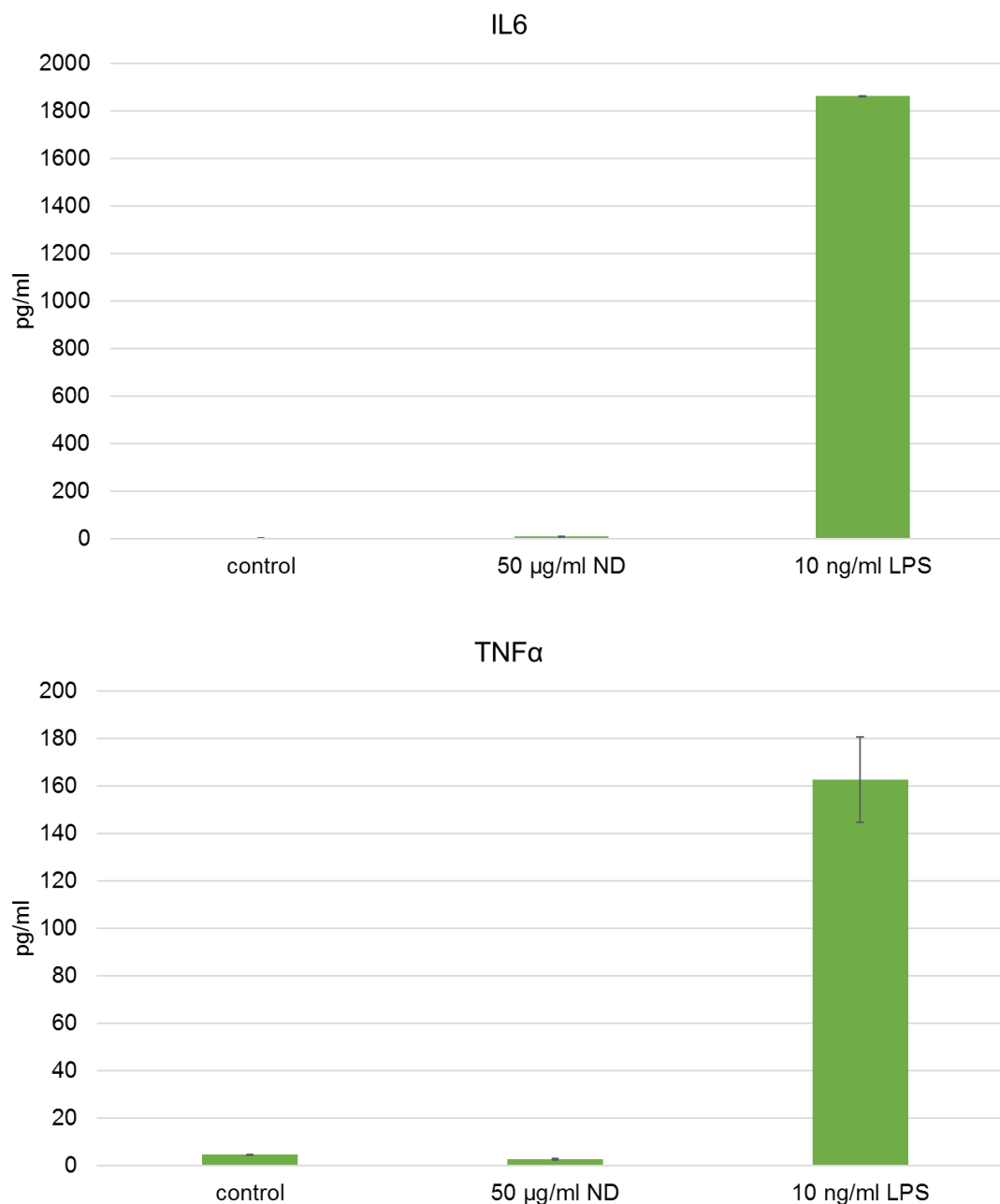


**Figure 4.18:** Cytokines ELISAs. BMDM were treated with or without 50 μg/ml ND or 10 ng/ml LPS. After 24 hours, media were replaced and cells were incubated for another 24 hours before collecting the supernatant for ELISAs. Results showed no effect of ND treatment on the expression of the tested cytokines except for CCL2. Results are average of two replicates  $\pm$  coefficient of variation (CV).

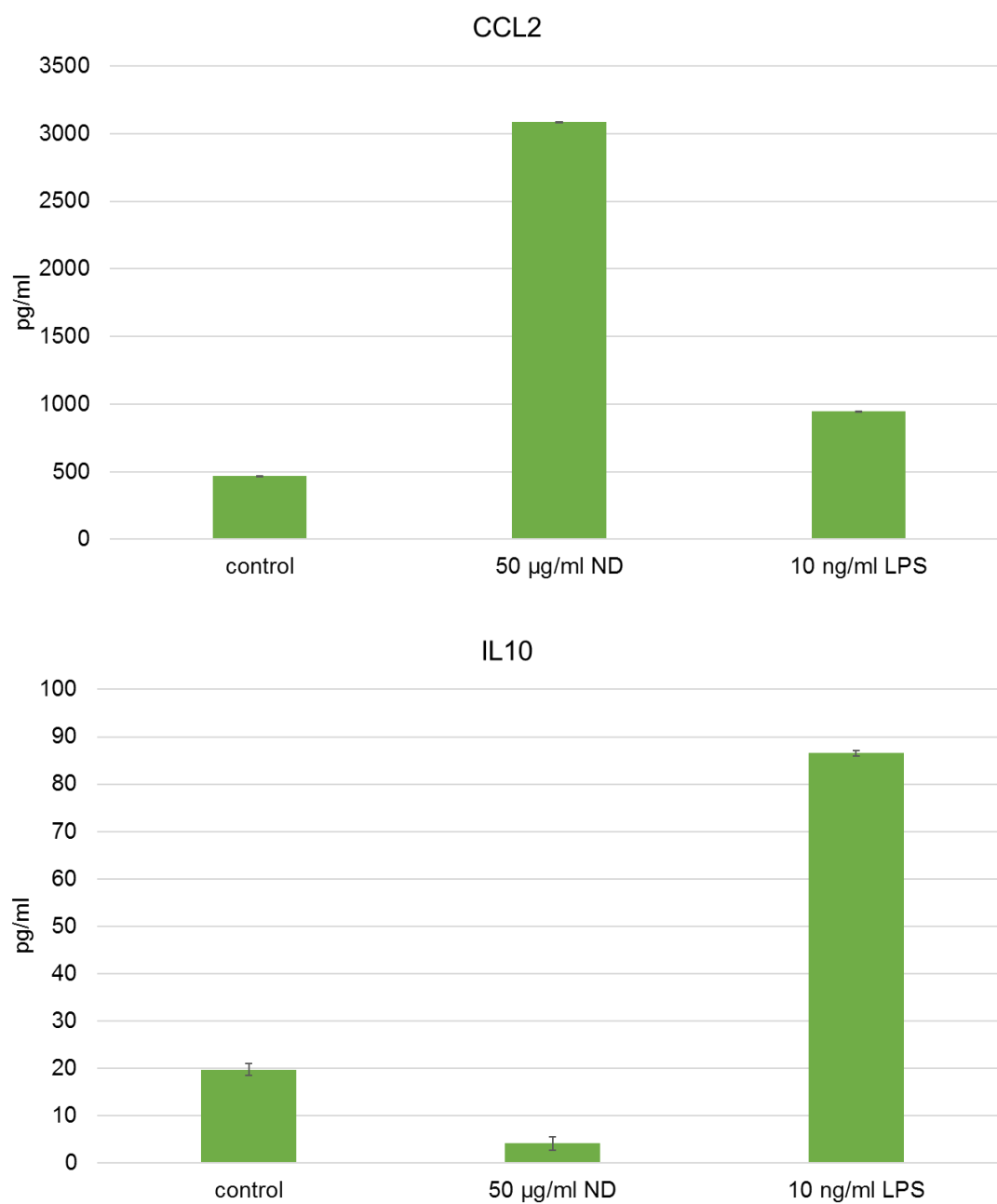


**Figure 4.18:** Continued.

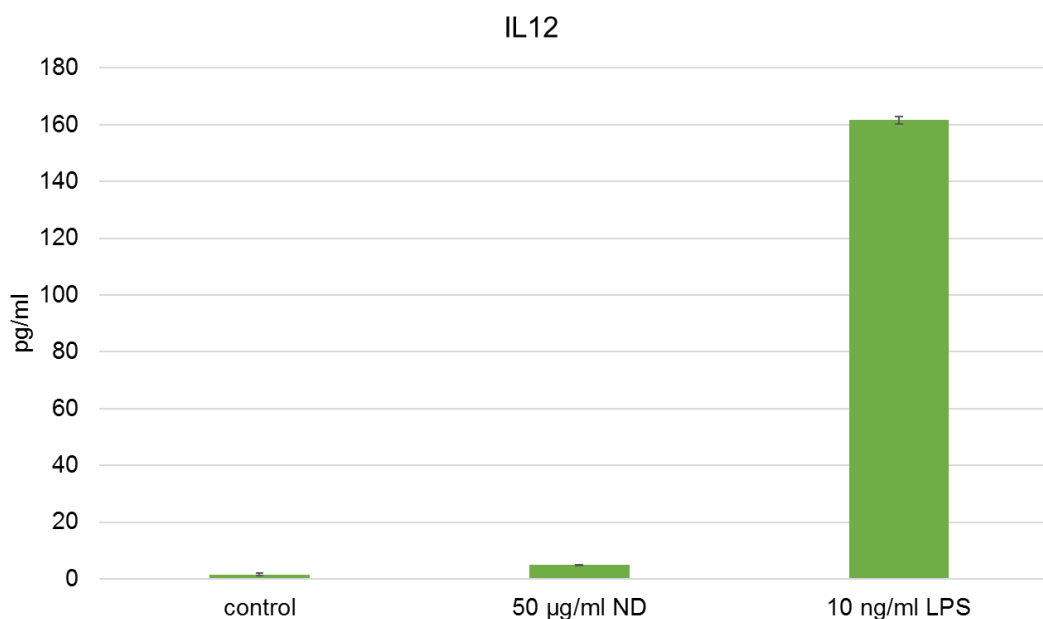


**Figure 4.18:** Continued.

#### 4.6 Effects of ND on macrophage functions and differentiation

Depending on the specific physical and chemical properties of the nanoparticle, essential cell functions can be influenced by nanoparticles. In the case of macrophages, the ability to endocytose and respond to known threats are important for the function of the immune system because they represent the first responding cells to initiate the immune response. I aimed to investigate the ability of ND-treated cells to respond to a highly potent immunogen, LPS, in a negative (suppression) or positive (enhancement) direction.

Macrophages cell line and BMDM were pre-treated with 50 µg/ml ND for 4 hours before exposing them to 10 ng/ml LPS. Response of the ND-treated and untreated cells to LPS was assessed using RT-qPCR. No significant changes in the expression of the

target genes were found between the ND-treated and untreated cells (Figure 4.19). Although not significant, the ND-treated macrophage cell line showed more variable expression in IL1 $\beta$ , a slight increase in IL6 and CXCL2, and downregulation of CCL2 while the primary BMDM expression was somehow unaffected by ND treatment.

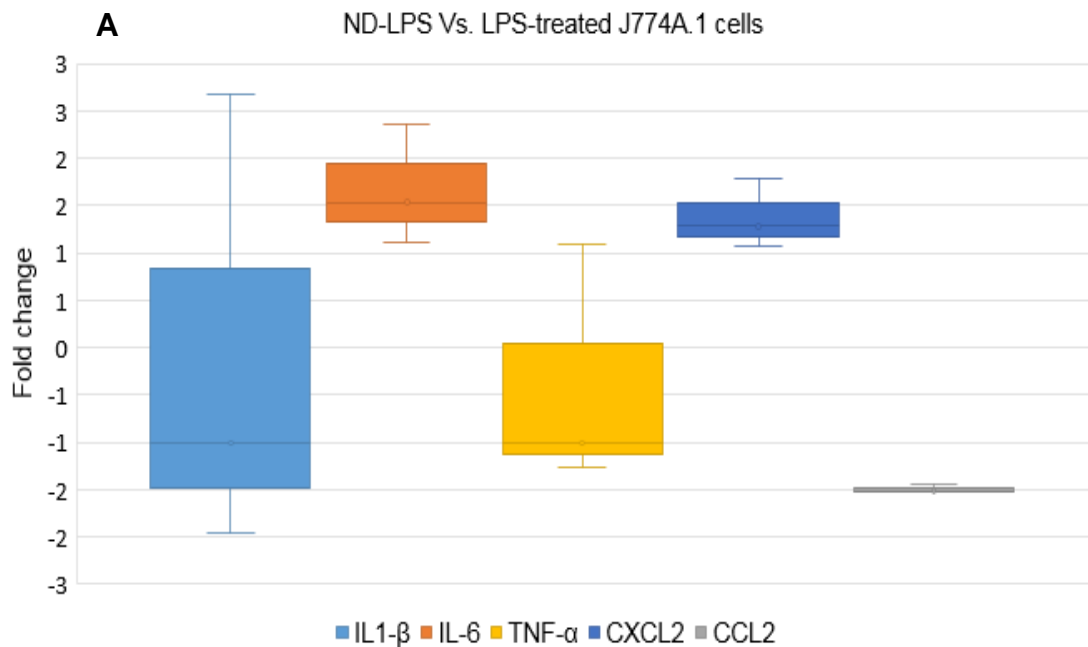


**Figure 4.19:** Effects of ND treatment on macrophages response to LPS. RT-qPCR results showing gene expression of cytokines in J774A.1 cells (**A**) and BMDM (**B**). Cells were pretreated with 50  $\mu$ g/ml ND for 4 hours before exposing them to LPS for 3 hours. The results represent the mean fold change  $\pm$ SEM calculated by  $\Delta\Delta$ ct method and averaged from at least three independent experiments.

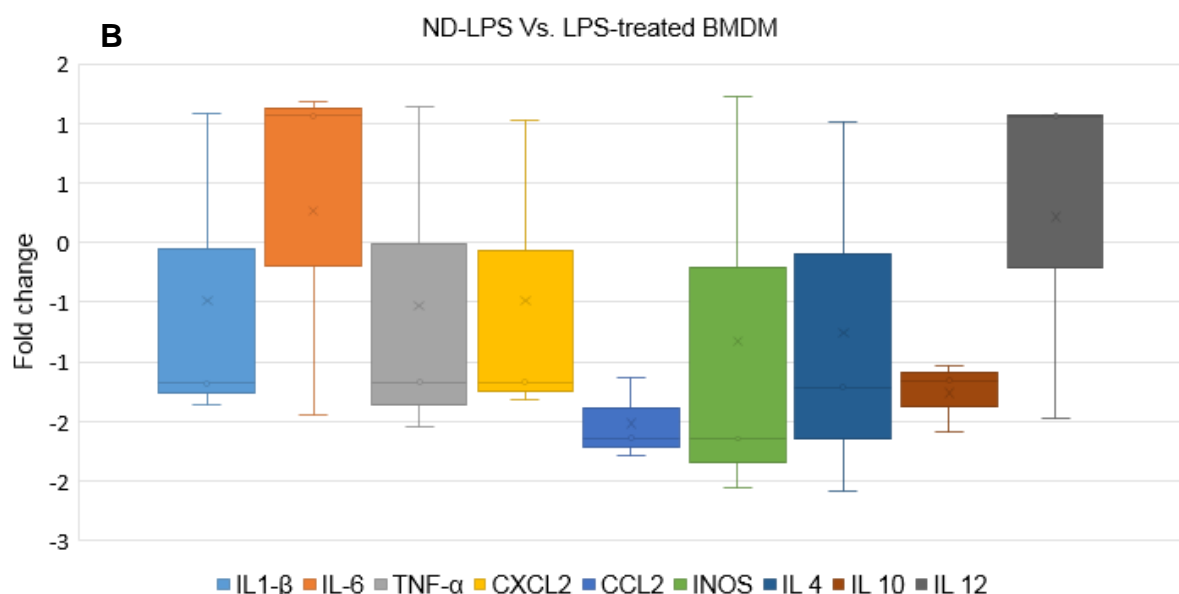


**Figure 4.19:** Continued.

Next, I studied the endocytic activity of ND-treated cells by exposing them to fluorescently-labeled dextran particles. The internalized dextran particles fluorescence was measured with FACS and compared with that in untreated cells. Results show that ND pre-treatment reduced the uptake of dextran particles significantly ( $p < 0.05$ ) (Figure 4.20). The reduction in cell internalization of dextran particle was irrespective to ND concentration, although the lowest uptake (and lowest P value, 0.019), was at the highest concentration used (50  $\mu\text{g/ml}$  ND).

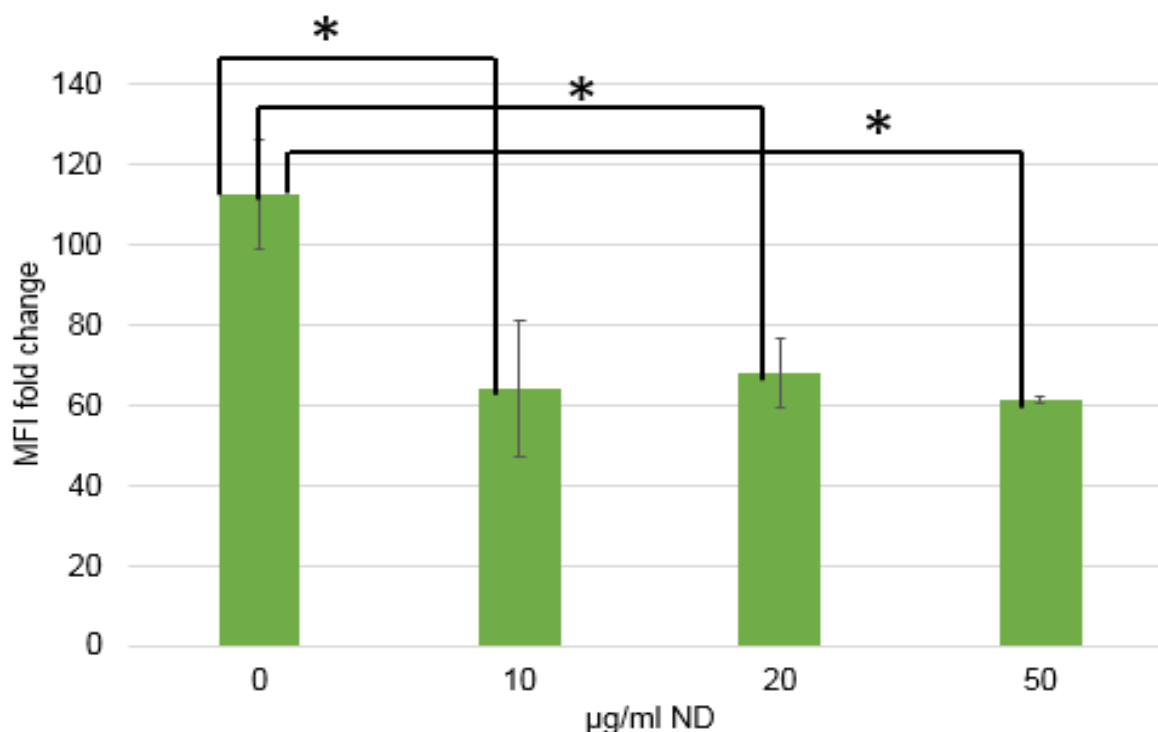


**Figure 4.20:** Endocytic activity. ND-treated and untreated BMDM were exposed to ND for 16 hours before exposing them to dextran for 45 minutes and the fluorescence signal from cells was measured using FACS. MFI results represent the mean  $\pm$ SEM from three independent experiments. One way ANOVA and Dunnett t for multiple comparisons were significant ( $p < 0.05$ ).

The myeloid progenitor cells reside in the bone marrow where they differentiate into different types of blood cells including monocytes which further differentiate into macrophages or dendritic cells (Figure 1.5). These cells have been used to prepare macrophages or dendritic cells to study their biology or for other investigations such as cytotoxicity studies. Many protocols have been used to prepare BMDM but in general,



these cells differentiate in culture under induction of M-CSF for 7 days. After differentiation, these cells are assessed usually for their expression of macrophage surface markers to confirm the macrophage phenotype.

Differentiation of macrophages is an important process to produce functional macrophages *in vivo*. The effect of ND on the differentiating bone marrow cells has not been studied. I investigated the effects of ND on the differentiation of these cells when they are exposed early (on day one after isolation from the bone) before they fully differentiated into BMDM. I assessed the cells morphology and expression of macrophages surface markers (CD11b and F4/80). The cell morphology did not appear to be affected by ND treatment (Figure 4.21). The ND-treated cells internalized the ND and they were able to re-adhere and form the normal cell shape after harvesting and re-culturing.

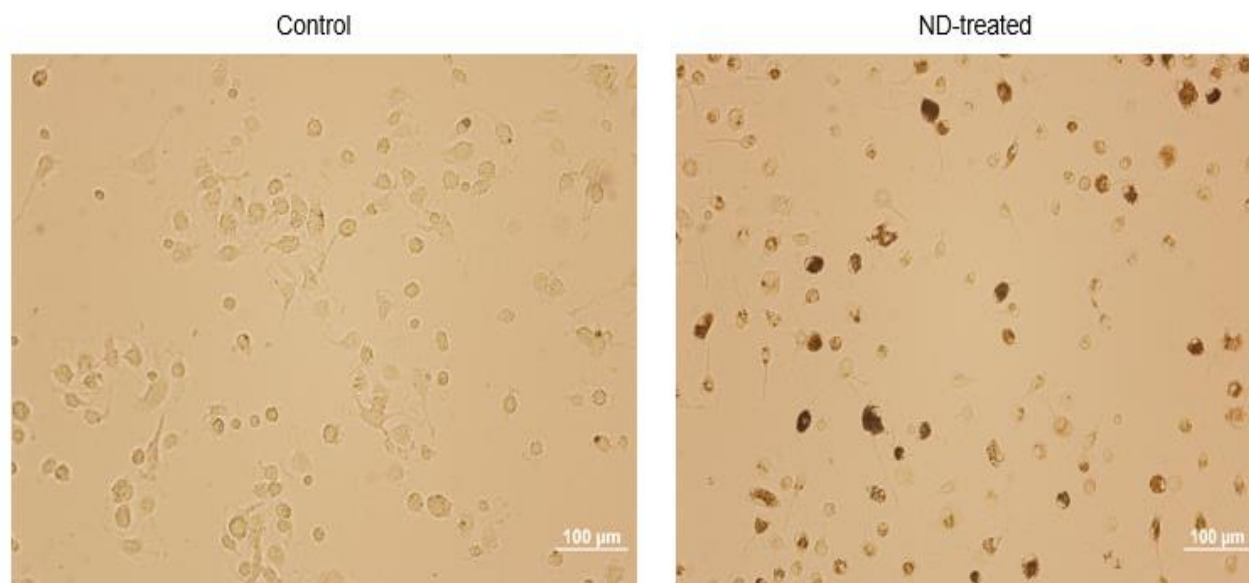


**Figure 4.21:** Microscopic images of BMDM differentiated in the presence of ND. Isolated bone marrow cells were exposed to 50  $\mu\text{g/ml}$  ND and incubate for 7 days with differentiation media. Bright field images showing ND-treated (right) and untreated (left) cells. ND did not appear to alter cell's morphology.

To determine the effects of ND treatment on the ability of BMDM to express macrophage surface markers, ND-treated and untreated cells were stained with FITC-CD11b and PE-F4/80 antibodies and assessed with FACS (Figure 4.22). Exposure of bone marrow cells to ND before differentiating them, did not affect the percent of cells expressing each surface marker (Figure 4.23 A), or the fraction double positive for the two markers (Figure 4.23 B). More than 90% of cells expressed each or both markers in the ND-treated or untreated cells. However, the fluorescence intensities were reduced

significantly ( $p$  value 0.042 for CD11b and 0.008 for F4/80) in the ND-treated cells (Figure 4.24). These results indicate that the number of cells expressing the surface markers (CD11b, F4/80, or both) was not affected by ND treatment while the number of each marker per cell is reduced in the ND-treated cells.

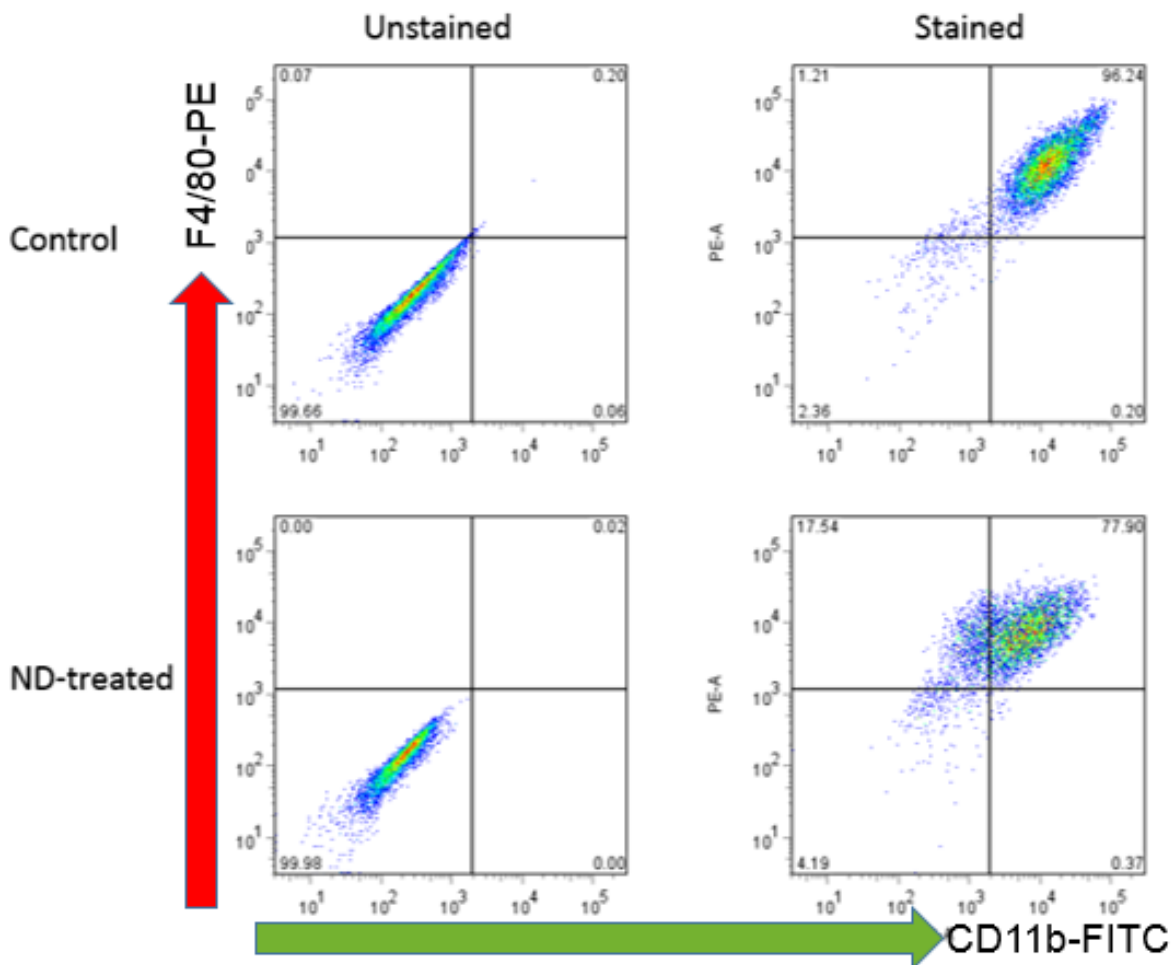


**Figure 4.22** FACS graphs for determination of effects of ND on surface markers expression. Representative graphs from FACS analysis showing the percent of cells expressing macrophage surface markers, FITC-CD11b and PE-F4/80.

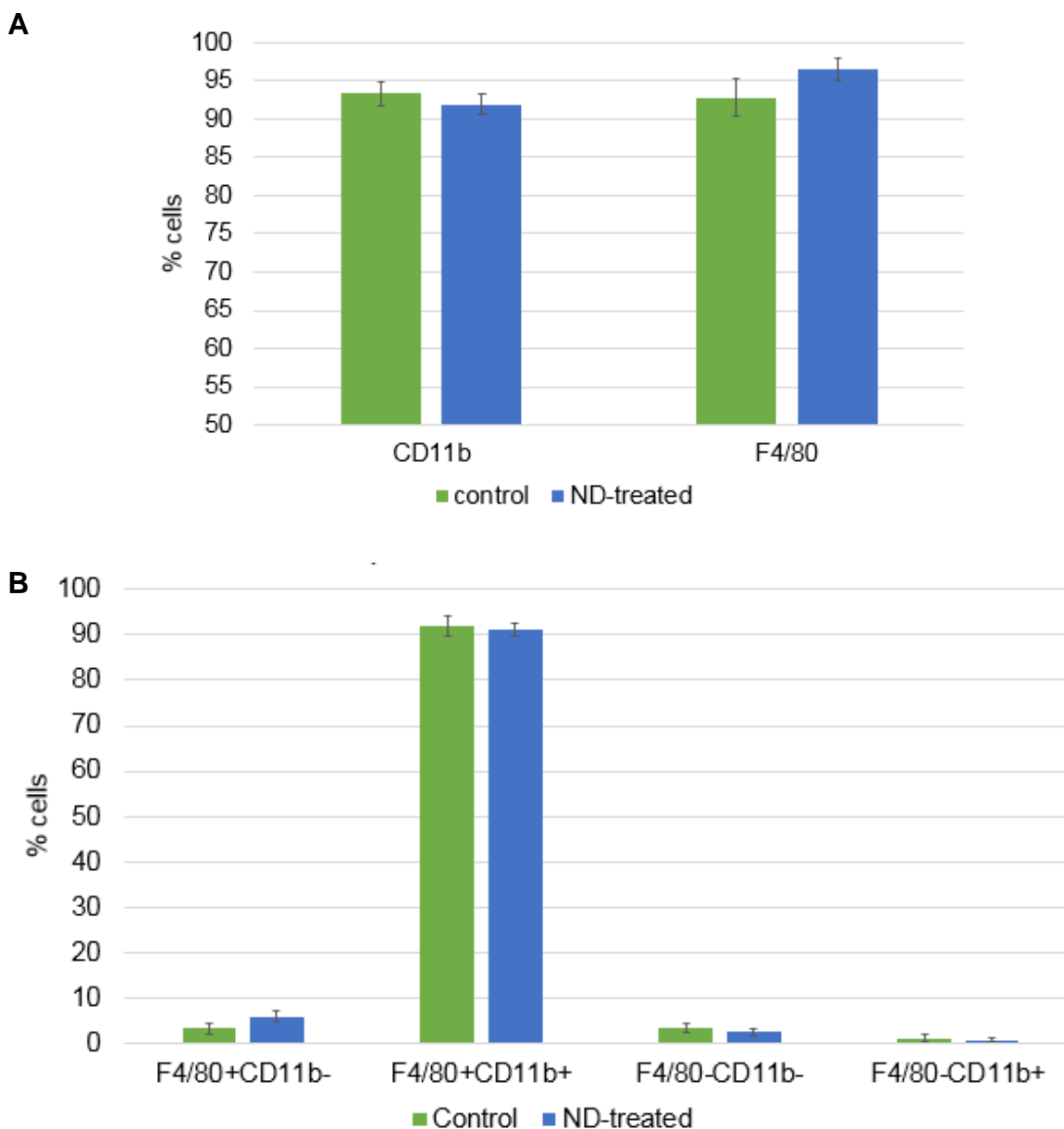


**Figure 4.23:** Expression of surface markers in ND-treated and untreated BMDM. Bone marrow cells were exposed to 50  $\mu$ g/ml ND and differentiated into macrophages under M-CSF induction for 7 days. Expression of cell surface markers was assessed with FITC-CD11b and PE-F4/40 antibodies. **(A)** Percent of cells expressing CD11b or F4/80. **(B)** Percent each cell population based on their surface markers.

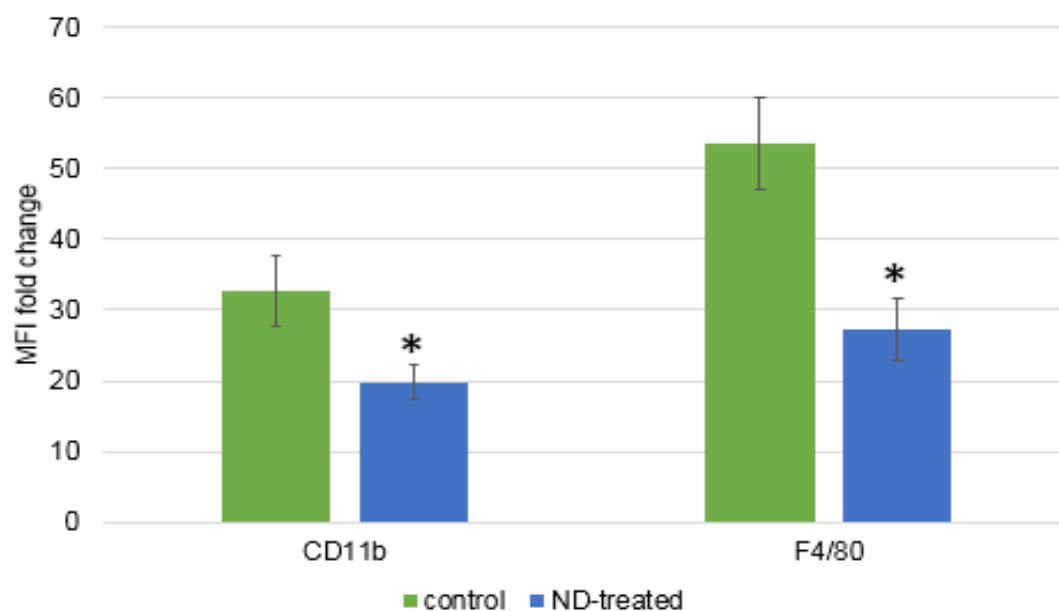


**Figure 4.24:** Effects of ND on the number of surface markers expressed per cell. Results represent fold change in MFI as compared to unstained control from four independent experiments. \*  $p < 0.05$ .

## **CHAPTER 5**

### **DISCUSSION**

Utilization of ND for biomedical applications is highly attractive but requires extensive studies to investigate their potential impacts. The chemical inertness of these particles does not imply biological inertness and therefore, I aimed to investigate the effects of ND on two macrophage cell types, J774A.1 cell line and BMDM. My studies involved assessment of the direct effect of ND on the cell and potential impacts on basic macrophage immune functions.

#### **5.1 Primary cells and macrophage-like cell line**

The macrophage cell line is widely used for cytotoxicity studies; however, these cells have a high mutational rate and the continual subculture of these immortalized cells results in the loss of genes that are not required for their survival, yet, are essential for immune functions of the cell (Marim et al. 2010; Kaur and Dufour 2012). In addition, the scientific community recommend the use of primary cells to add confidence in the study results due to the misidentification of cell lines that has been highly reported and requires authentication (Almeida et al. 2016; Horbach and Halffman 2017). Significant differences between macrophage-like cell lines (Including J774A.1) and BMDM has been reported (Chamberlain et al. 2009). Therefore, primary mouse macrophages, BMDM, were used in my studies because they may better represent the normal macrophages and to confirm results from my studies with the cell line.

The primary cells were differentiated under M-CSF induction, and their phenotype was confirmed with antibodies against the macrophage surface markers, CD11b and F4/80 (Figure 4.1). Other sources for M-CSF can be used to induce differentiation of BMDM such as L-929 fibroblast conditioned medium (Weischenfeldt and Porse 2008; Chamberlain et al. 2009; Marim et al. 2010). The mouse cell line, L-929, secretes M-CSF into the culture media which is usually collected and used to promote maturation of macrophages. To avoid any variability in the M-CSF concentration, I used the recombinant protein instead of the L-929 conditioned media.

## **5.2 Effects of ND on cell morphology**

Exposure of cells to nanoparticles may affect or interfere with vital processes in cells. The effect may show directly as changes in cells morphology, metabolic activity, viability, or apoptosis. I assessed the effect of ND on macrophage morphology and found that the shape of the cell did not change dramatically after ND treatment, nonetheless, these cells appeared to be larger in the microscopic images as compared to the untreated controls (Figure 4.2). However, ND-treated cells were smaller than untreated cells as measured with the FSC parameter in FACS analysis (Figure 4.3). The ND-treated cells looked darker in color due to the ND appearing as dark spots in cells while the control, untreated cells, are transparent and this may explain the large appearance of ND-treated cells in microscopic images.

Macrophages usually increase in size in response to stimuli such as LPS (Saxena et al. 2003; Pi et al. 2014). In addition to macrophages, HeLa cells and hepatocyte morphology were shown to be affected by ND treatment (Mytych et al. 2014; Mytych et

al. 2015). In these studies, both cell types were enlarged and showed cytotoxic effects such as inhibition of proliferation and oxidative stress after ND treatment. These toxic effects could be due to the smaller ND (<10 nm) that were used as well as differences between cell types. In general, smaller ND particles tend to exert more toxicity as compared to larger particles (Thomas et al. 2012; Keremidarska et al. 2014). Another study on detonation ND with different sizes showed size-specific and cell-type specific changes in morphology (Keremidarska et al. 2014). Detonation ND are prepared by detonation of graphene to produce smaller (4-5 nm) ND as compared to the larger HPHT-ND (100 nm) used in my work but these primary sizes may not represent the actual size of ND interacting with cells due to the formation of ND aggregates. Smaller ND (4-6 nm) were also shown to increase the number of flattened peritoneal macrophages in microscopic images which was not detected in my experiments (Shkurupy et al. 2015). Cellular granularity was assessed with FACS and results show that the granularity increased in a time- and dose-dependent manner (Figure 4.4). Similar changes in granularity were reported for macrophages incubated with smaller ND while measuring the granularity from microscopic images (Mytych et al. 2015).

### **5.3 Subcellular localization**

The confocal microscope uses optical sectioning (not physical sectioning) of cells to focus on a focal plan producing high resolution images (Inoué 2006). The focal plan passes through the cell at a specified depth and by moving in the Z plan, multiple images are taken at different focal plans to determine the presence or absence of ND in the nucleus. Confocal microscope images showed that ND are accumulated in the cytoplasm



but did not enter to the nuclei of macrophages (Figure 4.6). Other studies on 100 nm ND also showed the localization of ND in the cytoplasm but not in the nuclei of hepatocytes and lung cells, even at a much higher concentration (400  $\mu\text{g/ml}$ ) (Yu et al. 2005; Liu et al. 2007). Nuclear entry may be determined by the size of nuclear pore complex (about 50 nm). However, smaller (2-10 nm), detonation ND were also shown to be localized to the cytoplasm of HeLa cells (Li et al. 2010). It was important to determine the ability of nanoparticles to enter to the nucleus which depends primarily on their size and surface chemistry. Smaller particle (< 50 nm) with specific surface chemistry such as conjugated nuclear localization sequence (NLS), are more suitable to target the nucleus to deliver proteins or nucleic acids to the nucleus (Liu et al. 2007). Nevertheless, these smaller particles tend to exert more toxic effects by interfering with vital processes and biomolecules such as DNA and thus, larger particles are more suitable to avoid their entrance to the nucleus, while smaller particles are suitable to deliver drugs, proteins, or nucleic acids to the nucleus, depending on the intended application.

#### **5.4 Interference of ND with absorbance and fluorescence**

The ability of ND to absorb and emit light at different wavelengths is beneficial for different biomedical applications such as imaging and tracking. However, this can be problematic because it interferes with different assays to determine ND effects on cells. Different viability assays are colorimetric or fluorometric methods which rely on measuring the absorbance or fluorescence of the assay reagent to assess cytotoxicity. The absorbance of ND was measured at different wavelengths and I found that ND can absorb (Figure 4.7) and emit fluorescence signals (Figure 4.12) at different wavelengths.

The interference of ND was avoided in the MTS assay by transferring the formazan-containing cell culture supernatant into new wells before measuring the absorbance. Transfer of supernatant did not affect the overall proportion of absorbance among samples (Figure 4.8). To avoid ND interference with fluorescence signal from the apoptosis assay, the red-dead cell stain was not used and the percent of cells with a positive green signal that is associated with activated caspase 3/7, was used to determine the effects of ND on percent of cell death.

In a study to investigate nanoparticles interference with toxicity assays, 24 different nanoparticles were shown to interfere with optical measurements of assay reagents (Kroll et al. 2012). Interference of nanomaterial with assay reagent could also be due to other mechanisms. Carbon nanotubes have been shown to “fake” cytotoxic effect when assessed with the MTT assay but not with other viability assays (Worle-Knirsch et al. 2006). The study showed that carbon nanotubes do not affect the enzymatic reaction but the insoluble formazan crystals are lumped with nanotubes inside cells. The author concluded that the effect of nanomaterials should be assessed with more than one viability assay to avoid any unknown interference with assay reagents.

## **5.5 Cell viability**

The viability of cells treated with different concentrations of ND and for different time intervals was assessed using the MTS assay. Results showed a slight reduction, yet not significant, in the viability of the two cell types analyzed directly after the ND treatment or after 1, 2, or 3 days (Figures 4.10 and 4.11). The MTS or MTT assays, which is another variant of MTS, were used in several previous studies to assess the cytotoxicity of ND.

Lung A549 epithelial cells and HFL-1 fibroblasts were used to investigate the cytotoxicity of different sizes of ND using the MTT assay and showed that both the 5 and 100 nm ND-treated cells did not differ from the control significantly with these two cell types (Chao et al. 2007; Liu et al. 2007). Other studies used the MTT assay for macrophages, neuroblastoma cells, keratinocytes and PC-12 cells treated with functionalized or unfunctionalized ND and showed that the viability of these cells was not reduced by ND treatment (Schrand, Huang et al. 2007; Huang K et al. 2017). Another study by Schrand and coworkers (2007) showed a decrease in viability in macrophages, but not neuroblastoma cells, treated with ND (2-10 nm) at 50 µg/ml or higher (Schrand, Dai et al. 2007). However, the authors concluded that ND are biocompatible compared to the other carbon-based nanomaterials tested.

In these studies, and many others, the assay was performed directly or 48 hours after ND treatment. Evaluation of the cell metabolic activity directly after ND treatment may represent testing for acute cytotoxicity of ND. However, it can also be misleading because ND treatment may have a transient effect on cell metabolism which may return to its normal level with time. In addition, the toxic effects of the tested nanoparticle might be delayed until after being processed and interacting with cellular components. In my work, cell metabolic activity/viability was investigated in the two cell types directly after ND treatment, and after 1, 2, and 3 days after ND treatment. These experiments also investigated the effects of increasing the concentrations and treatment duration on the viability of macrophages. The MTS assay results suggest that these ND do not reduce cell viability significantly with the concentrations and treatment durations that were used.

The percent of dead cells in the ND-treated cells was assessed and compared to that of untreated cells as a negative control, and with the staurosporine- (10  $\mu$ M) or LPS-treated cells (100 ng/ml) as positive controls (Figure 4.13). The percent of dead cells in all ND-treated samples did not increase significantly. A previous study showed that 50 and 100  $\mu$ g/ml of small ND (<10 nm) were able to induce apoptotic cell death (Dworak et al. 2014). Their work also showed significant adverse effects on cell viability, proliferation, and DNA integrity in primary human lymphocytes. Prabhakar et al. (2017) suggested that cells couple endocytosis with exocytosis to eliminate the potential toxic effect of ND (Prabhakar et al. 2017). Different cells may have different endocytic or exocytic rates in addition to the uptake mechanism of different types of ND, which may explain inconsistency in results of ND toxicity studies.

## **5.6 Quantification of the ND uptake and uptake mechanism**

Quantification of the ND uptake using FACS showed that the uptake of ND increased in a time- and dose-dependent manner (Figure 4.14). Other studies also showed the time- and dose-dependent uptake of different sizes of ND in different cell types. The fluorescence intensities of 5 and 100 nm ND were previously compared using flow cytometry and it was shown that the intensity of the smaller particles was higher than that of the larger ones at equal doses with lung epithelial cells (Liu et al. 2007). Their study suggested that the higher fluorescence intensity of the smaller particles is due to the higher surface-to-volume ratio of the smaller particles or higher uptake of these particles. The uptake of ND by cells also depends on the cell type. In a study comparing the uptake of a 100 nm ND by cancer and non-cancer human lung cells, both cell types

internalized the ND but the cancerous cells showed a much higher uptake of ND as compared to the non-cancerous cells (Perevedentseva, Hong et al. 2013).

Nanoparticles are internalized into cells via different endocytic pathways depending on the nanoparticle characteristics and on the cell type being tested (Iversen et al. 2011). It is important to understand the mechanism of uptake to understand the possible fate of the nanoparticles inside the cell and their effects. Application of the endocytic pathways inhibitors showed that the ND uptake is mostly through an actin-dependent (about 40%) and clathrin-dependent (about 20%) endocytosis (Figure 4.15). Macrophages are professional phagocytes and thus, they can phagocytose small and large (Up to 10  $\mu\text{m}$ ) particles, but this does not preclude the uptake through other pathways.

Perevedentseva and coworkers (2013) showed that the uptake of 100 nm ND by lung adenocarcinoma cells and human bronchial epithelial cells was predominantly via clathrin-dependent endocytosis (Perevedentseva, Hong et al. 2013). Even though they used similar ND (100 nm), cell types were not like my cells and thus, this shows that different cells may use different uptake pathways to internalize ND. Another study also showed clathrin-dependent endocytosis of 140 nm ND by HeLa cells and fibroblastoid cells, but they also reported the involvement of actin filaments in the uptake process (Vaijayanthimala et al. 2009).

A recent study showed that internalization of 100 nm ND by RAW 264.7 macrophages was inhibited by about 23% by clathrin pathway inhibitor which is close to my findings for this inhibitor (Huang K et al. 2017). However, they did not find an effect of the actin inhibitor on ND internalization although they used a higher concentration of this

inhibitor (10  $\mu\text{g/ml}$  compared to 6  $\mu\text{g/ml}$  that I used). That study suggested clathrin-dependent endocytosis but not phagocytosis. These inhibitors are selective but not specific for any endocytic pathway and can still interfere with the other pathways. For example, actin is known to be required for clathrin-dependent endocytosis so inhibition of actin should affect the clathrin pathway (Kaksonen et al. 2006; Dutta and Donaldson 2012). In addition, the efficacy of these inhibitors varies in different cell types which can affect the results for determining the endocytic pathway of ND internalization.

The specific properties of ND in addition to the route by which ND are introduced to the body, affect their biodistribution and fate in the body. An *in vivo* study reported that about 60% of the 50 nm ND accumulated in the mouse liver, 0.5 hour after intravenous injection and lesser percentages were in the lung and spleen (Yuan et al. 2009). The study also showed that the values remained the same after 28 days and trace amounts of ND were detectable in urine and feces. Another study reported that the intradermally injected 100 nm ND are drained from injection sites by macrophages and accumulated in axillary lymph nodes (Vaijayanthimala et al. 2012). Su et al. (2017) used 100 nm ND to label human mesenchymal stem cells and quantitatively tracked the labeled cells or ND alone in miniature pigs and reported that most of the ND and ND-labeled cells accumulated in lungs after 48 hours of intravenous injection and lesser amounts in the liver then the spleen (Su et al. 2017). These studies showed the biodistribution of the 50 and 100 nm ND after intravenous and intradermal injections but it is still unknown whether these organs are able to eliminate or degrade the ND. In addition, the long-term effect of these entrapped particles is yet to be determined.

## 5.7 Effects of ND on gene expression

I investigated the inflammatory response in ND-treated macrophages at the mRNA level using RT-qPCRs of cytokines and chemokines. ND treatment (50  $\mu\text{g}/\text{ml}$  for 6-7 hours) did not induce a significant change in the expression of the tested cytokines although some differences were noted in the expression between the two cell types (Figure 4.17). The interleukin (IL) family member, IL1 $\beta$ , is a pro-inflammatory cytokine that is crucial for the inflammatory response and can affect almost all cell types in the body (Dinarello 1996). Therefore, secretion of the functional IL1 $\beta$  is strictly regulated and requires a priming step to induce expression of the pro-IL1 $\beta$ , which is an inactive precursor of IL1 $\beta$ , followed by further exposure to additional stimuli to induce its proteolytic cleavage by caspase 1 (Lopez-Castejon and Brough 2011). Activation of caspase 1 requires recruitment of the inflammasome which was shown to be formed in response to a range of nanoparticles; TiO<sub>2</sub>, SiO<sub>2</sub>, polystyrene, carbon nanotubes, carbon black, and silver nanoparticles (Yazdi et al. 2010; Lunov et al. 2011; Palomaki et al. 2011; Reissetter et al. 2011; Winter et al. 2011; Yang et al. 2012). These studies, and others, suggest that activation of inflammasome is a critical event in the immunotoxicity of nanoparticles which may worsen the immune response in subsequent exposures to pathogens (Wang X et al. 2013).

The inflammasome is a multimeric protein which can form in innate immune cells in response to certain stimuli (Guo et al. 2015). Activation of the inflammasome is a prerequisite for the activation of IL1 $\beta$  which in turn, can activate other immune cells and the subsequent activation of TNF $\alpha$ , IL6, CCL2, and CXCL2 (Dinarello 1996; Brabcova et al. 2014). The pro-inflammatory cytokine, TNF $\alpha$ , has central regulatory roles in the

inflammatory response and has been targeted in a range of inflammatory diseases (Bradley 2008). Most, if not all, inflammatory states have elevated levels of IL1, IL6, and TNF $\alpha$  (Scheller et al. 2011). IL6 can act as a pro or anti-inflammatory cytokine depending on its binding to the soluble or membrane-bound receptors, and it has roles in regulation of the transition from acute to chronic inflammation (Gabay 2006; Scheller et al. 2011). Chemokines such as CCL2 and CXCL2, are secreted by many cell types, but mainly by monocytes/macrophages in response to proinflammatory cytokines where they selectively recruit monocytes, neutrophils, and lymphocytes to the site of inflammation (Deshmane et al. 2009; Rouault et al. 2013).

Previous studies investigated the response of different cells (other than macrophages), to ND. Human natural killer (NK) cells were shown to upregulate their expression of IFN $\gamma$  but not TNF $\alpha$ , only in the presence of IL12 (Suarez-Kelly et al. 2017). Mytych et al. (2014) showed that ND (<10 nm) induced intracellular ROS production in total cell and in mitochondria of HeLa cells (Mytych et al. 2014). Intracellular ROS is an important signal for the activation of the inflammasome (Harijith et al. 2014). Secretion of cytokines were not altered in MSCs in response to ND treatment (Blaber et al. 2013).

Few studies have investigated the inflammatory response of macrophages to ND. Small (2-8 nm) ND were reported to have no effect on the expression of IL6, TNF $\alpha$ , and iNOS in RAW 264.7 murine macrophages (Huang et al. 2008). Another study using different sizes of ND (6, 60, 100, 250, and 500 nm) to assess expression of IL1 $\beta$ , TNF $\alpha$ , CXCL2, CCL2, platelet-derived growth factor (PDGF), and VEGF at the mRNA level in RAW 264.7 cells reported that ND treatment caused a down regulation in the tested genes irrespective to particle size (Thomas et al. 2012). Human monocytes were shown to



increase TNF $\alpha$  expression but not IFN $\gamma$ , in response to ND without displaying any increase in the expression of activation markers on their surfaces (Suarez-Kelly et al. 2017). Although I noted some upregulation in the inflammatory genes expression in J774A.1 cell line, my RT-qPCR results did not show any significant difference in gene expression in J774A.1 or BMDM which was not tested previously in these cell types. The difference in macrophage response to ND could be due to differences in the size or properties of the used ND or differences between cell types. My results are in agreement with a recent study that showed no significant production of pro-inflammatory cytokines in 100 nm ND-treated Raw 264.7 macrophages (Huang K et al. 2017).

Although I did not find a significant upregulation in the expression of CCL2 in response to ND at the mRNA level, a significant increase was noted at the protein level (Figure 4.18). The stability of the mRNA or coupling the transcription with translation in addition to the time that it is required for this chemokine to be transcribed and translated into a functional protein, may explain the increased protein concentration but not the mRNA levels. This chemokine is involved in the recruitment of monocytes, neutrophils, and lymphocytes to the site of inflammation and stimulate the release of IL1 and IL6 from macrophages/monocytes (Deshmane et al. 2009; Rouault et al. 2013). This chemokine was shown to be downregulated after exposure of RAW 264.7 macrophages to 60 nm ND for 24 hours (Thomas et al. 2012). Differences between cell types and ND types might cause this inconsistency in the expression results of CCL2. The extreme hardness of ND suggest that these particles may not be susceptible to biodegradation, though, susceptibility of ND to biodegradation is still unknown (Bhattacharya et al. 2016). The

increased expression of CCL2 by macrophages could be due to the inability of these cells to degrade ND and thus, trying to recruit other cells to eliminate them.

### **5.8 Effects of ND on macrophage response to LPS**

To assess the ability of ND-treated cells to respond to conventional immunogen, ND-treated and untreated cells were exposed to LPS, the TLR4 ligand, and their responses were compared with RT-qPCR. Both the ND-treated and untreated cells responded to the LPS with no significant difference between their responses (Figure 4.19). A study on the effects of gold nanoparticles on macrophage function showed that these particles inhibit the production of pro-inflammatory cytokines and attenuate the response of RAW264.7 and BMDM to CpG (TLR9 ligand) with some variations in the responses of the two cell types (Tsai et al. 2012). To my knowledge, the effects of ND on macrophages functions and more specifically, their response to LPS, has not been investigated. I found that ND-treated cells respond to LPS normally, like the untreated cells, at the concentration (50  $\mu\text{g/ml}$ ) and time of incubation (4 hours with ND then 3 hours with LPS) used. The effects of different ND, on functions of different cell types may vary and yet to be explored. In addition, other immune markers could be affected in macrophages exposed to ND and their responses to other immunogens could be affected after ND treatment.

### **5.9 Effects of ND on macrophage endocytic activity**

Another cell function was also investigated. ND-treated and untreated macrophages were exposed to fluorescently-labeled dextran particles and the

internalized dextran was measured with FACS. The uptake of dextran was significantly reduced in ND-treated cells irrespective to the ND concentration (Figure 4.20). Kodali et al. (2013) showed that interactions of macrophages with amorphous silica or superparamagnetic iron oxide nanoparticles caused extensive differential gene expression in response to LPS and reduced the cells' ability to phagocytose *Streptococcus pneumoniae* significantly (Kodali et al. 2013). Interestingly, the two nanoparticles did not cause direct cytotoxicity or production of pro-inflammatory cytokines; rather, they impaired the macrophages' responses and ability to transition from the M1 to M2 phenotype (Kodali et al. 2013). Iron oxide nanoparticles did not induce the production of TNF $\alpha$ , IL6, or IL1 $\beta$  in primary human monocytes; nonetheless, they suppressed the LPS-induced production of the pro-inflammatory cytokines (Grosse et al. 2016). Amino-functionalized polystyrene nanoparticles were shown to inhibit phagocytosis of *E. coli* in M1 and M2 macrophages and again, no reduction in cell viability or expression of M1 surface markers (Fuchs et al. 2016). Macrophages exposed to TiO<sub>2</sub> nanoparticles were reported to have lower chemotactic, phagocytic, and bactericidal activities with no cytotoxicity in these cells while inducing the expression of pro-inflammatory cytokines and inhibition of M2 markers (Huang C et al. 2017). These studies showed that nanoparticles can impair the innate immune functions in macrophages or modulate their activation state but not necessarily cause cell death.

The effects of ND on macrophages phagocytic or more generally, endocytic activity has not been studied. My results showed a significant reduction in the macrophages endocytic function with all the ND concentrations used. The mechanism by which these particles affect endocytosis in macrophages is yet to be investigated. A recent study on

the effect of ND on macrophage cell line, RAW 264.7, bactericidal activity showed that ND-treated macrophages were able to decrease the number of *E. coli* colonies and reported no effect of ND treatment (Huang K et al. 2017). However, that study did not investigate ND effects on other macrophage functions.

### **5.10 Differentiation of BMDM in the presence of ND**

Effects of ND on differentiating bone marrow cells has not been studied and therefore, I exposed the isolate bone marrow cells to ND (50 µg/ml) and assessed their morphology and expression of the macrophage surface markers. The results showed that ND treatment did not affect the cell morphology or the percent of cells expressing the macrophage surface markers (Figures 4.21, 4.22, and 4.23). However, the number of the surface markers on each cell was reduced significantly (Figure 4.24). These results suggest that most of the cells were able to acquire the macrophage phenotype (were double positive for the two markers, CD11b and F4/80), while showing a reduction in the expression of these markers which may indicate some effects on macrophage function.

The macrophage surface marker, CD11b, is a subunit of macrophage-1 antigen (Mac-1) which mediates cell adhesion, spreading and migration among other immune processes (Solovjov et al. 2005). Mac-1, also known as complement receptor 3 (CR3), can bind to inactive complement fragment 3 (iC3b) and is expressed on many leukocytes (Todd 1996). In addition to its roles in immune processes, CD11b has been used to identify macrophages when it is expressed along with F4/80 on the cell surface (Austyn and Gordon 1981; Weischenfeldt and Porse 2008). The reduction in the expression of

CD11b and F4/80 on macrophages may indicate an inhibition or attenuation of some immune functions such as migration and binding to complement components.

Monocytes differentiate from myeloid progenitor cells in the bone marrow and leave to the blood where they circulate for days before they move to other tissues (Murphy 2011). Upon injury or exposure to an immunogen, monocytes migrate from the blood into the injured tissue and differentiate into mature macrophages where they participate in the immune response. Immune cells, including macrophages, present at the injured or inflamed location secrete inflammatory cytokines and chemokines to recruit and activate other immune cells. Recruitment of immune cells through chemokine gradient to the site depends on the ability of the cell to express adhesion molecules on its surface to promote migration. Exposure of the cells to ND altered their ability of expressing these markers by reducing the number of each marker per cell and maybe other surface receptors or activation markers that would need further investigations.

Studies on the effect of ND on immune cells function and differentiation have been elusive. Huang K et al. (2017) investigated the effect of HPHT ND (100 nm) on RAW 264.7 macrophages bactericidal function (Huang K et al. 2017). They found that the number of bacterial colonies formed in the ND-treated sample was similar to that in the control cells. The authors concluded that these ND are biocompatible and do not affect macrophage bactericidal function (Huang K et al. 2017).

A recent study on the effects of nanoparticles on human THP-1 macrophages function showed that phagocytosis of opsonized beads was decreased while phagocytosis of unopsonized beads was increased by SiO<sub>2</sub>, FeO<sub>3</sub>, CeO<sub>2</sub>, TiO<sub>2</sub>, and Ag/SiO<sub>2</sub> nanoparticles treatments, while ZnO reduced both (deLoid et al. 2016). I suggest

that the reduction in phagocytosis of the opsonized beads could be due to a reduction in the expression of complement receptors, such as Mac-1, or other surface receptors on these macrophages in response to nanoparticles. Comparative work with ND may reveal their effects on phagocytosis of opsonized and unopsonized particles. Another study showed that introduction of ND into chicken embryos led to a significant reduction in the vascularization of the heart and the density of branched vessels (Wierzbicki et al. 2013). Their work showed that ND can affect differentiation through downregulation of basic fibroblast growth factor during embryogenesis leading to a reduction in the formation of new blood vessels. This confirms that ND can affect the ability of cells to express certain genes during differentiation which is in agreement of my finding regarding the ability of macrophages to express CD11b and F4/80 during differentiation after ND treatment. On the other hand, ND were reported to have no negative effects on embryonic development of *C. elegans* (Mohan et al. 2010). Reduction in CD11b and F4/80 in BMDM could be due to ND interfering with signaling cascades that usually induce the expression of these markers. Bone marrow cells are usually incubated with M-CSF to differentiate into BMDM under normal culture conditions. Exposure of these cells to ND before they differentiate into BMDM might affect their responses to M-CSF induction, which is the driving factor towards macrophage differentiation.

Several studies investigated the cytotoxicity of ND using different viability assays and most of these reported ND biocompatibility in different cell types. However, fewer studies focused on the effects of ND on immune cell functions. The effect of ND on differentiating cells may vary depending on the type of ND and the model system used. Meanwhile, their effect on differentiating bone marrow cells has not been investigated.

The above-mentioned studies showed an inconsistency in results which could be due to the nature of the tested ND in addition to differences in the animal model or cell type. With the wide range of ND sizes, shapes, surface chemistry and charge, it is impossible to generalize the toxic/nontoxic effect of different types of ND.

### **5.11 Size-dependent effects**

Nanoparticles are currently produced with different sizes of the material to find the suitable size for the intended application. The size-dependent toxicity of nanoparticles has been reported in several studies (Carlson et al. 2008; Manolova et al. 2008; Kunzmann et al. 2011; Tsai et al. 2012). Small ND (6-100 nm) has also been shown to induce toxic effects in different cell types (Thomas et al. 2012; Dworak et al. 2014; Keremidarska et al. 2014; Mytych et al. 2014; Mytych et al. 2015). In these studies, ND induced a reduction in metabolic activity and cell viability, inhibition of proliferation, DNA oxidative damage, or apoptosis among other toxic effects. On the other hand, other studies reported no toxic effects of 2-100 nm ND (Chao et al. 2007; Liu et al. 2007; Schrand, Huang et al. 2007; Huang K et al. 2017). Although it's hard to generalize but, the 100 nm ND seems to be at the border between the toxic/nontoxic effects. Small ND (such as 5 nm) have higher surface-to-volume ratio than the larger particles (100 nm) and they may have higher uptake by the same cell type at the same doses than the larger particles (Liu et al. 2007). These differences between smaller and larger particles may indicate more potential interactions of the smaller particles with biomolecules and processes and thus, more potential effects on cells.

Small (<10 nm) ND may enter the cell through endocytic or non-endocytic pathways (Passive transport or diffusion). Diffusing ND can spread in the cytoplasm while the endocytosed particles were shown to co-localize with endosomes/lysosomes (Huang K et al. 2017). The particle size of ND has not been linked with the ability of ND to enter to the nucleus although the smaller particles (<50 nm) can, theoretically, fit into the nuclear pore complex. Small (2-10 nm) and large (100 nm) ND were shown, in my work, and other studies to localize to the cytoplasm but not into the nucleus of different cell types (Yu et al. 2005; Liu et al. 2007; Liu et al. 2009; Li et al. 2010; Perevedentseva, Hong et al. 2013). This finding implies that any toxic effect from the small or large ND is not induced by direct interactions of ND with DNA or other nuclear components.

The size of ND does not seem to be the factor that would determine whether ND will induce an inflammatory response in cells or not. The macrophage cell line RAW 264.7 has been shown to assess the inflammatory response to ND and results showed that small (2-8 nm) ND did not affect the expression of inflammatory cytokines while varying sizes (6-500 nm) ND have been shown to downregulate the expression of these genes in the same cell line (Huang et al. 2008; Thomas et al. 2012). The different effect of ND in these macrophages could be due to differences in the type of ND used in these studies. In addition, the 100 nm ND did not affect the expression of inflammatory cytokine in that same cell line in a recent study which agrees with my results in J774A.1 and BMDM (Huang K et al. 2017).



## CHAPTER 6

### CONCLUSION AND FUTURE WORK

Utilization of ND in the biomedical field is gaining more interest with highly promising results for *in vivo* imaging and theragnostic applications. These applications require more in-depth investigations on the safety and interactions of ND with different cells and systems at the molecular level. I hypothesized that ND can affect macrophages and interfere with their functions and I aimed to study interactions of ND with these cells to better understand the potential impact of ND on the immune system. I found that ND do not affect the macrophages' morphology or cell viability significantly. My results show that ND can interfere with MTT and MTS assay results due to the ability of ND to absorb light at different wavelengths. Fluorescence of ND is beneficial for ND tracking inside the cell and for imaging and quantification of ND uptake among others. However, this fluorescence can be problematic because it can interfere with fluorescence signals from other assays reagents such as the red-dead cell stain in the apoptosis assay kit. During my search for viability assays, all the assays I found were based on measuring absorbance or fluorescence signals of assay reagents to indicate cell viability. Therefore, care should be taken when interpreting colorimetric and fluorometric assays results because ND can give false positive signals which may be hard to avoid in such assays. The uptake of ND by macrophages via phagocytic and clathrin-dependent endocytosis, is time- and dose-dependent. These particles localize to the cytoplasm of macrophages without entering the nucleus or inducing an inflammatory response. Exposure of

macrophages to ND do not affect the expression of IL1 $\beta$ , IL4, IL6, IL10, IL12, TNF $\alpha$ , iNOS, CCL2, or CXCL2 at the mRNA level significantly. On the other hand, the chemokine CCL2 was upregulated at the protein level. Exposure of macrophages to ND did not affect or interfere with their responses to LPS, at least, in the immune markers that were tested. However, the ability of macrophages to endocytose dextran particles was significantly reduced at high and low ND doses. In addition, pre-treatment of the isolated bone marrow cells with ND before they differentiate into BMDM did not cause changes in their morphology or the percent of cells expressing macrophage surface markers. Nonetheless, ND treatment reduced the number of surface markers (CD11b and F4/80) expressed per cell.

My results suggest that ND are not cytotoxic to macrophages at the concentrations used. On the other hand, ND can interfere with macrophage functions and differentiation. Future work will investigate other cell functions such as the required steps for antigen presentation (Figure 1.7, recognition, internalization, acidification and fusion with lysosomes, degradation, and expression on MHC-II on cell surface), and explore the mechanisms by which ND are interfering with macrophages functions. The downstream effect of the reduction in endocytic activity and reduction in macrophages surface markers expression are yet to be determined. Response of these cells to other immunogens such as CpG (TLR9 ligand), might be affected by ND treatment and need to be studied. In addition, a more comprehensive study to evaluate gene expression patterns using a microarray or RNA sequencing of mRNA, may reveal changes in gene expression in ND-treated cells which may affect vital biological or immunological pathways in these cells. ND with different sizes and surface chemistries may have different effects on

macrophages and should be studied. In addition, these particles may be internalized into macrophages through different endocytic pathways. Other approaches to determine the endocytic pathway include genetic blocking of specific genes or proteins to selectively block a specific pathway which would be more reliable than the use of the endocytic pathway inhibitors (Dutta and Donaldson 2012). Other than macrophages, interactions of ND with other immune cells and their effects on the expression of other immune mediators are also needed. Due to the key roles of macrophages in the immune system, I believe that the effects of ND on these cells will impact the overall immune system function. However, these effects could be different in the presence of other immune system components and therefore the impact of ND on the immune system should be investigated in animal models to better assess the immunocompatibility of ND. Previous *in vivo* study showed that macrophages drain ND (100 nm) from injection sites to the axillary lymph nodes (Vaijayanthimala et al. 2012). However, the fate of ND-loaded macrophages is still unknown. In addition, other *in vivo* studies reported that ND accumulate in the lung, liver, and the spleen but these studies did not investigate the long-term effect of ND in these organs or their ability to eliminate or degrade them (Yuan et al. 2009; Su et al. 2017). The size of these particles (100 nm) suggest that they may not be eliminated with urine. In addition, their outstanding hardness suggest that they may not be biodegradable and thus, they may accumulate in vital organs for a long time. Therefore, a longer-term *in vivo* study to determine the fate of ND in the body is required. Other types of nanoparticles (Titanium dioxide), has been shown to prime a specific activation state in macrophages where these cells became inflammatory and decreased the macrophage chemotactic, bactericidal, and phagocytic activity (Huang C et al. 2017). Although ND did not induce

inflammatory state in macrophages, some immune functions of macrophages are affected and additional studies are needed to investigate the other macrophage functions. These particles could be inducing a special state in macrophages where cells are not dead, but their responsiveness and some functions are affected by ND treatment.

## REFERENCES

- Abbas AK, Lichtman AHH, Pillai S. 2015. Cellular and molecular immunology. 8th ed. Philadelphia (PA): Elsevier Health Sciences.
- Ajayan PM. 1999. Nanotubes from carbon. Chemical Reviews. 99(7):1787-1800.
- Akiladevi D, Basak S. 2011. Carbon nanotubes (CNTs) production, characterization and its applications. International Journal of Advances in Pharmaceutical Sciences. 1(3):187-195.
- Almeida JL, Cole KD, Plant AL. 2016. Standards for cell line authentication and beyond. PLoS Biology. 14(6):[9 p.] e1002476.
- Ando Y, Zhao X. 2006. Synthesis of Carbon Nanotubes by Arc-Discharge Method. New diamond frontier carbon technol. 16(3): 123-137.
- Arbogast JW, Darmany AP, Foote CS, Diederich FN, Whetten RL, Rubin Y, Alvarez MM, Anz SJ. 1991. Photophysical properties of sixty atom carbon molecule (C<sub>60</sub>). The Journal of Physical Chemistry. 95(1):11-12.
- Arranja AG, Pathak V, Lammers T, Shi Y. 2017. Tumor-targeted nanomedicines for cancer theranostics. Pharmacological Research. 115(Supplement C):87-95.
- Austyn JM, Gordon S. 1981. F4/80, a monoclonal antibody directed specifically against the mouse macrophage. European journal of immunology. 11(10):805-815.
- Baker PA, Thompson RG, Catledge SA. 2016. A wear simulation study of nanostructured CVD diamond-on-diamond articulation involving concave/convex mating surfaces. Journal of coatings technology and research. 13(2):385-393.
- Bellingan GJ, Caldwell H, Howie SE, Dransfield I, Haslett C. 1996. In vivo fate of the inflammatory macrophage during the resolution of inflammation: inflammatory macrophages do not die locally, but emigrate to the draining lymph nodes. Journal of immunology (Baltimore, Md : 1950). 157(6):2577-2585.

- Benoit M, Desnues B, Mege JL. 2008. Macrophage polarization in bacterial infections. *J Immunol.* 181(6):3733-3739.
- Bhattacharya K, Mukherjee SP, Gallud A, Burkert SC, Bistarelli S, Bellucci S, Bottini M, Star A, Fadeel B. 2016. Biological interactions of carbon-based nanomaterials: from coronation to degradation. *Nanomedicine.* 12(2):333-351.
- Bisker G, Iverson NM, Ahn J, Strano MS. 2015. A pharmacokinetic model of a tissue implantable insulin sensor. *Adv Healthc Mater.* 4(1):87-97.
- Blaber SP, Hill CJ, Webster RA, Say JM, Brown LJ, Wang S-C, Vesey G, Herbert BR. 2013. Effect of labeling with iron oxide particles or nanodiamonds on the functionality of adipose-derived mesenchymal stem cells. *Plos One.* 8(1):[10 p.]. e52997.
- Bosi S, Da Ros T, Spalluto G, Prato M. 2003. Fullerene derivatives: an attractive tool for biological applications. *European Journal of Medicinal Chemistry.* 38(11):913-923.
- Brabcova E, Kolesar L, Thorburn E, Striz I. 2014. Chemokines induced in human respiratory epithelial cells by IL-1 family of cytokines. *Folia biologica.* 60(4):180-186.
- Bradley JR. 2008. TNF-mediated inflammatory disease. *The Journal of pathology.* 214(2):149-160.
- Brown DM, Kinloch IA, Bangert U, Windle AH, Walter DM, Walker GS, Scotchford CA, Donaldson K, Stone V. 2007. An in vitro study of the potential of carbon nanotubes and nanofibres to induce inflammatory mediators and frustrated phagocytosis. *Carbon.* 45(9):1743-1756.
- Cai Y, Postnikova EN, Bernbaum JG, Yú S, Mazur S, Deiuliis NM, Radoshitzky SR, Lackemeyer MG, McCluskey A, Robinson PJ et al. 2015. Simian hemorrhagic fever virus cell entry is dependent on CD163 and uses a clathrin-mediated endocytosis-like pathway. *Journal of Virology.* 89(1):844-856.

- Carlson C, Hussain SM, Schrand AM, K. Braydich-Stolle L, Hess KL, Jones RL, Schlager JJ. 2008. Unique cellular interaction of silver nanoparticles: size-dependent generation of reactive oxygen species. *The Journal of Physical Chemistry B*. 112(43):13608-13619.
- Caster JM, Patel AN, Zhang T, Wang A. 2017. Investigational nanomedicines in 2016: a review of nanotherapeutics currently undergoing clinical trials. *Wiley interdisciplinary reviews Nanomedicine and nanobiotechnology*. 9(1):[18 p.].
- Catledge SA, Thomas V, Vohra YK. 2013. Nanostructured diamond coatings for orthopaedic applications. *Woodhead publishing series in biomaterials*. 2013:105-150.
- Cha C, Shin SR, Annabi N, Dokmeci MR, Khademhosseini A. 2013. Carbon-based nanomaterials: multifunctional materials for biomedical engineering. *ACS nano*. 7(4):2891-2897.
- Chamberlain LM, Godek ML, Gonzalez-Juarrero M, Grainger DW. 2009. Phenotypic non-equivalence of murine (monocyte-) macrophage cells in biomaterial and inflammatory models. *Journal of Biomedical Materials Research Part A*. 88A(4):858-871.
- Chao J-I, Perevedentseva E, Chung P-H, Liu K-K, Cheng C-Y, Chang C-C, Cheng C-L. 2007. Nanometer-sized diamond particle as a probe for biolabeling. *Biophysical Journal*. 93(6):2199-2208.
- Chaplin DD. 2010. Overview of the immune response. *The Journal of allergy and clinical immunology*. 125(2 Suppl 2): S3-23.
- Choi HS, Ashitate Y, Lee JH, Kim SH, Matsui A, Insin N, Bawendi MG, Semmler-Behnke M, Frangioni JV, Tsuda A. 2010. Rapid translocation of nanoparticles from the lung airspaces to the body. *Nat Biotech*. 28(12):1300-1303.
- Chow EK, Zhang XQ, Chen M, Lam R, Robinson E, Huang H, Schaffer D, Osawa E, Goga A, Ho D. 2011. Nanodiamond therapeutic delivery agents mediate

- enhanced chemoresistant tumor treatment. *Science translational medicine*. 3(73):[11p.]. 73ra21.
- Colin S, Chinetti-Gbaguidi G, Staels B. 2014. Macrophage phenotypes in atherosclerosis. *Immunological Reviews*. 262(1):153-166.
- Conner SD, Schmid SL. 2003. Regulated portals of entry into the cell. *Nature*. 422(6927):37-44.
- da Silva RP, Gordon S. 1999. Phagocytosis stimulates alternative glycosylation of macrosialin (mouse CD68), a macrophage-specific endosomal protein. *The Biochemical journal*. 338 (Pt 3):687-694.
- Davies G, Hamer MF. 1976. Optical studies of the 1.945 eV vibronic band in diamond. *Proceedings of the Royal Society of London Series A, Mathematical and Physical Sciences*. 348(1653):285-298.
- Davies G, Lawson SC, Collins AT, Mainwood A, Sharp SJ. 1992. Vacancy-related centers in diamond. *Physical review B, Condensed matter*. 46(20):13157-13170.
- Davies LC, Jenkins SJ, Allen JE, Taylor PR. 2013. Tissue-resident macrophages. *Nat Immunol*. 14(10):986-995.
- Davies LC, Taylor PR. 2015. Tissue-resident macrophages: then and now. *Immunology*. 144(4):541-548.
- Davis MJ, Tsang TM, Qiu Y, Dayrit JK, Freij JB, Huffnagle GB, Olszewski MA. 2013. Macrophage M1/M2 polarization dynamically adapts to changes in cytokine microenvironments in *Cryptococcus neoformans* infection. *mBio*. 4(3):[10 p.]. e00264-00213.
- DeLoid G, Casella B, Pirela S, Filoramo R, Pyrgiotakis G, Demokritou P, Kobzik L. 2016. Effects of engineered nanomaterial exposure on macrophage innate immune function. *NanoImpact*. 2:70-81.



- Deshmane SL, Kremlev S, Amini S, Sawaya BE. 2009. Monocyte chemoattractant protein-1 (mcp-1): an overview. *Journal of Interferon & Cytokine Research*. 29(6):313-326.
- Dinareello CA. 1996. Biologic basis for interleukin-1 in disease. *Blood*. 87(6):2095-2147.
- Duluc D, Delneste Y, Tan F, Moles MP, Grimaud L, Lenoir J, Preisser L, Anegon I, Catala L, Ifrah N et al. 2007. Tumor-associated leukemia inhibitory factor and IL-6 skew monocyte differentiation into tumor-associated macrophage-like cells. *Blood*. 110(13):4319-4330.
- Dutta D, Donaldson JG. 2012. Search for inhibitors of endocytosis: Intended specificity and unintended consequences. *Cellular Logistics*. 2(4):203-208.
- Dutta D, Sundaram SK, Teeguarden JG, Riley BJ, Fifield LS, Jacobs JM, Addleman SR, Kaysen GA, Moudgil BM, Weber TJ. 2007. Adsorbed proteins influence the biological activity and molecular targeting of nanomaterials. *Toxicological sciences: an official journal of the Society of Toxicology*. 100(1):303-315.
- Dworak N, Wnuk M, Zebrowski J, Bartosz G, Lewinska A. 2014. Genotoxic and mutagenic activity of diamond nanoparticles in human peripheral lymphocytes in vitro. *Carbon*. 68:763-776.
- Eatemadi A, Daraee H, Karimkhanloo H, Kouhi M, Zarghami N, Akbarzadeh A, Abasi M, Hanifehpour Y, Joo SW. 2014. Carbon nanotubes: properties, synthesis, purification, and medical applications. *Nanoscale Research Letters*. 9(1):393-405.
- Elias KL, Price RL, Webster TJ. 2002. Enhanced functions of osteoblasts on nanometer diameter carbon fibers. *Biomaterials*. 23(15):3279-3287.
- Fang CY, Vaijayanthimala V, Cheng CA, Yeh SH, Chang CF, Li CL, Chang HC. 2011. The exocytosis of fluorescent nanodiamond and its use as a long-term cell tracker. *Small*. 7(23):3363-3370.

- Feng L, Wu L, Qu X. 2013. New horizons for diagnostics and therapeutic applications of graphene and graphene oxide. *Advanced Materials*. 25(2):168-186.
- Ferrante CJ, Leibovich SJ. 2012. Regulation of macrophage polarization and wound healing. *Advances in Wound Care*. 1(1):10-16.
- Fisher C, E. Rider A, Jun Han Z, Kumar S, Levchenko I, Ostrikov K. 2012. Applications and nanotoxicity of carbon nanotubes and graphene in biomedicine. *Journal of Nanomaterials*. 2012:[19 p.].
- Friedman SH, DeCamp DL, Sijbesma RP, Srdanov G, Wudl F, Kenyon GL. 1993. Inhibition of the HIV-1 protease by fullerene derivatives: model building studies and experimental verification. *Journal of the American Chemical Society*. 115(15):6506-6509.
- Friedman SH, Ganapathi PS, Rubin Y, Kenyon GL. 1998. Optimizing the binding of fullerene inhibitors of the HIV-1 protease through predicted increases in hydrophobic desolvation. *Journal of Medicinal Chemistry*. 41(13):2424-2429.
- Fu CC, Lee HY, Chen K, Lim TS, Wu HY, Lin PK, Wei PK, Tsao PH, Chang HC, Fann W. 2007. Characterization and application of single fluorescent nanodiamonds as cellular biomarkers. *Proc Natl Acad Sci U S A*. 104(3):727-732.
- Fuchs A-K, Syrovets T, Haas KA, Loos C, Musyanovych A, Mailänder V, Landfester K, Simmet T. 2016. Carboxyl- and amino-functionalized polystyrene nanoparticles differentially affect the polarization profile of M1 and M2 macrophage subsets. *Biomaterials*. 85(Supplement C):78-87.
- Gabay C. 2006. Interleukin-6 and chronic inflammation. *Arthritis Research & Therapy*. 8(Suppl 2):S3-S3.
- Geim AK, Novoselov KS. 2007. The rise of graphene. *Nat Mater*. 6(3):183-191.
- Gerondopoulos A, Jackson T, Monaghan P, Doyle N, Roberts LO. 2010. Murine norovirus-1 cell entry is mediated through a non-clathrin-, non-caveolae-,

- dynammin- and cholesterol-dependent pathway. The Journal of general virology. 91(Pt 6):1428-1438.
- Ghoneum M, Pan D, Katano H. 2014. Enhancement of human T lymphocyte proliferation by nanodiamond and nanoplatinum in liquid, DPV576. JSM Nanotechnol Nanomed. 2(2): 1031-1036.
- Gibson AE, Noel RJ, Herlihy JT, Ward WF. 1989. Phenylarsine oxide inhibition of endocytosis: effects on asialofetuin internalization. The American journal of physiology. 257(2 Pt 1):C182-184.
- Giersing BK, Dastgheyb SS, Modjarrad K, Moorthy V. 2016. Status of vaccine research and development of vaccines for *Staphylococcus aureus*. Vaccine. 34(26):2962-2966.
- Gong H, Anasori B, Dennison CR, Wang K, Kumbur EC, Strich R, Zhou JG. 2015. Fabrication, biodegradation behavior and cytotoxicity of Mg-nanodiamond composites for implant application. Journal of Materials Science: Materials in Medicine. 26(2):110.
- Gordon S. 2003. Alternative activation of macrophages. Nat Rev Immunol. 3(1):23-35.
- Gracio JJ, Fan QH, Madaleno JC. 2010. Diamond growth by chemical vapour deposition. Journal of Physics D: Applied Physics. 43(37):[57 p.]. 374017.
- Gregory A, Williamson D, Titball R. 2013. Vaccine delivery using nanoparticles. Frontiers in Cellular and Infection Microbiology. 3:[13 p.].
- Grosse S, Stenvik J, Nilsen AM. 2016. Iron oxide nanoparticles modulate lipopolysaccharide-induced inflammatory responses in primary human monocytes. International Journal of Nanomedicine. 11:4625-4642.
- Gruber A, Dräbenstedt A, Tietz C, Fleury L, Wrachtrup J, Borczykowski Cv. 1997. Scanning confocal optical microscopy and magnetic resonance on single defect centers. Science. 276(5321):2012-2014.

- Guo H, Callaway JB, Ting JPY. 2015. Inflammasomes: mechanism of action, role in disease, and therapeutics. *Nature Medicine*. 21:677-687.
- Gutensohn K, Beythien C, Bau J, Fenner T, Grewe P, Koester R, Padmanaban K, Kuehn P. 2000. In vitro analyses of diamond-like carbon coated stents. *Thrombosis Research*. 99(6):577-585.
- Harijith A, Ebenezer DL, Natarajan V. 2014. Reactive oxygen species at the crossroads of inflammasome and inflammation. *Frontiers in physiology*. 5:[11 p.].
- Haziza S, Mohan N, Loe-Mie Y, Lepagnol-Bestel A-M, Massou S, Adam M-P, Le XL, Viard J, Plancon C, Daudin R et al. 2017. Fluorescent nanodiamond tracking reveals intraneuronal transport abnormalities induced by brain-disease-related genetic risk factors. *Nat Nano*. 12(4):322-328.
- Hemelaar SR, de Boer P, Chipaux M, Zuidema W, Hamoh T, Martinez FP, Nagl A, Hoogenboom JP, Giepmans BNG, Schirhagl R. 2017. Nanodiamonds as multi-purpose labels for microscopy. *Scientific Reports*. 7:720-728.
- Hirsch A, Brettreich M. 2005. *The Chemistry of the Fullerenes*. Germany: Wiley-VCH Verlag GmbH. Chapter 1, The Parent Fullerenes; p. 1-36.
- Horbach SPJM, Halffman W. 2017. The ghosts of HeLa: How cell line misidentification contaminates the scientific literature. *Plos one*. 12(10):[16 p.]. e0186281.
- Howard JB, McKinnon JT, Makarovskiy Y, Lafleur AL, Johnson ME. 1991. Fullerenes C60 and C70 in flames. *Nature*. 352(6331):139-141.
- Huang C, Sun M, Yang Y, Wang F, Ma X, Li J, Wang Y, Ding Q, Ying H, Song H et al. 2017. Titanium dioxide nanoparticles prime a specific activation state of macrophages. *Nanotoxicology*. 11(6):737-750.
- Huang H, Pierstorff E, Osawa E, Ho D. 2008. Protein-mediated assembly of nanodiamond hydrogels into a biocompatible and biofunctional multilayer nanofilm. *ACS nano*. 2(2):203-212.

- Huang H-C, Barua S, Sharma G, Dey SK, Rege K. 2011. Inorganic nanoparticles for cancer imaging and therapy. *Journal of Controlled Release*. 155(3):344-357.
- Huang KJ, Lee CY, Lin YC, Lin CY, Perevedentseva E, Hung SF, Cheng CL. 2017. Phagocytosis and immune response studies of macrophage-nanodiamond Interactions in vitro and in vivo. *Journal of biophotonics*. 1(2):[12 p.].
- Igarashi R, Yoshinari Y, Yokota H, Sugi T, Sugihara F, Ikeda K, Sumiya H, Tsuji S, Mori I, Tochio H et al. 2012. Real-Time Background-Free Selective Imaging of Fluorescent Nanodiamonds in Vivo. *Nano letters*. 12(11):5726-5732.
- Iijima S. 1991. Helical microtubules of graphitic carbon. *Nature*. 354(6348):56-58.
- Inoué S. 2006. Foundations of confocal scanned imaging in light microscopy. In: Pawley J, editor. *Handbook of biological confocal microscopy*. Boston (MA): Springer; p. 1-19.
- Iversen T-G, Skotland T, Sandvig K. 2011. Endocytosis and intracellular transport of nanoparticles: Present knowledge and need for future studies. *Nano Today*. 6(2):176-185.
- Iverson NM, Barone PW, Shandell M, Trudel LJ, Sen S, Sen F, Ivanov V, Atolia E, Farias E, McNicholas TP et al. 2013. In vivo biosensing via tissue-localizable near-infrared-fluorescent single-walled carbon nanotubes. *Nat Nano*. 8(11):873-880.
- Kaksonen M, Toret CP, Drubin DG. 2006. Harnessing actin dynamics for clathrin-mediated endocytosis. *Nat Rev Mol Cell Biol*. 7(6):404-414.
- Kaur G, Dufour JM. 2012. Cell lines: Valuable tools or useless artifacts. *Spermatogenesis*. 2(1):1-5.
- Kaur R, Badea I. 2013. Nanodiamonds as novel nanomaterials for biomedical applications: drug delivery and imaging systems. *Int J Nanomedicine*. 8:203-220.
- Kaushik BK, Majumder MK. 2015. Carbon Nanotube Based VLSI Interconnects. India: Springer. Chapter 2, Carbon Nanotube: Properties and Applications; p. 17-37

- Keremidarska M, Ganeva A, Mitev D, Hikov T, Presker R, Pramatarova L, Krasteva N. 2014. Comparative study of cytotoxicity of detonation nanodiamond particles with an osteosarcoma cell line and primary mesenchymal stem cells. *Biotechnology, Biotechnological Equipment*. 28(4):733-739.
- Khabashesku VN, Margrave JL, Barrera EV. 2005. Functionalized carbon nanotubes and nanodiamonds for engineering and biomedical applications. *Diamond and Related Materials*. 14(3):859-866.
- Khang D, Sato M, Price RL, Ribbe AE, Webster TJ. 2006. Selective adhesion and mineral deposition by osteoblasts on carbon nanofiber patterns. *International Journal of Nanomedicine*. 1(1):65-72.
- Kodali V, Littke MH, Tilton SC, Teeguarden JG, Shi L, Frevert CW, Wang W, Pounds JG, Thrall BD. 2013. Dysregulation of macrophage activation profiles by engineered nanoparticles. *ACS nano*. 7(8):6997-7010.
- Kolosnjaj-Tabi J, Volatron J, Gazeau F. 2017. Basic principles of in vivo distribution, toxicity, and degradation of prospective inorganic nanoparticles for imaging. In: Bulte JWM, Modo MMJ, editors. *Design and applications of nanoparticles in biomedical imaging*. Cham: Springer International Publishing; p. 9-41.
- Kong H, Wang L, Zhu Y, Huang Q, Fan C. 2015. Culture medium-associated physicochemical insights on the cytotoxicity of carbon nanomaterials. *Chemical Research in Toxicology*. 28(3):290-295.
- Kong X, Huang LC, Liao SC, Han CC, Chang HC. 2005. Polylysine-coated diamond nanocrystals for MALDI-TOF mass analysis of DNA oligonucleotides. *Anal Chem*. 77(13):4273-4277.
- Kong XL, Huang LC, Hsu CM, Chen WH, Han CC, Chang HC. 2005. High-affinity capture of proteins by diamond nanoparticles for mass spectrometric analysis. *Anal Chem*. 77(1):259-265.

- Kratschmer W, Lamb LD, Fostiropoulos K, Huffman DR. 1990. Solid C60: a new form of carbon. *Nature*. 347(6291):354-358.
- Kroll A, Pillukat MH, Hahn D, Schnekenburger J. 2012. Interference of engineered nanoparticles with in vitro toxicity assays. *Archives of toxicology*. 86(7):1123-1136.
- Kroto HW, Heath JR, O'Brien SC, Curl RF, Smalley RE. 1985. C60: Buckminsterfullerene. *Nature*. 318(6042):162-163.
- Krusic PJ, Wasserman E, Keizer PN, Morton JR, Preston KF. 1991. Radical reactions of C60. *Science*. 254(5035):1183-1185.
- Kruss S, Hilmer AJ, Zhang J, Reuel NF, Mu B, Strano MS. 2013. Carbon nanotubes as optical biomedical sensors. *Advanced Drug Delivery Reviews*. 65(15):1933-1950.
- Kunzmann A, Andersson B, Vogt C, Feliu N, Ye F, Gabrielsson S, Toprak MS, Buerki-Thurnherr T, Laurent S, Vahter M et al. 2011. Efficient internalization of silica-coated iron oxide nanoparticles of different sizes by primary human macrophages and dendritic cells. *Toxicology and Applied Pharmacology*. 253(2):81-93.
- Li J, Zhu Y, Li W, Zhang X, Peng Y, Huang Q. 2010. Nanodiamonds as intracellular transporters of chemotherapeutic drug. *Biomaterials*. 31(32):8410-8418.
- Li YL, Van Cuong N, Hsieh M-F. 2014. Endocytosis pathways of the folate tethered star-shaped PEG-PCL micelles in cancer cell lines. *Polymers*. 6(3):634-650.
- Lim DG, Kim KH, Kang E, Lim SH, Ricci J, Sung SK, Kwon MT, Jeong SH. 2016. Comprehensive evaluation of carboxylated nanodiamond as a topical drug delivery system. *Int J Nanomedicine*. 11:2381-2395.
- Lin YC, Wu KT, Lin ZR, Perevedentseva E, Karmenyan A, Lin MD, Cheng CL. 2016. Nanodiamond for biolabelling and toxicity evaluation in the zebrafish embryo in vivo. *Journal of Biophotonics*. 9(8):827-836.

- Liu B, Hu X, Chai J, Zhu J, Yang B, Li Y. 2016. Application of nanodiamonds in Cu(ii)-based rhodamine B probes for NO detection and cell imaging. *Journal of materials chemistry B*. 4(19):3358-3364.
- Liu J, Cui L, Losic D. 2013. Graphene and graphene oxide as new nanocarriers for drug delivery applications. *Acta biomaterialia*. 9(12):9243-9257.
- Liu KK, Cheng CL, Chang CC, Chao JI. 2007. Biocompatible and detectable carboxylated nanodiamond on human cell. *Nanotechnology*. 18(32):[10 p.]. 325102.
- Liu KK, Wang CC, Cheng CL, Chao JI. 2009. Endocytic carboxylated nanodiamond for the labeling and tracking of cell division and differentiation in cancer and stem cells. *Biomaterials*. 30(26):4249-4259.
- Liu T, Shi Y, Du J, Ge X, Teng X, Liu L, Wang E, Zhao Q. 2016. Vitamin D treatment attenuates 2,4,6-trinitrobenzene sulphonic acid (TNBS)-induced colitis but not oxazolone-induced colitis. *Scientific Reports*. 6:[10 p.]. 32889.
- Lopez-Castejon G, Brough D. 2011. Understanding the mechanism of IL-1 $\beta$  secretion. *Cytokine & Growth Factor Reviews*. 22(4):189-195.
- Lunov O, Syrovets T, Loos C, Nienhaus GU, Mailander V, Landfester K, Rouis M, Simmet T. 2011. Amino-functionalized polystyrene nanoparticles activate the NLRP3 inflammasome in human macrophages. *ACS nano*. 5(12):9648-9657.
- Maleki Dizaj S, Mennati A, Jafari S, Khezri K, Adibkia K. 2015. Antimicrobial activity of carbon-based nanoparticles. *Advanced Pharmaceutical Bulletin*. 5(1):19-23.
- Malhotra V, Warren G, Mellman I. 2011. Protein trafficking between membranes. In: Cassimeris L, Lingappa VR, Plopper G, Lewin B, editors. *Lewin's cells*. 2nd ed. Sudbury (MA): Jones & Bartlett Learning; p. 345-389.
- Manolova V, Flace A, Bauer M, Schwarz K, Saudan P, Bachmann MF. 2008. Nanoparticles target distinct dendritic cell populations according to their size. *European journal of immunology*. 38(5):1404-1413.



- Marim FM, Silveira TN, Lima DS, Zamboni DS. 2010. A method for generation of bone marrow-derived macrophages from cryopreserved mouse bone marrow cells. *Plos One*. 5(12):[8 p.]. e15263.
- Markovic Z, Trajkovic V. 2008. Biomedical potential of the reactive oxygen species generation and quenching by fullerenes (C60). *Biomaterials*. 29(26):3561-3573.
- Martinez FO, Gordon S. 2014. The M1 and M2 paradigm of macrophage activation: time for reassessment. *F1000Prime Reports*. 6:[13 p.].
- Martinon F, Chen X, Lee A-H, Glimcher LH. 2010. Toll-like receptor activation of XBP1 regulates innate immune responses in macrophages. *Nature immunology*. 11(5):411-418.
- Mashino T, Shimotohno K, Ikegami N, Nishikawa D, Okuda K, Takahashi K, Nakamura S, Mochizuki M. 2005. Human immunodeficiency virus-reverse transcriptase inhibition and hepatitis C virus RNA-dependent RNA polymerase inhibition activities of fullerene derivatives. *Bioorganic & medicinal chemistry letters*. 15(4):1107-1109.
- Mauter MS, Elimelech M. 2008. Environmental applications of carbon-based nanomaterials. *Environmental Science & Technology*. 42(16):5843-5859.
- Mayor S and Pagano RE. 2007. Pathways of clathrin-independent endocytosis. *Nature Reviews. Molecular Cell Biology* 8(8):603-12.
- Min Y, Caster JM, Eblan MJ, Wang AZ. 2015. Clinical translation of nanomedicine. *Chemical Reviews*. 115(19):11147-11190.
- Mitchell LA, Lauer FT, Burchiel SW, McDonald JD. 2009. Mechanisms for how inhaled multiwalled carbon nanotubes suppress systemic immune function in mice. *Nat Nanotechnol*. 4(7):451-456.
- Mochalin VN, Shenderova O, Ho D, Gogotsi Y. 2011. The properties and applications of nanodiamonds. *Nat Nanotechnol*. 7(1):11-23.

- Mohan N, Chen C-S, Hsieh H-H, Wu Y-C, Chang H-C. 2010. In vivo imaging and toxicity assessments of fluorescent nanodiamonds in *Caenorhabditis elegans*. *Nano letters*. 10(9):3692-3699.
- Moore L, Gatica M, Kim H, Osawa E, Ho D. 2013. Multi-protein delivery by nanodiamonds promotes bone formation. *J Dent Res*. 92(11):976-981.
- Mosser DM, Zhang X. 2008. Activation of murine macrophages. *Current protocols in immunology*. Chapter 14: Unit 14.12. doi:10.1002/0471142735.im1402s83.
- Murphy FA, Schinwald A, Poland CA, Donaldson K. 2012. The mechanism of pleural inflammation by long carbon nanotubes: interaction of long fibers with macrophages stimulates them to amplify pro-inflammatory responses in mesothelial cells. *Particle and Fiber Toxicology*. 9:8-8.
- Murphy KM. 2011. *Janeway's Immunobiology*. 8th ed. London & New York: Taylor & Francis Group. Chapter 1, Basic concepts in immunology; p. 1-36.
- Mytych J, Lewinska A, Bielak-Zmijewska A, Grabowska W, Zebrowski J, Wnuk M. 2014. Nanodiamond-mediated impairment of nucleolar activity is accompanied by oxidative stress and DNMT2 upregulation in human cervical carcinoma cells. *Chemico-biological interactions*. 220:51-63.
- Mytych J, Lewinska A, Zebrowski J, Wnuk M. 2015. Nanodiamond-induced increase in ROS and RNS levels activates NF- $\kappa$ B and augments thiol pools in human hepatocytes. *Diamond and Related Materials*. 55(Supplement C):95-101.
- Nayak TR, Jian L, Phua LC, Ho HK, Ren Y, Pastorin G. 2010. Thin films of functionalized multiwalled carbon nanotubes as suitable scaffold materials for stem cells proliferation and bone formation. *ACS nano*. 4(12):7717-7725.
- Nobel prize.org. The Nobel Prize in Chemistry. 1996. Nobel Media AB 2014. Web. [accessed 2017 Nov 14].  
<[http://www.nobelprize.org/nobel\\_prizes/chemistry/laureates/1996/](http://www.nobelprize.org/nobel_prizes/chemistry/laureates/1996/)>

- Novoselov KS, Falko VI, Colombo L, Gellert PR, Schwab MG, Kim K. 2012. A roadmap for graphene. *Nature*. 490(7419):192-200.
- Osterholzer JJ, Chen G-H, Olszewski MA, Zhang Y-M, Curtis JL, Huffnagle GB, Toews GB. 2011. Chemokine receptor 2-mediated accumulation of fungicidal exudate macrophages in mice that clear cryptococcal lung infection. *The American Journal of Pathology*. 178(1):198-211.
- Palomaki J, Valimaki E, Sund J, Vippola M, Clausen PA, Jensen KA, Savolainen K, Matikainen S, Alenius H. 2011. Long, needle-like carbon nanotubes and asbestos activate the NLRP3 inflammasome through a similar mechanism. *ACS nano*. 5(9):6861-6870.
- Payne CK, Jones SA, Chen C, Zhuang X. 2007. Internalization and trafficking of cell surface proteoglycans and proteoglycan-binding ligands. *Traffic*. 8(4):389-401.
- Perevedentseva E, Hong S-F, Huang K-J, Chiang I-T, Lee C-Y, Tseng Y-T, Cheng C-L. 2013. Nanodiamond internalization in cells and the cell uptake mechanism. *Journal of Nanoparticle Research*. 15(8):1834-1838.
- Perevedentseva E, Lin YC, Jani M, Cheng CL. 2013. Biomedical applications of nanodiamonds in imaging and therapy. *Nanomedicine*. 8(12):2041-2060.
- Pi J, Li T, Liu J, Su X, Wang R, Yang F, Bai H, Jin H, Cai J. 2014. Detection of lipopolysaccharide induced inflammatory responses in RAW264.7 macrophages using atomic force microscope. *Micron*. 65(Supplement C):1-9.
- Prabhakar N, Khan MH, Peurla M, Chang H-C, Hänninen PE, Rosenholm JM. 2017. Intracellular trafficking of fluorescent nanodiamonds and regulation of their cellular toxicity. *ACS Omega*. 2(6):2689-2693.
- Reisetter AC, Stebounova LV, Baltrusaitis J, Powers L, Gupta A, Grassian VH, Monick MM. 2011. Induction of inflammasome-dependent pyroptosis by carbon black nanoparticles. *The Journal of biological chemistry*. 286(24):21844-21852.

- Rizzo LY, Theek B, Storm G, Kiessling F, Lammers T. 2013. Recent progress in nanomedicine: therapeutic, diagnostic and theranostic applications. *Current opinion in biotechnology*. 24(6):1159-1166.
- Rodal SK, Skretting G, Garred O, Vilhardt F, van Deurs B, Sandvig K. 1999. Extraction of cholesterol with methyl-beta-cyclodextrin perturbs formation of clathrin-coated endocytic vesicles. *Molecular biology of the cell*. 10(4):961-974.
- Roszer T. 2015. Understanding the mysterious M2 macrophage through activation markers and effector mechanisms. *Mediators of Inflammation*. 2015:[16 p.]. article ID 816460. doi:10.1155/2015/816460
- Rouault C, Pellegrinelli V, Schilch R, Cotillard A, Poitou C, Tordjman J, Sell H, Clément K, Lacasa D. 2013. Roles of chemokine ligand-2 (CXCL2) and neutrophils in influencing endothelial cell function and inflammation of human adipose tissue. *Endocrinology*. 154(3):1069-1079.
- Roy RK, Lee KR. 2007. Biomedical applications of diamond-like carbon coatings: a review. *J Biomed Mater Res B Appl Biomater*. 83(1):72-84.
- Salaam AD, Hwang P, McIntosh R, Green HN, Jun HW, Dean D. 2014. Nanodiamond-DGEA peptide conjugates for enhanced delivery of doxorubicin to prostate cancer. *Beilstein journal of nanotechnology*. 5:937-945.
- Salvador-Morales C, Flahaut E, Sim E, Sloan J, H. Green ML, Sim RB. 2006. Complement activation and protein adsorption by carbon nanotubes. *Molecular Immunology*. 43(3):193-201.
- Sampath P, Pollard TD. 1991. Effects of cytochalasin, phalloidin and pH on the elongation of actin filaments. *Biochemistry*. 30(7):1973-1980.
- Santoro A, Ferrante MC, Di Guida F, Pirozzi C, Lama A, Simeoli R, Clausi MT, Monnolo A, Mollica MP, Mattace Raso G et al. 2015. Polychlorinated biphenyls (PCB 101, 153, and 180) impair murine macrophage responsiveness to lipopolysaccharide:

- involvement of NF-kappaB pathway. *Toxicological sciences: an official journal of the Society of Toxicology*. 147(1):255-269.
- Saxena RK, Vallyathan V, Lewis DM. 2003. Evidence for lipopolysaccharide induced differentiation of RAW264.7 murine macrophage cell line into dendritic like cells. *Journal of Biosciences*. 28(1):129-134.
- Schanen BC, Karakoti AS, Seal S, Drake DR, 3rd, Warren WL, Self WT. 2009. Exposure to titanium dioxide nanomaterials provokes inflammation of an in vitro human immune construct. *ACS nano*. 3(9):2523-2532.
- Scheller J, Chalaris A, Schmidt-Arras D, Rose-John S. 2011. The pro- and anti-inflammatory properties of the cytokine interleukin-6. *Biochimica et Biophysica Acta (BBA) - Molecular Cell Research*. 1813(5):878-888.
- Schinazi RF, Sijbesma R, Srdanov G, Hill CL, Wudl F. 1993. Synthesis and virucidal activity of a water-soluble, configurationally stable, derivatized C60 fullerene. *Antimicrobial Agents and Chemotherapy*. 37(8):1707-1710.
- Schirhagl R, Chang K, Loretz M, Degen CL. 2014. Nitrogen-vacancy centers in diamond: nanoscale sensors for physics and biology. *Annu Rev Phys Chem*. 65:83-105.
- Schrand AM, Dai L, Schlager JJ, Hussain SM, Osawa E. 2007. Differential biocompatibility of carbon nanotubes and nanodiamonds. *Diamond and Related Materials*. 16(12):2118-2123.
- Schrand AM, Huang H, Carlson C, Schlager JJ, Omacr Sawa E, Hussain SM, Dai L. 2007. Are diamond nanoparticles cytotoxic? *J Phys Chem B*. 111(1):2-7.
- Shamsul HM, Hasebe A, Iyori M, Ohtani M, Kiura K, Zhang D, Totsuka Y, Shibata K. 2010. The Toll-like receptor 2 (TLR2) ligand FSL-1 is internalized via the clathrin-dependent endocytic pathway triggered by CD14 and CD36 but not by TLR2. *Immunology*. 130(2):262-272.

- Shenderova O, Koscheev A, Zaripov N, Petrov I, Skryabin Y, Detkov P, Turner S, Van Tendeloo G. 2011. Surface chemistry and properties of ozone-purified detonation nanodiamonds. *The Journal of Physical Chemistry C*. 115(20):9827-9837.
- Shenderova OA, McGuire GE. 2015. Science and engineering of nanodiamond particle surfaces for biological applications. *Biointerphases*. 10(3):[23 p.]. 030802.
- Shenderova OA, Zhirnov VV, Brenner DW. 2002. Carbon nanostructures. *Critical Reviews in Solid State and Materials Sciences*. 27(3-4):227-356.
- Shkurupy VA, Arkhipov SA, Neshchadim DV, Akhramenko ES, Troitskii AV. 2015. In vitro effects of nanosized diamond particles on macrophages. *Bulletin of Experimental Biology and Medicine*. 158(4):500-503.
- Slegerova J, Hajek M, Rehor I, Sedlak F, Stursa J, Hruby M, Cigler P. 2015. Designing the nanobiointerface of fluorescent nanodiamonds: highly selective targeting of glioma cancer cells. *Nanoscale*. 7(2):415-420.
- Solovjov DA, Pluskota E, Plow EF. 2005. Distinct roles for the alpha and beta subunits in the functions of integrin alphaMbeta2. *The Journal of biological chemistry*. 280(2):1336-1345.
- Stout DA, Webster TJ. 2012. Carbon nanotubes for stem cell control. *Materials Today*. 15(7):312-318.
- Su LJ, Wu MS, Hui YY, Chang BM, Pan L, Hsu PC, Chen YT, Ho HN, Huang YH, Ling TY et al. 2017. Fluorescent nanodiamonds enable quantitative tracking of human mesenchymal stem cells in miniature pigs. *Scientific Reports*. 7(45607):[11 p.].
- Suarez-Kelly LP, Campbell AR, Rampersaud IV, Bumb A, Wang MS, Butchar JP, Tridandapani S, Yu L, Rampersaud AA, Carson WE. 2017. Fluorescent nanodiamonds engage innate immune effector cells: A potential vehicle for targeted anti-tumor immunotherapy. *Nanomedicine: Nanotechnology, Biology and Medicine*. 13(3):909-920.

- Taylor R, Langley GJ, Kroto HW, Walton DRM. 1993. Formation of C<sub>60</sub> by pyrolysis of naphthalene. *Nature*. 366(6457):728-731.
- Thomas V, Halloran BA, Ambalavanan N, Catledge SA, Vohra YK. 2012. In vitro studies on the effect of particle size on macrophage responses to nanodiamond wear debris. *Acta biomaterialia*. 8(5):1939-1947.
- Todd RF. 1996. The continuing saga of complement receptor type 3 (CR3). *Journal of Clinical Investigation*. 98(1):1-2.
- Tsai CY, Lu SL, Hu CW, Yeh CS, Lee GB, Lei HY. 2012. Size-dependent attenuation of TLR9 signaling by gold nanoparticles in macrophages. *J Immunol*. 188(1):68-76.
- Tsai L, Lin Y, Perevedentseva E, Lugovtsov A, Priezzhev A, Cheng C. 2016. Nanodiamonds for medical applications: Interaction with blood in vitro and in vivo. *International Journal of Molecular Sciences*. 17(7):1111.
- Turcheniuk K, Mochalin VN. 2017. Biomedical applications of nanodiamond. *Nanotechnology*. 28(25):[27 p.].252001.
- Vaijayanthimala V, Cheng PY, Yeh SH, Liu KK, Hsiao CH, Chao JI, Chang HC. 2012. The long-term stability and biocompatibility of fluorescent nanodiamond as an in vivo contrast agent. *Biomaterials*. 33(31):7794-7802.
- Vaijayanthimala V, Lee DK, Kim SV, Yen A, Tsai N, Ho D, Chang HC, Shenderova O. 2015. Nanodiamond-mediated drug delivery and imaging: challenges and opportunities. *Expert opinion on drug delivery*. 12(5):735-749.
- Vaijayanthimala V, Tzeng YK, Chang HC, Li CL. 2009. The biocompatibility of fluorescent nanodiamonds and their mechanism of cellular uptake. *Nanotechnology*. 20(42):[9 p.]. 425103.
- Vega-Figueroa K, Santillán J, García C, González-Feliciano JA, Bello SA, Rodríguez YG, Ortiz-Quiles E, Nicolau E. 2017. Assessing the suitability of cellulose-nanodiamond composite as a multifunctional biointerface material for bone tissue regeneration. *ACS Biomaterials Science & Engineering*. 3(6):960-968.

- Vlasov II, Shiryaev AA, Rendler T, Steinert S, Lee S-Y, Antonov D, Voros M, Jelezko F, Fisenko AV, Semjonova LF et al. 2014. Molecular-sized fluorescent nanodiamonds. *Nat Nano*. 9(1):54-58.
- Wang C, Yu X, Cao Q, Wang Y, Zheng G, Tan TK, Zhao H, Zhao Y, Wang Y, Harris DC. 2013. Characterization of murine macrophages from bone marrow, spleen and peritoneum. *BMC Immunology*. 14(1):[10 p.].
- Wang D, Tong Y, Li Y, Tian Z, Cao R, Yang B. 2013. PEGylated nanodiamond for chemotherapeutic drug delivery. *Diamond and Related Materials*. 36:26-34.
- Wang F, Fang RH, Luk BT, Hu C-MJ, Thamphiwatana S, Dehaini D, Angsantikul P, Kroll AV, Pang Z, Gao W et al. 2016. Nanoparticle-based antivirulence vaccine for the management of methicillin-resistant *Staphylococcus aureus* Skin Infection. *Advanced Functional Materials*. 26(10):1628-1635.
- Wang LH, Rothberg KG, Anderson RG. 1993. Mis-assembly of clathrin lattices on endosomes reveals a regulatory switch for coated pit formation. *The Journal of cell biology*. 123(5):1107-1117.
- Wang Q, Ni H, Lan L, Wei X, Xiang R, Wang Y. 2010. Fra-1 protooncogene regulates IL-6 expression in macrophages and promotes the generation of M2d macrophages. *Cell research*. 20(6):701-712.
- Wang X, Reece SP, Brown JM. 2013. Immunotoxicological impact of engineered nanomaterial exposure: mechanisms of immune cell modulation. *Toxicol Mech Methods*. 23(3):168-177.
- Wang Y, Li Z, Wang J, Li J, Lin Y. 2011. Graphene and graphene oxide: biofunctionalization and applications in biotechnology. *Trends in Biotechnology*. 29(5):205-212.
- Weischenfeldt J, Porse B. 2008. Bone marrow-derived macrophages (BMM): isolation and applications. *CSH protocols*. 3(12):[7 p.]. doi: 10.1101/pdb.prot5080.



- Weng M-F, Chiang S-Y, Wang N-S, Niu H. 2009. Fluorescent nanodiamonds for specifically targeted bioimaging: Application to the interaction of transferrin with transferrin receptor. *Diamond and Related Materials*. 18(2):587-591.
- West MA, Bretscher MS, Watts C. 1989. Distinct endocytotic pathways in epidermal growth factor-stimulated human carcinoma A431 cells. *The Journal of Cell Biology*. 109(6 Pt 1):2731-2739.
- Wierzbicki M, Sawosz E, Grodzik M, Hotowy A, Prasek M, Jaworski S, Sawosz F, Chwalibog A. 2013. Carbon nanoparticles downregulate expression of basic fibroblast growth factor in the heart during embryogenesis. *International Journal of Nanomedicine*. 8:3427-3435.
- Winter M, Beer HD, Hornung V, Kramer U, Schins RP, Forster I. 2011. Activation of the inflammasome by amorphous silica and TiO<sub>2</sub> nanoparticles in murine dendritic cells. *Nanotoxicology*. 5(3):326-340.
- Wörle-Knirsch JM, Pulskamp K, Krug HF. 2006. Oops they did it again! carbon nanotubes hoax scientists in viability assays. *Nano letters*. 6(6):1261-1268.
- Wu X, Bruschi M, Waag T, Schweeney S, Tian Y, Meinhardt T, Stigler R, Larsson K, Funk M, Steinmüller-Nethl D et al. 2017. Functionalization of bone implants with nanodiamond particles and angiopoietin-1 to improve vascularization and bone regeneration. *Journal of Materials Chemistry B*. 5(32):6629-6636.
- Xaus J, Comalada M, Valledor AF, Lloberas J, Lopez-Soriano F, Argiles JM, Bogdan C, Celada A. 2000. LPS induces apoptosis in macrophages mostly through the autocrine production of TNF- $\alpha$ . *Blood*. 95(12):3823-3831
- Yamago S, Tokuyama H, Nakamura E, Kikuchi K, Kananishi S, Sueki K, Nakahara H, Enomoto S, Ambe F. 1995. In vivo biological behavior of a water-miscible fullerene: <sup>14</sup>C labeling, absorption, distribution, excretion and acute toxicity. *Chemistry & biology*. 2(6):385-389.

- Yang E-J, Kim S, Kim JS, Choi I-H. 2012. Inflammasome formation and IL-1 $\beta$  release by human blood monocytes in response to silver nanoparticles. *Biomaterials*. 33(28):6858-6867.
- Yang L, Sheldon BW, Webster TJ. 2009. Orthopedic nano diamond coatings: Control of surface properties and their impact on osteoblast adhesion and proliferation. *Journal of Biomedical Materials Research Part A*. 91A(2):548-556.
- Yang Y, Asiri AM, Tang Z, Du D, Lin Y. 2013. Graphene based materials for biomedical applications. *Materials Today*. 16(10):365-373.
- Yazdi AS, Guarda G, Riteau N, Drexler SK, Tardivel A, Couillin I, Tschopp J. 2010. Nanoparticles activate the NLR pyrin domain containing 3 (Nlrp3) inflammasome and cause pulmonary inflammation through release of IL-1 $\alpha$  and IL-1 $\beta$ . *Proceedings of the National Academy of Sciences of the United States of America*. 107(45):19449-19454.
- Yin PT, Shah S, Chhowalla M, Lee K-B. 2015. Design, synthesis, and characterization of graphene–nanoparticle hybrid materials for bioapplications. *Chemical Reviews*. 115(7):2483-2531.
- Yu S-J, Kang M-W, Chang H-C, Chen K-M, Yu Y-C. 2005. Bright fluorescent nanodiamonds: no photobleaching and low cytotoxicity. *Journal of the American Chemical Society*. 127(50):17604-17605.
- Yuan Y, Chen Y, Liu J-H, Wang H, Liu Y. 2009. Biodistribution and fate of nanodiamonds in vivo. *Diamond and Related Materials*. 18(1):95-100.
- Zhang Q, Mochalin VN, Neitzel I, Knoke IY, Han J, Klug CA, Zhou JG, Lelkes PI, Gogotsi Y. 2011. Fluorescent PLLA-nanodiamond composites for bone tissue engineering. *Biomaterials*. 32(1):87-94.
- Zhang Y, Leu Y-R, Aitken RJ, Riediker M. 2015. Inventory of engineered nanoparticle-containing consumer products available in the Singapore retail market and

likelihood of release into the aquatic environment. *International Journal of Environmental Research and Public Health*. 12(8):8717-8743.

Zhu Y, Li J, Li W, Zhang Y, Yang X, Chen N, Sun Y, Zhao Y, Fan C, Huang Q. 2012. The biocompatibility of nanodiamonds and their application in drug delivery systems. *Theranostics*. 2(3):302-312.

## APPENDIX

9/11/2017

RightsLink Printable License

### THE AMERICAN ASSOCIATION FOR THE ADVANCEMENT OF SCIENCE LICENSE TERMS AND CONDITIONS

Sep 11, 2017

This Agreement between Old Dominion University -- Maisoun Bani Hani ("You") and The American Association for the Advancement of Science ("The American Association for the Advancement of Science") consists of your license details and the terms and conditions provided by The American Association for the Advancement of Science and Copyright Clearance Center.

License Number	4185930173146
License date	Sep 11, 2017
Licensed Content Publisher	The American Association for the Advancement of Science
Licensed Content Publication	Science Translational Medicine
Licensed Content Title	Nanodiamond Therapeutic Delivery Agents Mediate Enhanced Chemoresistant Tumor Treatment
Licensed Content Author	Edward K. Chow,Xue-Qing Zhang,Mark Chen,Robert Lam,Erik Robinson,Houjin Huang,Daniel Schaffer,Eiji Osawa,Andrei Goga,Dean Ho
Licensed Content Date	Mar 9, 2011
Licensed Content Volume	3
Licensed Content Issue	73
Volume number	3
Issue number	73
Type of Use	Thesis / Dissertation
Requestor type	Scientist/individual at a research institution
Format	Print and electronic
Portion	Figure
Number of figures/tables	1
Order reference number	
Title of your thesis / dissertation	THE EFFECT OF CARBOXYLATED, HIGH PRESSURE HIGH TEMPERATURE NANODIAMONDS ON MACROPHAGES DURING AND AFTER DIFFERENTIATION
Expected completion date	Dec 2017

<https://s100.copyright.com/AppDispatchServlet>

1/8

9/12/2017

Rightslink® by Copyright Clearance Center



RightsLink®

Home

Account  
Info

Help



Title:

Surface Chemistry and  
Properties of Ozone-Purified  
Detonation Nanodiamonds

Author:

O. Shenderova, A. Koscheev, N.  
Zaripov, et al

Publication:

The Journal of Physical  
Chemistry C

Publisher:

American Chemical Society

Date:

May 1, 2011

Copyright © 2011, American Chemical Society

Logged in as:

Malsoun Bani Hani  
Old Dominion UniversityAccount #:  
3001193639

LOGOUT

**PERMISSION/LICENSE IS GRANTED FOR YOUR ORDER AT NO CHARGE**

This type of permission/license, instead of the standard Terms & Conditions, is sent to you because no fee is being charged for your order. Please note the following:

- Permission is granted for your request in both print and electronic formats, and translations.
- If figures and/or tables were requested, they may be adapted or used in part.
- Please print this page for your records and send a copy of it to your publisher/graduate school.
- Appropriate credit for the requested material should be given as follows: "Reprinted (adapted) with permission from (COMPLETE REFERENCE CITATION). Copyright (YEAR) American Chemical Society." Insert appropriate information in place of the capitalized words.
- One-time permission is granted only for the use specified in your request. No additional uses are granted (such as derivative works or other editions). For any other uses, please submit a new request.

If credit is given to another source for the material you requested, permission must be obtained from that source.

BACK

CLOSE WINDOW

Copyright © 2017 Copyright Clearance Center, Inc. All Rights Reserved. [Privacy statement](#). [Terms and Conditions](#).  
Comments? We would like to hear from you. E-mail us at [customercare@copyright.com](mailto:customercare@copyright.com)

<https://s100.copyright.com/AppDispatchServlet#formTop>

11/23/2017

RightsLink Printable License

**NATURE PUBLISHING GROUP LICENSE  
TERMS AND CONDITIONS**

Nov 23, 2017

---

This Agreement between Old Dominion University -- Maisoun Bani Hani ("You") and Nature Publishing Group ("Nature Publishing Group") consists of your license details and the terms and conditions provided by Nature Publishing Group and Copyright Clearance Center.

License Number	4234810564730
License date	Nov 23, 2017
Licensed Content Publisher	Nature Publishing Group
Licensed Content Publication	Nature Immunology
Licensed Content Title	Tissue-resident macrophages
Licensed Content Author	Luke C Davies, Stephen J Jenkins, Judith E Allen, Philip R Taylor
Licensed Content Date	Sep 18, 2013
Licensed Content Volume	14
Licensed Content Issue	10
Type of Use	reuse in a dissertation / thesis
Requestor type	academic/educational
Format	print and electronic
Portion	figures/tables/illustrations
Number of figures/tables/illustrations	1
High-res required	no
Figures	Table 1
Author of this NPG article	no
Your reference number	
Title of your thesis / dissertation	Effects of carboxylated nanodiamonds on macrophages during and after differentiation
Expected completion date	Dec 2017
Estimated size (number of pages)	150

<https://s100.copyright.com/AppDispatchServlet>

## VITA

**Maisoun E. Bani Hani**

### Address

Department of Biological Sciences, Old Dominion University, Norfolk VA 23529

### Education

- Ph.D. Biomedical Sciences, December 2017, Old Dominion University, Norfolk VA
- M.S. Applied Biological Sciences, June 2012, Jordan University of Science and Technology, Jordan
- B.S. Environmental Sciences, June 2007, Jordan University of Science and Technology, Jordan

### Publications

- Karasneh J, Bani-Hani M, Alkhateeb A, Hassan A, Alzoubi F, Thornhill M. TLR2, TLR4 and CD86 gene polymorphisms in recurrent aphthous stomatitis. Journal of oral pathology & medicine: official publication of the International Association of Oral Pathologists and the American Academy of Oral Pathology. 2015; 44(10):857-63.
- Karasneh JA, Bani-Hani ME, Alkhateeb AM, Hassan AF, Thornhill MH. Association of MMP but not TIMP-1 gene polymorphisms with recurrent aphthous stomatitis. Oral diseases. 2014; 20(7):693-9.
- Karasneh J, Bani Hani M, Hassan A, Thornhill M. Toll-like receptor and metalloproteinase genes polymorphisms in Jordanian RAS patients. Oral Diseases 2012, 18, 26-26.
- Bani Hani M, Osgood C. Effects of carboxylated nanodiamonds on macrophages during and after differentiation. (In progress).